AD-A069 113 ILLINOIS UNIV AT URBANA-CHAMPAIGN DEPT OF CIVIL ENGIN--ETC F/G 13/13
BOUNDARY INTEGRAL EQUATION SOLUTION OF PLANE ELASTICITY PROBLEM--ETC(U)
APR 79 H NIKOOYEH, A R ROBINSON N00014-75-C-0164
UNCLASSIFIED UILU-ENG-79-2005 NL

1 OF 2
AD A069113

UILU-ENG-79-2005

CIVIL ENGINEERING STUDIES
STRUCTURAL RESEARCH SERIES NO. 461

LEVEL II

BOUNDARY INTEGRAL EQUATION SOLUTION OF PLANE ELASTICITY PROBLEMS WITH HIGH STRESS CONCENTRATIONS

See 1473 in back.

By
H. NIKOOYEH
A. R. ROBINSON

A Technical Report of
Research Sponsored by
THE OFFICE OF NAVAL RESEARCH
DEPARTMENT OF THE NAVY
Contract No. N00014-75-C-0164
Project No. NR 064-183

UNIVERSITY OF ILLINOIS
at URBANA-CHAMPAIGN
URBANA, ILLINOIS
APRIL 1979

BOUNDARY INTEGRAL EQUATION SOLUTION OF PLANE ELASTICITY PROBLEMS WITH HIGH STRESS CONCENTRATIONS

by

H. Nikooyeh

A. R. Robinson

A Technical Report of

Research Sponsored by

THE OFFICE OF NAVAL RESEARCH
DEPARTMENT OF THE NAVY

Contract No. N00014-75-C-0614

Project No. NR 064-183

University of Illinois
at Urbana-Champaign
Urbana, Illinois

April 1979

ACKNOWLEDGMENT

This report was prepared as a doctoral dissertation by Mr. Hassan Nikooyeh and was submitted to the Graduate College of the University of Illinois at Urbana-Champaign in partial fulfillment of the requirements for the degree of Doctor of Philosophy in Civil Engineering. The work was done under the supervision of Dr. Arthur R. Robinson, Professor of Civil Engineering.

The investigation was conducted as part of a research program supported by the Office of Naval Research under Contract N00014-75-C-0164, "Numerical and Approximate Methods of Stress Analysis."

The authors wish to thank Dr. A. R. Eubanks, Professor of Civil Engineering and Dr. Leonard Lopez, Associate Professor of Civil Engineering, for their assistance.

The numerical results were obtained with the use of the IBM 360-75 and CYBER-75 computer systems of the Office of Computer Services at the University of Illinois at Urbana-Champaign.

TABLE OF CONTENTS

LIST OF TABLES

LIST OF FIGURES

1. INTRODUCTION

1.1 Object and Scope

The object of this study is to determine accurately the stresses and displacements in two-dimensional elastic bodies with high stress concentrations using a form of the boundary integral equation technique. Major emphasis will be placed on treating boundary value problems for bodies where at some points the radius of curvature of the boundary becomes very small. Example of such configurations are notches where the root of the notch is curved and parallel-sided cracks of finite but small width (wide crack). An improvement of a previously developed procedure for treating the case of an infinitesimal crack provides a considerable advantage in the solution of the wide crack problem as well.

The material of the body is assumed to be homogeneous, isotropic and linearly elastic. The displacements are taken small enough that the linear theory of elasticity is applicable.

The technical importance of the problems under consideration needs no emphasis. The purpose of the sample problems solved is to display the versatility and accuracy of the procedure rather than to give numerical solution to actual problems of engineering significance.

1.2 General Remarks on Boundary Integral Equation Method

The boundary integral equation (BIE) method provides a powerful tool for solving boundary value problems in potential theory and classical elasticity. Historically, according to Love [1][1], the integral equation method was first applied in theory of elasticity by Betti in 1872.

[1] Numbers in brackets refer to entries in the list of references.

Further work was done in this area by Somigliana in the 1880's. The general elasticity problem[1] is solved in the Somigliana approach [2] by applying Betti's law to the actual state of stress and the state of stress arising from the Kelvin's fundamental solutions.[2] The method overcomes the inherent difficulty of Betti's approach which requires construction of Green's type functions for the solution of the same problem.

The advent of digital computers has been responsible for the development of interest in the numerical treatment of elasticity problems using the boundary integral equation approach. The method has been modified and extended in a number of investigations to solve two- and three-dimensional problems in isotropic elastic media, and even in elasto-plastic and anisotropic media [5-12].

The method has also been extended to the solution of bodies with infinite stress gradients such as cracks and sharp re-entrant corners (for example, see Ref. 12-17). One method of special interest was developed by Barone and Robinson [18]. This method makes use of Williams' solutions [19, 20] with unknown coefficients to represent the stress and displacement field in the vicinity of the sharp notches or cracks. This work unlike other methods using the Williams' representation, employs new auxiliary solutions for the determination of the unknown coefficients. This method will be used extensively in this study. A more detailed explanation of the method is given in Section 2.4.

---

[1] In this study we shall consider only the so-called "first" boundary-value problem in plane elasticity which is to determine the displacements in the interior of an elastic body where the body force and boundary tractions are prescribed. Extension to other well-set boundary value problems does not appear to involve essential changes.

[2] These solutions are sometimes called auxiliary solutions in the BIE method.

1.3 Motivation and General Description of the Proposed Method

As mentioned before, the major emphasis will be placed on treating bodies with notches where the root of the notch is curved (fillet problem), and also bodies with a "wide" crack. The solution of these problems using the ordinary BIE method requires the introduction of many points in a small, localized region of the boundary. This will cause the number of the unknowns to increase and contributes to poor conditioning of the final equations.[1] Indeed, in the limit, as the configuration approaches that of a sharp notch, the method breaks down.

The overall stragegy of the proposed procedure is to modify the process which has been found to work for the sharp notch. The modification will run into difficulty only if the radius of the notch is not small with respect to that of the body, in which case the ordinary BIE method is economically applicable, and one would not speak of a stress-concentration problem.

The method is therefore based on the Barone and Robinson [18] solution technique. In that method the Williams' forms [19, 20] are used right up to the singular point. In the proposed modification a small body containing the fillet is removed and an extended Williams' form holds in an annular region outside this inner piece (see Fig. 4). The inner piece is treated as a smooth body where the details of the configuration of the fillet are taken into account by the specified geometry of the boundary points. The process involves matching the smooth solution for the inner piece to the

---

[1] It should be noted that since the equations of the BIE method are not banded, the computational penalty, even without regard to round-off error, is severe.

analytic Williams' field on the annulus. The generalized displacements specifying the Williams' field are determined in much the same way as in Ref. [18], except that the body in question has a hole (the part removed as the inner body). After these generalized displacements are found, the full solution in the inner piece can be constructed and the detailed stress pattern found near the fillet.

The solution of the wide crack problem is essentially the same as for the notch with a fillet of small radius, except that before developing the series solution for the annular region, it is necessary to perturb the Williams' solution for the corresponding infinitesimal crack in order to satisfy the homogeneous boundary conditions on the actual boundary of the crack. Finally, an altered form of the Barone and Robinson solution technique for the infinitesimal crack is used to avoid certain mathematical problems, as is explained in Appendix A.

1.4 Notation

The symbols used in this study are defined where they first appear. For convenient reference, the more important symbols are listed below. Some symbols are assigned more than one meaning, however ambiguities do not occur in the context of their use.

A_m, B_m	m-th eigenfunction
C_{1m}, C_{2m}, C_{3m}, C_{4m}	m-th eigenvector
D	region occupied by two-dimensional body

D_ε	circular sub-region of D with radius ε
D_ρ, D_ϕ	displacements of perturbed Williams' solution in polar coordinates
E	young modulus of elasticity
f	density function
g	kernel of integral equations
G(s)	= f·g, product of density function and kernel, Eq. (5.1)
h, h_j	spacing of node points on the boundary
$I_L, I(\varepsilon)$	line integral
K	m-th generalized displacement
k	boundary curvature
L	boundary curve of region D
L_ε	boundary curve of sub-region D_ε
ℓ, m	direction cosine of normal $\hat{n}$
N_L	number of node points in L
$\hat{n}(Q)$	outward normal at point Q on L
P	an interior point of D+L
P,Q	boundary points on L
Q_ε	boundary point on L_ε
r, r(P,Q)	distance between two points P and Q
$\hat{s}(Q)$	tangent to the boundary L at point Q
$S_{\rho\rho}$, $S_{\phi\phi}$, $S_{\rho\phi}$	stresses of perturbed Williams' solutions

$t_j(Q)$	actual far-field tractions at point Q
$t^*_{ij}(P,Q)$	far-field traction at point Q due to auxiliary field at point P
$u_j(Q)$	actual far-field displacement at point Q
$u^*_{ij}(P,Q)$	far-field displacement at point Q due to auxiliary field at point P
u_ρ, u_ϕ	displacements of the Williams' solution forms
$\bar{u}_\rho$, $\bar{u}_\phi$	displacements of the modified Williams' solution or modified perturbed solution
W_L, V_L	net reciprocal work along L
x,y	rectangular coordinates
z	= x + iy complex number
$\bar{z}$	conjugate of z
ϵ	radius of circular region D_ϵ
θ_0	included angle of a notch
λ_m	m-th eigenvalue
ρ, ϕ	polar coordinates
$\sigma_{\rho\rho}$, $\sigma_{\phi\phi}$, $\sigma_{\rho\phi}$	stresses from Williams' solutions form
$\bar{\sigma}_{\rho\rho}$, $\bar{\sigma}_{\phi\phi}$, $\bar{\sigma}_{\rho\phi}$	stresses from modified Williams' solution or modified perturbed solution

The summation convention is used on the repeated subscripts j in the integral relationships.

2. THE BOUNDARY INTEGRAL EQUATION METHOD AND ITS EXTENSION TO CORNERS

2.1 Introduction

As mentioned in Chapter 1, the method of solution in this study is based on an integral equation formulation of the problems. A brief review of the boundary integral equation (BIE) method for bodies with smooth boundaries will be given in Section 2.2. In order to extend the BIE method to bodies with irregular boundary point[1] it is convenient to use a field that represents the character of displacements at that point. Such an extension was developed by Barone and Robinson [18] and will be discussed in Section 2.4. Before the extension of the BIE method to irregular points can be developed, it is necessary to know the behavior of the displacements in the vicinity of such points. The basic elasticity solutions which define this behavior, the so-called Williams' solutions [19,20], are described in Section 2.3. It will be shown in Chapter 3 and Chapter 4 how these solutions can be modified to be applicable for certain regions in problems of notches with fillet of small radius and in problems with cracks of finite but small width.

2.2 The Boundary Integral Equation Method

2.2.1 General Remarks

In recent years much attention has been given to the numerical solution of boundary value problems using integral equations. The method has been

---

[1] Irregular boundary points are those at which the tangent to the boundary does not turn smoothly or a sudden change in the nature of the boundary conditions occurs. These include corners, notch tips, crack tips, and an edge of a contact region. This is not to be confused with Kellogg's definition of regular boundaries and surfaces [37].

used successfully for solving a wide range of problems in applied mechanics (for example, see Refs. 5-23). The main advantage of the boundary integral equation is that for the solution of a given problem, the unknown boundary values are expressed entirely in terms of boundary data. This is in contrast to the finite difference and finite element methods which use interior field values in addition to the boundary values as unknowns for the solution of the same problem.

The formulation of the boundary integral equation method for the theory of elasticity is based on Betti's law [1]. The two sets of displacement and corresponding stress fields used in Betti's law will be the actual system and another, auxiliary system. The object is determination of unknown displacements and stresses of the actual system using the known fields of the auxiliary system as well as whatever boundary values of the actual system are known.

The success of the BIE method depends on the choice of the auxiliary solution. It is desirable to have auxiliary fields corresponding to loads which pick out a component of displacement at an interior point. Such auxiliary fields are those resulting from the point loads acting on a body in the direction of the desired displacements. A proper choice of other auxiliary loadings is the key to the convenient extension of the BIE method to be discussed in Section 2.4.

2.2.2 Kelvin Solution for the Infinite Plate

Concentrated force solutions, the so-called Kelvin solutions, are auxiliaries that will be used extensively in this study. The tractions

and displacement $t^*_{ij}(P,Q)$ and $u^*_{ij}(P,Q)$[1] at a boundary point Q due to a concentrated force in the i-th coordinate direction at a point P are:

a) Tractions

$$t^*_{11}(P,Q)=A(r_x{}^2 + B)\frac{r_n}{r} \quad ; \quad t^*_{12}(P,Q)=A(r_x r_y r_n + Br_s)\frac{1}{r}$$
$$t^*_{22}(P,Q)=A(r_y{}^2 + B)\frac{r_n}{r} \quad ; \quad t^*_{21}(P,Q)=A(r_x r_y r_n - Br_s)\frac{1}{r} \tag{2.1}$$

b) Displacements

$$u^*_{11}(P,Q)=Ln(r) + cr_x{}^2 \quad ; \quad u^*_{12}(P,Q)=Cr_x r_y$$
$$u^*_{22}(P,Q)=Ln(r) + cr_y{}^2 \quad ; \quad u^*_{21}(P,Q)=Cr_x r_y \tag{2.2}$$

where $r = r(P,Q)$ and the subscripts x, y, n, s indicate differentiation with respect to the x, y, n, and s coordinates (see Fig. 1). The constants A, B, and C for the case of plane strain are:

$$A=\frac{2E}{(1+\nu)(3-4\nu)} \quad ; \quad B=\frac{1}{2}(1-2\nu) \quad ; \quad C=\frac{1}{3-4\nu} \tag{2.3}$$

In Eqs. (2.3), E is Young modulus of elasticity and ν is Poisson's ratio.

2.2.3 Integral Equation for Regular Boundary Points

Consider a two-dimensional isotropic elastic body in plane strain with boundary contour L (see Fig. 1). The Kelvin field resulting from a concentrated force applied at a point P of the body in the i-th coordinate direction will be used as auxiliary. Since the auxiliary solution is unbounded at P, a small region D_ε with boundary L_ε is removed from the body.

---

[1] The first script, (i = 1,2) refers to direction of the load and the second (j = 1,2) refers to x, y coordinates.

Betti's law can now be written for the remaining region in the form:[1]

$$\int_{L_\varepsilon} t_j(Q_\varepsilon)\, u^*_{ij}(P,Q_\varepsilon)ds(Q_\varepsilon) + \int_{L-L_\varepsilon} t_j(Q)\, u^*_{ij}(P,Q)ds(Q) =$$

$$\int_{L_\varepsilon} u_j(Q_\varepsilon)\, t^*_{ij}(P,Q_\varepsilon)ds(Q_\varepsilon) + \int_{L-L_\varepsilon} u_j(Q)\, t^*_{ij}(P,Q)ds(Q) \tag{2.4}$$

where Q_ε represent the point on the circular boundary L_ε. The kernels $t^*_{ij}(P,Q)$ and $u^*_{ij}(P,Q)$ are defined in the previous section. The $u_j(Q)$ and $t_j(Q)$ are the boundary displacement and traction at point Q. After taking the limit $\varepsilon \to 0$, we obtain

$$\alpha_{ij}u_j(P) = \int_L t_j(Q)\, u^*_{ij}(P,Q)ds - \int_L u_j(Q)\, t^*_{ij}(P,Q)ds, \tag{2.5}$$

$$\lim_{\varepsilon\to 0} \int_{L_\varepsilon} t_j(Q_\varepsilon)\, u^*_{ij}(P,Q_\varepsilon)ds(Q_\varepsilon) = 0, \tag{2.6}$$

$$\lim_{\varepsilon\to 0} \int_{L_\varepsilon} u_j(Q_\varepsilon)\, t^*_{ij}(P,Q_\varepsilon)ds(Q_\varepsilon) = \alpha_{ij}u_j(P) \tag{2.7}$$

In Eq. (2.5) the integrals are to be understood in the Cauchy principal value sense. The displacement vector at an interior point P is denoted by $u_j(P)$. The value of the α_{ij} for an interior point or a regular boundary point is:

$$\begin{aligned} \alpha_{ij} &= 0 && \text{for } i \neq j \\ \alpha_{ij} &= -\theta_0 A(B + 0.25) && \text{for } i = j \end{aligned} \tag{2.8}$$

---

[1] In the equations of this section the summation convention is used for lower case subscripts.

where $\theta_0 = 2\pi$ for an interior point and $\theta_0 = \pi$ for a point on a smooth boundary. The value of α_{ij} for a sharp corner is:[1]

$$\alpha_{ij} = -(A/4)[\cos(2\beta_0 + 2\theta_0) - \cos(2\beta_0)] \qquad \text{for } i \neq j \tag{2.9}$$

$$\alpha_{ij} = -\{\theta_0 A(B + 0.25) \pm (A/4)[\sin(2\beta_0 + 2\theta_0) - \sin(2\beta_0)]\} \qquad \text{for } i = j$$

where the positive sign holds for j=1 and negative sign for j=2. The angle θ_0 is the internal angle of the notch and β_0 is shown in Fig. 2.

2.3 The Williams' Solutions

2.3.1 Introduction

In the development of the proposed method of this study, extensive use will be made of the displacement field in the neighborhood of an irregular boundary point. Analytical results for determination of the character of the displacement and stress fields are well known [19,20]. A more recent approach by O. K. Aksentian [24], which is based on a three-dimensional elastic analysis of the problem, provides a somewhat more general solution of the problem in the form of asymptotic expressions. A brief description of the Williams' solution for two-dimensional bodies in plane strain will be given here.

The displacement field in the neighborhood of an irregular point in polar coordinates may be written in the form

$$u_\rho = A(\phi)\rho^\lambda$$
$$u_\phi = B(\phi)\rho^\lambda \tag{2.10}$$

[1] The Kelvin auxiliaries are used to pick out only the rigid body displacements at a sharp corner (see Section 3.5).

Solving the differential equations of equilibrium for the functions $A(\phi)$ and $B(\phi)$ gives

$$A(\phi)=(\lambda-3+4\nu)[c_1\cos(\lambda-1)\phi+c_2\sin(\lambda-1)\phi]+c_3\cos(\lambda+1)\phi+c_4\sin(\lambda+1)\phi$$
$$B(\phi)=(\lambda+3-4\nu)[-c_1\sin(\lambda-1)\phi+c_2\cos(\lambda-1)\phi]-c_3\sin(\lambda+1)\phi+c_4\cos(\lambda+1)\phi \quad (2.11)$$

where the c's are arbitrary constants of integration and ν is Poisson's ratio. The corresponding stresses in polar coordinates are:

$$\sigma_{\rho\rho} = P(\phi)\rho^{\lambda-1}$$
$$\sigma_{\phi\phi} = Q(\phi)\rho^{\lambda-1} \quad (2.12)$$
$$\sigma_{\rho\phi} = R(\phi)\rho^{\lambda-1}$$

where

$$P(\phi)=2\mu\lambda\{(\lambda-1)[c_1\cos(\lambda-1)\phi+c_2\sin(\lambda-1)\phi]+c_3\cos(\lambda+1)\phi+c_4\sin(\lambda+1)\phi\}$$
$$Q(\phi)=-2\mu\lambda\{(\lambda+1)[c_1\cos(\lambda-1)\phi+c_2\sin(\lambda-1)\phi]+c_3\cos(\lambda+1)\phi+c_4\sin(\lambda+1)\phi\} \quad (2.13)$$
$$R(\phi)=2\mu\lambda\{(\lambda-1)[-c_1\sin(\lambda-1)\phi+c_2\cos(\lambda-1)\phi]-c_3\sin(\lambda+1)\phi+c_4\cos(\lambda+1)\phi\}$$

and μ is the shear modulus.

The constants c_i must be determined so that displacements and stresses satisfy the imposed boundary conditions. If the body is a wedge, boundary conditions will be given along the sides of the wedge. For example, specifications of two homogeneous tractions boundary conditions along each edge leads to an eigenvalue problem [19,24] with characteristic equation of the form

$$\sin^2\lambda\theta_0=\lambda^2\sin^2\theta_0 \quad (2.14)$$

where θ_0 is the internal angle of the wedge. There are an infinite number of eigenvalues (λ_m,m = 1,2,3,..) which satisfy Eq. (2.14) and lead to an infinite number of eigenfunctions, each of which is determined to within a multiplicative constant.

2.3.2 Series Representation of the Displacement Field

It was shown that there are an infinite number of displacement fields each of which satisfies the homogeneous boundary conditions. In general, the results occur in complex conjugate pairs of solutions, each pair leading to two real solutions. Detailed representation of these fields are given by Barone [18]. For simplicity of the arguments, the eigenfunctions will be considered in the form $\rho^{\lambda}\psi(\phi)$ even if λ is complex.

Any combination of the Williams' solutions is also a solution. That is, the following expressions are possible solutions of the homogeneous problem.

$$
\begin{aligned}
u_\rho &= \sum_m K_m u_{\rho m} \quad ; \quad u_{\rho m} = A_m(\phi)\rho^{\lambda m} \\
u_\phi &= \sum_m K_m u_{\phi m} \quad ; \quad u_{\phi m} = B_m(\phi)\rho^{\lambda m} \\
\sigma_{\rho\rho} &= \sum_m K_m \sigma_{\rho\rho m} \quad ; \quad \sigma_{\rho\rho m} = P_m(\phi)\rho^{\lambda m-1} \\
\sigma_{\phi\phi} &= \sum_m K_m \sigma_{\phi\phi m} \quad ; \quad \sigma_{\phi\phi m} = Q_m(\phi)\rho^{\lambda m-1} \\
\sigma_{\rho\phi} &= \sum_m K_m \sigma_{\rho\phi m} \quad ; \quad \sigma_{\rho\phi m} = R_m(\phi)\rho^{\lambda m-1}
\end{aligned}
\tag{2.15}
$$

In the Barone and Robinson solution techniques [18], the K's serve as generalized displacements. In order to insure that the displacements in Eqs. (2.15) are bounded, the real part of each eigenvalue λ_m must be greater or equal to zero. Such solutions will be termed "proper" Williams' solutions. However, in Eq. (2.14) if λ_m is a solution, then $-\lambda_m$ is also a solution.[1] A solution with the real part of the eigenvalue less than zero will be called an "improper" Williams' solution.[2] As will be seen, these improper solutions are used as auxiliaries for the determination of the generalized displacements. They can be given as

$$
\begin{aligned}
u_\rho^* &= \sum_m K_m^* u_{\rho m}^* \quad ; & u_{\rho m}^* &= A_m^*(\phi)\rho^{\lambda_m^*} \\
u_\phi^* &= \sum_m K_m^* u_{\phi m}^* \quad ; & u_{\phi m}^* &= B_m^*(\phi)\rho^{\lambda_m^*-1} \\
\sigma_{\rho\rho}^* &= \sum_m K_m^* \sigma_{\phi\phi m}^* \quad ; & \sigma_{\rho\rho m}^* &= P_m^*(\phi)\rho^{\lambda_m^*} \\
\sigma_{\phi\phi}^* &= \sum_m K_m^* \sigma_{\phi\phi m}^* \quad ; & \sigma_{\phi\phi m}^* &= Q_m^*(\phi)\rho^{\lambda_m^*-1} \\
\sigma_{\rho\phi}^* &= \sum_m K_m^* \sigma_{\rho\phi m}^* \quad ; & \sigma_{\rho\phi m}^* &= R_m^*(\phi)\rho^{\lambda_m^*-1}
\end{aligned}
\tag{2.16}
$$

The proper Williams' solutions appear to provide a complete set for expanding an arbitrary distribution of self-equilibrated tractions on an artificial circular boundary in a body, having the irregular point as its center. The numerical verification of this has been carried out in several

---

[1] It is shown in Ref. 18 that solution exists for these eigenvalues which satisfy the homogeneous boundary conditions for well-set problems.

[2] Improper Williams' solutions correspond to unbounded strain energy near the singular point.

cases. For example, let us take a disk with a crack such that tip of the crack is at center of the disk (see Fig. 16). For an arbitrary self-equilibrated tractions on the boundary of the disk one can take a large enough number of eigenfunctions in an expansion to reduce the error on the boundary of the disk below any prescribed value. As a numerical example, the disk is loaded by radial tension and Eqs. (2.15) were used for the expansion. Table 1 gives the coefficients of the expansion and Table 2 the computed tractions for points on the boundary. The results will be discussed fully in Chapter 5.

It seems that the circular shape of the boundary is not an unimportant factor in the convergence of the solution, for the results are not satisfactory on some bodies with non-circular boundaries, using say, a collocation method [25]. It is also shown by Barone and Robinson [18] that the displacement field of the irregular point is valid in a small region about the irregular point. One might expand the region by adding to the number of eigenfunctions in the expansion expression and still retain accuracy. However, the region for which the expansion is valid can not include other singular points on the boundary of the body. These are inevitable at any corner or any point where the boundary condition changes suddenly. These observations make it reasonable to limit the area where the Williams' series is used to a fairly small region around its generating singularity.

In general, the proper and improper Williams' solution taken together (the "extended" Williams' solution) will be needed to represent a field in an annulus having two circular boundaries. The analogy with spherical and cylindrical harmonics suggests that singular solutions must be considered when the origin is not part of the body.

2.4 The Solution Technique of Barone and Robinson

The formulation of the boundary integral equations for elastic bodies with irregular boundary points is given by Barone and Robinson [18]. In this method the proper Williams' solution Eqs. (2.15), with K's as unknown generalized displacements are used to represent the displacement field in the vicinity of the irregular boundary point up to so-called transition points. The integral equation for the regular boundary points are then written as described in Section 2.2.3. For irregular boundary points a new kernel was derived which turns out to be the eigenfunctions of the improper Williams' solution Eqs. (2.16). These auxiliary solutions are used to pick out the unknown generalized displacements. However, for the first two K's corresponding to rigid-body displacements the Kelvin auxiliary solutions are used.

Since the improper Williams' solutions are singular at an irregular point, a small circular piece of radius ϵ containing the irregular point is removed from the body before the reciprocal theorem is applied to the actual and auxiliary solution. The reciprocity relation for the body after taking the limit $\epsilon \to 0$ is

$$\sum_{m=3}^{M} -\alpha_{im} K_m + \int_L t^*_{ij}(P,Q)\, u_j(Q)\, ds(Q) = \int_L u^*_{ij}(P,Q)\, t_j(Q)\, ds(Q) \tag{2.17}$$

where in Eq. (2.17) the standard summation convention is used on the lower case subscripts. The $t^*_{ij}(P,Q)$ and $u^*_{ij}(P,Q)$ are tractions and displacements

of the i-th improper Williams' solution. The $t_j(Q)$ and $u_j(Q)$ are the traction and the displacement of the boundary point Q in the j-th coordinate direction and P is the irregular point at which the auxiliary solutions are singular. Here M is the total number of proper Williams' solutions used, including the three rigid-body motions.[1] Furthermore,

$$\alpha_{im} = 0 \qquad \text{for} \qquad i \neq m$$

$$\alpha_{im} = F_{im} \qquad \text{for} \qquad i = m \quad , \quad m \geq 3$$

where F_{im} is given by Eq. (C.5).

As can be seen, the m-th auxiliary solution pick out the m-th generalized displacement and relates it to the far field boundary values. The ordinary integral equations at regular points along with these new ones form a coupled system involving the generalized displacements and other boundary values as unknowns. This leads to a strongly diagonal system of linear algebraic equations which is solved for the unknown values. As mentioned before, the generalized displacements depend on the boundary values at fairly remote points. This appears to contribute to a numerically stable solution. Physically, the generalized displacements must depend on the applied loads in the far field. The fact that this dependence is explicit in the numerical procedure is one advantage of the method.

---

[1] The two translations are "picked out" by Kelvin solutions. The rigid-body rotation is in the set of Williams' solutions.

3. APPROXIMATE DETERMINATION OF STRESSES AND DISPLACEMENTS NEAR A NOTCH WITH A SMALL FILLET

3.1 Introduction

The main objective of this Chapter is to develop an effective numerical scheme for the determination of stresses and displacements at points in a small region containing the fillet (the inner region). This is done by developing a set of solutions for the inner region and tying them to the rest of the body by expanding the solutions in a series with unknown coefficients. This procedure allows us to overcome the poor conditioning of equations which would arise by including the details of the boundary of the small fillet in the same calculation as the boundary of the large body.

As will be seen, the proper Williams' solutions (Eqs. 2.15) corresponding to the sharp notch are sufficient for developing the inner solutions, but the extended (full) Williams' solutions must be used for the series expansion in the so-called annular region.

3.2 The Solution of the Inner and Annular Regions

We take a two-dimensional body with a notch where the root of the notch is curved (see Fig. 3). We shall consider three regions of the body:

i. An inner piece containing the fillet and bounded by a circle centered at the intersection of the two straight edges of the notch (Point P, Fig. 4);

ii. An annular region adjacent to the inner piece having as its outer boundary a circle passing through the transition points; and

iii. The outer body, or the large body, which consists of the rest of the body exterior to the annulus and the annulus itself.

Let us analyze the inner body by the ordinary BIE method as described in Section 2.2.3, for one of the proper Williams' tractions applied to its outer boundary. A field which is determined in this way for the inner body and its boundary is termed a "unit field." Now the displacements as well as the tractions are available on the circle ABC (see Fig. 4) separating the inner body from the annulus. As analytic solution consisting of Williams' solutions is sought in the annulus which matches the displacements and stresses on ABC and thus completely guarantees continuity of displacements and tractions between the inner body and the annulus. In general this will require improper as well as proper Williams' solutions.

To this end, let us expand the computed field for the annular region (ABC-FED, Fig. 5) in a series using the proper and improper Williams' solutions (Eqs. 2.15 and 2.16), which were heuristically justified in Section 2.3. What results is termed a "modified Williams' solution." It is modified by the presence of the fillet, for if the notch were sharp, the result would have been the single proper Williams' solution corresponding to the applied tractions.

It might seem incorrect to use only proper Williams' tractions to find the unit fields and then to match these unit fields to the field on the annulus with both improper and proper solutions. However, as was mentioned in Section 2.3, any traction on the circle can be expanded in proper Williams' tractions. The inclusion of the improper ones in addition

would lead to non-uniqueness of the coefficients. It should be remembered that the series representation in the annulus matches displacements as well as tractions.

The general solution for the annular region is now expressed in a series of the modified Williams' solutions, the unknown coefficients of which are generalized coordinates for the outer body.[1] Once these coefficients are determined, the solution for the inner body is just a linear combination of the previously calculated inner solutions (unit fields).

3.3 Calculation of the Modified Williams' Solution

3.3.1 Series Representation of the Solution

As described earlier, in order to develop a new solution to represent the displacement field of the annular region it is necessary to remove the inner piece from the body. This piece is loaded by tractions corresponding to one of the proper eigenfunctions of the Williams' solution for the sharp notch, say the m-th one. The pointwise displacements are then computed using the ordinary BIE method. This process is carried out for the first M eigenfunctions of the Williams' solution. Therefore, corresponding to each eigenfunction a new field is developed which reflects the

---

[1] At first sight, the procedure would seem to be open to Hadamard's objection to solution of an elliptic problem with Cauchy initial data [29, 32]. It should be remembered, however, that here the coefficients are finally determined by the conditions at the outer boundary of the body. All that has been done is to partition the total extended set of the Williams' solutions in a way convenient for calculation. It is, however, important that the number of proper Williams' solutions (the ones that grow with ρ) be equal to the number of K's. This is automatic in the present procedure.

influence of the fillet on the displacement and stress fields. The results of each solution are now represented in series of the form:

$$
\begin{aligned}
\bar{u}_{\rho m} &= \sum_{j=-N}^{M} \alpha_{mj}\, u_{\rho j} && ; \quad u_{\rho j} = A_j(\phi)\rho^{\lambda_j} \\
\bar{u}_{\phi m} &= \sum_{j=-N}^{M} \alpha_{mj}\, u_{\phi j} && ; \quad u_{\phi j} = B_j(\phi)\rho^{\lambda_j} \\
\bar{\sigma}_{\rho\rho m} &= \sum_{j=-N}^{M} \alpha_{mj}\, \sigma_{\rho\rho j} && ; \quad \sigma_{\rho\rho j} = P_j(\phi)\rho^{\lambda_j - 1} \\
\bar{\sigma}_{\phi\phi m} &= \sum_{j=-N}^{M} \alpha_{mj}\, \sigma_{\phi\phi j} && ; \quad \sigma_{\phi\phi j} = Q_j(\phi)\rho^{\lambda_j - 1} \\
\bar{\sigma}_{\rho\phi m} &= \sum_{j=-N}^{M} \alpha_{mj}\, \sigma_{\rho\phi j} && ; \quad \sigma_{\rho\phi j} = R_j(\phi)\rho^{\lambda_j - 1}, \quad |j| \geq 4
\end{aligned}
\tag{3.1}
$$

where the α_{mj}'s are the unknown coefficients and the expansion functions are the eigenfunctions corresponding to the sharp notch. They include the real as well as the complex eigenfunctions. However, here the bar on the displacements or stresses does not represent the complex conjugate, rather the notation is used to represent the modified Williams' solution for the annular region. The scripts $j<0$ are used to represent the eigenfunctions with the eigenvalues $\lambda_j<0$; $j>0$ means $\lambda_j>0$. The relation $|j|\geq 4$ indicates that the three rigid body motions are excluded in the expansion.

3.3.2 Matching of the Field of the Inner and Annular Regions

Betti's law is used for the determination of the α_{mj}'s, the unknown coefficients of the m-th modified Williams' solution. The objective is to connect the fields of the inner and annular regions smoothly.

Consider a smaller annulus in the body with outer radius $R_2<R_1$ (ABCA'B'C', Fig. 5). This piece is loaded along the boundary ABC with the tractions of the m-th unit field of the inner piece, and along the boundary A'B'C' with the tractions of the series representation of the same solution. The k-th improper Williams' solution is now chosen as an auxiliary.

Betti's law applied to this annular piece results in

$$\Gamma^*_{mk} = \sum_{j=-N}^{M} \alpha_{mj} F^*_{jk} R_2^{\lambda_j + \lambda^*_k}, \tag{3.2}$$

$$\Gamma^*_{mk} = \int_0^{\theta_0} \{[\bar{u}_{\rho m} \sigma^*_{\rho\rho k} + \bar{u}_{\phi m} \sigma^*_{\rho\phi k}] - [\bar{\sigma}_{\rho\rho m} u^*_{\rho k} + \bar{\sigma}_{\rho\phi m} u^*_{\phi k}]\} R_0 d\phi \tag{3.3}$$

where R_0 is the radius the inner piece and the F^*_{mk} is given by Eq. (C.5) in Appendix C. It is also shown in that Appendix that:

$$F^*_{jk} = 0 \quad \text{for} \quad j \neq k \quad \text{or} \quad \lambda^*_k + \lambda_j \neq 0 \tag{3.4}$$

$$F^*_{jk} \neq 0 \quad \text{for} \quad j = k \quad \text{or} \quad \lambda^*_k + \lambda_j = 0 \tag{3.5}$$

Therefore,

$$\alpha_{mj} = \Gamma^{*}_{mj}/F^{*}_{mjj} \qquad -N < j > M\ ,\ |J| \geq 4 \qquad (3.6)$$

As can be seen, the α_{mj}'s are functions of the outer radius R_0, of the inner piece only. A question naturally arises: What should be the size of the inner piece? As mentioned earlier, the inner piece must be large enough to include the whole fillet so that the boundaries in the annular region are straight. This will insure homogeneous boundary conditions for the edges of the annular region. The inner piece should also be small enough that the stress gradients are not much larger than the maximum stress divided by the diameter. This should guarantee accurate results by the ordinary numerical integral equation process.

In this study the radius of the inner piece is taken to be 2.5 times of the radius of the fillet.

3.4 Series Representation of the Displacement Field for the Annulus

Once the unknown coefficients of the modified Williams' solution are determined, we have a solution for the annular region which takes account of the fillet of the inner piece. This solution can be written in series form

$$\begin{aligned}
u_\rho &= \sum_{m=1}^{M} K_m \bar{u}_{\rho m} \\
u_\phi &= \sum_{m=1}^{M} K_m \bar{u}_{\phi m} \\
\sigma_{\rho\rho} &= \sum_{m=1}^{M} K_m \bar{\sigma}_{\rho\rho m} \qquad (3.7) \\
\sigma_{\rho\phi} &= \sum_{m=1}^{M} K_m \bar{\sigma}_{\rho\phi m} \\
\sigma_{\rho\phi} &= \sum_{m=1}^{M} K_m \bar{\sigma}_{\rho\phi m}
\end{aligned}$$

where the K's are generalized displacements and the expansion functions are the modified Williams' solution. Here M is the total number of modified functions for the solution of a specific problem. Note that the first three functions in the series are the displacement field for rigid body motions which are identical for both modified and original Williams' solutions.

3.5 Solution for the Large Body (Loaded Body)

The solution procedure for the large body is essentially the same as was described in Section 2.4 for the solution of the body with a sharp notch using the BIE method. In fact, the same improper Williams' solutions used as auxiliaries for the sharp notch problem also serve as auxiliaries for the large body formed by the removal of the inner piece.[1] These auxiliaries will pick out the unknown generalized displacements given in Eqs. (3.7).

The inner piece may be considered as the counterpart of the piece of radius ϵ centered at the irregular point in the sharp notch problem. This infinitesimally small piece had to be taken out from the body to insure applicability of Betti's law.

For evaluation of integrals along the boundary formed by the removal of the finite inner piece (Fig. 6), an equivalent path of integration can be

---

[1] Here, just as the case of the sharp notch, the Kelvin auxiliaries are used to pick out the rigid body translations.

chosen in order to simplify the computation of the integrals. One simple path of integration consists of the boundary edges of the fictitious sharp notch formed by the extension of the two straight parts of the boundary of the inner piece (see Fig. 7). The following consideration will show that this is an equivalent path of integration. Of course, it should be observed that for the actual body the modified Williams' solutions developed in Section 3.4 are not valid for any point inside the inner body. However, these solutions do satisfy the equilibrium equations and are continuous in the whole region except possibly at the tip of the fictitious notch. Now let us write Betti's work integral for the body ABCDEF of Fig. 7, using as the applied field the modified Williams' solutions and as the auxiliary field the displacements and tractions from a source outside the body. We then have

$$I_{ABC} + I_{CDEFA} = 0 \quad ; \quad I_{ABC} = -I_{CDEFA} \tag{3.8}$$

The boundaries ABC and CDEFA are shown in Fig. 7 and

$$I_{(\cdot)} = \int_{(\cdot)} [t_j u_j^* - u_j t_j^*] ds \tag{3.9}$$

Since some of the solutions are unbounded at point E a small piece with radius ε centered at this point is removed from the body before application of the Betti's law to the larger body. Details of the approximation of the integral expressions and determination of the unknowns are given in Chapter 5.

Once the integral equations are approximated and the final linear equations solved for the unknown generalized displacements K's and other unknown boundary values, the displacements and stresses at any point in the annulus can be determined using Eqs. (3.5). The unknown fields for points in the inner piece can be determined by applying Eq. 2.5 with already computed boundary data.

4. APPROXIMATE DETERMINATION OF STRESSES AND DISPLACEMENTS NEAR THE TIP OF A PARALLEL-SIDED CRACK OF FINITE WIDTH

4.1 Introduction

The main object of this chapter is to develop a numerical scheme for evaluation of stresses and displacements at points close to the tip of a parallel-sided crack of finite but small width. For the sake of brevity, this problem will be called the "wide crack" problem. The main features of the procedure will closely follow those described in Chapter 3 for the notch with a small fillet.

There is, however, one significant difference between the problem of the notch with small fillet and the wide crack problem. The Williams' solutions used in Chapter 3 satisfy the homogeneous boundary conditions on the notch boundary in the annular region. By contrast, here, the Williams' solutions corresponding to the infinitesimal crack give non-zero tractions on the edges of the wide crack. In order to satisfy the homogeneous boundary conditions along the edges of the wide crack, the tractions will be removed by a boundary perturbation scheme. What results will be termed a "perturbed Williams' solution" for the wide crack. These solutions will play the same role in the wide crack problem as the ordinary Williams' solutions played in the problem of the notch with a small fillet.

4.2 Determination of the Perturbed Williams' Solutions

4.2.1 Boundary Conditions for the Perturbation Functions

An ordinary or unperturbed Williams' solution leaves tractions on the actual boundary because the traction boundary conditions were imposed at the center line of the crack, not on the actual crack edges. A perturbation sequence of solutions will be introduced to remove these undesired tractions on the real crack edges. The perturbation functions will be found as the solution of boundary value problems with the center line of the crack as the boundary, in much the same way as the homogeneous boundary tractions for the unperturbed Williams' solutions were imposed on the center line of the crack. It should also be mentioned that the unperturbed Williams' solutions are eigenfunctions (see Section 2.3), with respect to these center-line boundary conditions. Some care must then be exercised in avoiding those perturbation functions which only change the magnitude of the any eigenfunction present in the entire solution. This will keep the perturbations as small as possible.

For clarity and computational ease, symmetric and anti-symmetric cases are treated separately. This will make it possible to deal with just a single boundary. Perturbation of the Williams' solutions will be such that the symmetric or anti-symmetric character of the original solution is preserved.

It is convenient to use the single complex function $\Phi = S_{yy} + iS_{yx}$ to represent two components of the stress field of the perturbed solution. The relations $\Phi(x, \pm d) = 0$ for $x < 0$ express the desired boundary conditions

for the wide crack problem. Let us write the function Φ in the form.

$$\Phi = \sum_{n=0}^{M} \delta^n \Phi_n \tag{4.1}$$

where M is total number of perturbations and Φ_n gives the stresses corresponding to the n-th perturbation. Here δ is a dimensionless measure of width, equal to the half width of the crack d, divided by the radius of the inner body (as in Section 3.2).

Let us express the stresses along the boundary edge $x < 0$ and $y = d$ by expanding Eq. (4.1) in a power series about $y = 0$ for $x < 0$.

$$\begin{aligned}
\Phi_0(x,\delta) &= \Phi_0 + \frac{\delta}{1!}\frac{\partial \Phi_0}{\partial y} + \frac{\delta^2}{2!}\frac{\partial^2 \Phi_0}{\partial y^2} + \frac{\delta^3}{3!}\frac{\partial^3 \Phi_0}{\partial y^3} + \ldots . \\
\delta . \Phi_1(x,\delta) &= \delta . \Phi_1 + \frac{\delta^2}{1!}\frac{\partial \Phi_1}{\partial y} + \frac{\delta^3}{2!}\frac{\partial^2 \Phi_1}{\partial y^2} + \ldots . \\
\delta^2 . \Phi_2(x,\delta) &= \delta^2 . \Phi_2 + \frac{\delta^3}{1!}\frac{\partial \Phi_2}{\partial y} + \ldots .
\end{aligned} \tag{4.2}$$

In Eqs. (4.2) all the functions and their derivatives are evaluated along the half line $y = 0$, $x < 0$. The function Φ_0 corresponds to one of the Williams' solutions for the infinitesimal crack. It is either symmetric or anti-symmetric and is determined so that $\Phi(x,0) = 0$ for $x < 0$. In order to determine the boundary conditons for the subsequent functions in the perturbation, we set

$$\frac{1}{1!}\frac{\partial \Phi_0}{\partial y} + \Phi_1 = 0$$

$$\frac{1}{2!}\frac{\partial^2 \Phi_0}{\partial y^2} + \frac{1}{1!}\frac{\partial \Phi_1}{\partial y} + \Phi_2 = 0$$

$$\frac{1}{3!}\frac{\partial^3 \Phi_0}{\partial y^3} + \frac{1}{2!}\frac{\partial^2 \Phi_1}{\partial y^2} + \frac{\partial \Phi_2}{\partial y} + \Phi_3 = 0 \qquad (4.3)$$

. . . . . .

. . . . . .

$$\frac{1}{n!}\frac{\partial^n \Phi_0}{\partial y^n} + \frac{1}{(n-1)!}\frac{\partial^{n-1} \Phi_1}{\partial y^{n-1}} + \cdots + \frac{\partial \Phi_{n-1}}{\partial y} + \Phi_n = 0$$

By solving for the unknown functions we get

$$\Phi_1 = -\frac{\partial \Phi_0}{\partial y}$$

$$\Phi_2 = -\frac{1}{2!}\frac{\partial^2 \Phi_0}{\partial y^2} - \frac{1}{1!}\frac{\partial \Phi_1}{\partial y}$$

$$\Phi_3 = -\frac{1}{3!}\frac{\partial^3 \Phi_0}{\partial y^3} - \frac{1}{2!}\frac{\partial^2 \Phi_1}{\partial y^2} - \frac{1}{1!}\frac{\partial \Phi_2}{\partial y} \qquad (4.4)$$

. . . . . .

$$\Phi_n = -\frac{1}{n!}\frac{\partial^n \Phi_0}{\partial y^n} \frac{1}{(n-1)!}\frac{\partial^{n-1} \Phi_1}{\partial y^{n-1}} - \cdots - \frac{1}{1!}\frac{\partial \Phi_{n-1}}{\partial y}$$

(all evaluated at $y = 0$, $x < 0$)

The boundary condition for the function ϕ_1 can now be determined using the first equation. After Φ_1, satisfying the given boundary condition is found, the second equation can be used to determine the boundary conditions for the Φ_2, and so on.

It should be noted that the procedure as described defines the boundary conditions for the perturbation functions on the edges of the corresponding infinitesimal crack, rather than on the actual boundary. This will permit determination of the perturbation functions in forms similar to those encountered in Chapter 2 in the solution of the Williams' problem for an infinitesimal crack. The main difference is that for the perturbation functions, solutions will be sought with specified non-zero values on the half line $\phi = \pm\pi$ as opposed to the zero tractions of the Williams' case.

4.2.2 Determination of the Perturbation Functions from their Boundary Conditions

The Φ_n functions (Eq. 4.1) have to be determined subject to the boundary conditions given by Eqs. (4.4). The general form of the function will be taken as

$$\Phi_k = \sum_{J=1}^{N} \beta_{jk}\psi_{jk} \tag{4.5}$$

The β's are unknown coefficients and the ψ's are certain general solution forms (see Appendix E). The general solution forms that will be used include solutions similar to those of Williams' type. However, it turns out that these solutions alone cannot satisfy the boundary conditions given by Eqs. (4.4), requiring the introduction of other solutions.

The difficulty may be seen by the following considerations. A perturbation solution must in general satisfy two real non-homogeneous boundary conditions (Eqs. 4.4), on the line $\phi = \pm\pi$. The first perturbation function, Φ, has boundary tractions varying as ρ^{λ_m-2}. For the infinitesimal crack problem λ_{m-1} is also an eigenvalue if λ_m is. This means that there are tractions varying as ρ^{λ_m-2} in an eigenfunction solution and as a consequence, there is only one non-zero boundary value that can be removed using the single non-eigenfunction solution.[1] Another form of solution is then needed. Considering λ_m as a parameter, the general Williams' form (having no pre-assigned boundary conditions) can be differentiated with respect to the parameter λ_m to obtain a new solution form[2]. The variation of tractions with ρ in this new solution involves a logarithmic term $\rho^{\lambda_m-2}\mathrm{Ln}(\rho)$. Note that two symmetric and two anti-symmetric solutions have arisen, not one of each as was wanted. However, the $\rho^{\lambda_m-2}\mathrm{Ln}(\rho)$ traction must be removed at the same time as the ρ^{λ_m-2}, for these are comparable in magnitude. It turns out that this can be done only if the coefficients of the logarithmic term are in the same proportion as the eigenfunction for λ_m-1 (in the displacement). Thus a single new solution results which can, in fact, remove the ρ^{λ_m-2} traction and introduces no new traction going like $\rho^{\lambda_m-2}\mathrm{Ln}(\rho)$ on the boundary $\phi = \pm\pi$.

---

[1] We have divided the Williams' solutions corresponding to the infinitesimal crack into two groups, one symmetric and the other anti-symmetric. For each case we have two constants of integration (the c's in Eqs. 2.11) in our disposal. Since one of the two independent solutions that can be derived is an eigenfunction, there remains only one non-eigenfunction.

[2] See Appendix B.

In the second perturbation four functions will be needed to remove the tractions going like ρ^{λ_m-3} and $\rho^{\lambda_m-3}\mathrm{Ln}(\rho)$ from the boundary edge $\phi = \pi$. Two of the functions will be similar in form to those used in the first perturbation (with an exponent less by one). The other two functions have to remove the boundary tractions going like $\rho^{\lambda_m-3}\mathrm{Ln}(\rho)$. A second logarithmic solution will also be used; here the coefficients of the logarithmic part will not be taken as an eigenfunction. For the fourth solution form, a second differentiation of the general Williams' form with respect to λ_m is needed. This solution involve terms going like ρ^{λ_m-3}, $\rho^{\lambda_m-3}\mathrm{Ln}(\rho)$ and $\rho^{\lambda_m-3}\mathrm{Ln}^2(\rho)$. Just as in the case of the first perturbation, the coefficients of the last term are taken to be proportional to the eigefunction corresponding to λ_m-2 (in displacement)[1]; the process continues in this fashion. In general for the n-th perturbation, 2n functions will be needed in order to remove the tractions on the boundary going like $\mathrm{Ln}^r(\rho)$, $(r = 0, 1, 2\ldots, n-1)$.

As an example, the solution forms and their participation coefficients for the first perturbation are given in Appendix E.

4.3 Determination of the Modified Perturbed Solutions

Once the perturbed Williams' solutions are determined, a small inner piece of the body surrounding the crack tip (see Fig. 9) is removed from the body. This piece is loaded by the tractions corresponding to one of the perturbed Williams' solutions.[1] The pointwise displacements are then computed using the ordinary BIE method. As in Section 3.3.1 the results

---

[1] This way the term going like $\rho^{\lambda_m-3}\mathrm{Ln}^2(\rho)$ will satisfy homogeneous boundary condition along $\phi = \pi$.

will be called the a unit field. This unit field is then represented in a series of the form.

$$\bar{u}_{\rho m} = \sum_{J=-N}^{M} \alpha_{mj} D_{\rho j}$$

$$\bar{u}_{\phi m} = \sum_{J=-N}^{M} \alpha_{mj} D_{\phi j} \qquad (4.9)$$

$$\bar{\sigma}_{\rho\rho m} = \sum_{J=-N}^{M} \alpha_{mj} S_{\rho\rho j}$$

$$\bar{\sigma}_{\phi\phi m} = \sum_{J=-N}^{M} \alpha_{mj} S_{\phi\phi j}$$

$$\bar{\sigma}_{\rho\phi m} = \sum_{J=-N}^{M} \alpha_{mj} S_{\rho\phi j}, \quad |j| \geq 4$$

where the α_{mj}'s are expansion coefficients, to be determined and the expansion functions are the perturbed Williams' solutions which consist of a series of the Williams' solution forms as well as the Williams' logarithmic functions. The integers M and N are defined as in Section 3.3. What results will be called the m-th "modified perturbed solution" corresponding to the m-th eigenfunction of the infinitesimal crack.

---

[1] To insure the equilibrium of the applied tractions, a solution corresponding to a concentrated force passing through the center of the inner piece and parallel to the crack (a Williams' logarithmic solution with $\lambda = 0$) is added to the perturbed solution.

The process is carried out for the first n perturbed Williams' solutions. As mentioned in Section 3.3.2, these sets of solutions tie the inner piece to the annular region of the large body.

4.4 Evaluation of the Unknown Coefficients of the Modified Perturbed Solutions

Consider an annular region of the body with the inner radius fixed at R_o and the outer radius at R (see Fig. 10) with the two extra regions ABCD and A'B'C'D' added to it to make a full 360° (slit) annulus. This is done for computational ease as will be clear shortly. The annulus is loaded along the boundary L_1 with the traction and displacements of the m-th unit field. The displacement field for the inner boundary of the added regions BD and B'D' will be defined by any smooth extrapolation.[1] Along the outer boundary L_2 and the edges AB and A'B', the annulus is loaded with the tractions and displacements of the modified perturbed solutions of the unit field as given by Eqs. (4.9).

The k-th Williams' solution corresponding to an infinitesimal crack is chosen as an auxiliary. The work integral is now written for the extended annular region as follows.

$$\Gamma^*_{mk} = \sum_{J=-N}^{M} \alpha_{mj} \left[V^*_{jk} - W^*_{jk}(\phi = 0) + W^*_{jk}(\phi = 2\pi)\right], \quad M \geq k \geq -N \tag{4.10}$$

[1] The traction field is just the analytic continuation of the expressions given in Eqs. (2.12) and (B.7).

Taking the limit as $R \to R_0$, we get

$$\Gamma^*_{mk} = \sum_{j=-N}^{M} \alpha_{mj} V^*_{jk} \tag{4.11}$$

where

$$\Gamma^*_{mk} = \int_{\phi=0}^{\phi=2\pi} \{[\bar{u}_{\rho m} \sigma^*_{\rho\rho k} - \bar{u}_{\phi m} \sigma^*_{\rho\phi k}] - [\bar{\sigma}_{\rho\rho m} u^*_{\rho k} + \bar{\sigma}_{\rho\phi m} u^*_{\phi k}]\} R_0 d\phi \ , \tag{4.12}$$

$$V^*_{jk} = \int_{\phi=0}^{\phi=2\pi} \{[D_{\rho j} \sigma^*_{\rho\rho k} + D_{\phi j} \sigma^*_{\rho\phi k}] - [S_{\rho\rho j} u^*_{\rho k} + S_{\rho\phi j} u^*_{\phi k}]\} R_0 d\phi \tag{4.13}$$

The V^*_{jk} can be evaluated using the orthogonality conditions of Appendix D.[1]

The approximation of the integral expressions (4.10) for all k give us M + N-6 simultaneous linear equations with the α's as unknowns. This strongly diagonal system of equations is then solved for the α's. This process is repeated to obtain the series representation of each unit load.

4.5. Over-all Solution for the Loaded Body Having a Wide Crack

Once the unknown coefficients defining the modified perturbed solutions are determined, the general solution form for the annulus

---

[1] The results of Appendix D are applicable only because adding the two pieces ABCD and A'B'C'D' (see Fig. 10) made the limits of integration the same for the inner and outer boundaries of the annulus. This was, of course, the reason for the extension of the annulus as described earlier in this section.

can be represented by Eqs. (3.8) with the K's as unknown generalized displacement.

The solution for the large body formed by the removal of the inner piece is similar to the solution for the case of the notch with a fillet of small radius, given in Section 3.5. However, the method will be modified by splitting the body as described in Appendix A for the body with an infinitesimal crack. As explained in that Appendix, the straightforward ordinary BIE method will fail for the infinitesimal crack. This implies that the equations will be poorly conditioned for the problem of the so-called wide crack in a straightforward computation without splitting the body.

In order to simplify the computation of the integrals along the boundary of the annulus (ABCDE in Fig. 11) an equivalent path of integration is chosen[1] (EFA in the same figure). This path lies inside the corresponding infinitesimal crack region in which the modified perturbed solutions are continuous (except possibly at point E, the tip of the fictitious crack). The path also takes into account the possible jump of the solutions across the half line $\phi = \pi$. Since some of the solutions are singular at point E, a piece of small radius ε centered at E is taken out from the body before application of Betti's law to the large body.

---

[1] Compare Section 3.5.

5. NUMERICAL TREATMENT OF BOUNDARY VALUE PROBLEMS AND SOLUTION OF SOME SAMPLE PROBLEMS

5.1 Numerical Treatment of Boundary Value Problems

5.1.1 Preliminary Remarks

The new boundary integral equation method developed in Chapters 3 and 4 reduces the solution of the problems under consideration to solutions of sets of singular integral equations. These equations must then be approximated and the resulting linear algebraic equations solved simultaneously for the unknown boundary values.

In order to approximate the integral equations, the closed boundary L is divided into N_L segments by N_L nodal points. In the intervals with regular boundary points the tractions and displacements are specified at the nodal points. In the intervals with an irregular boundary point, the proper Williams' solutions (Eqs. 2.15) with unknown generalized displacements represent the boundary values from the irregular point up to the so-called transition points. Similarly, in the fillet and the crack problems discussed in Chapter 3 and 4 the boundary data on the annulus are characterized by the generalized displacements of the extended Williams' solutions (Eq. 3.7).

The general form of the integral equations for regular boundary points is given by Eq. (2.5). The kernels of this equation are the field values of the Kelvin concentrated force solutions. A second type of integral equation, given by Eq. (2.17), is used for the region where the boundary values are represented by either the proper or the extended Williams' solutions. The kernels of this equation are the field values of the improper Williams' solutions.

The general form of the integrals involved can be written as

$$I = \int_L G(s)ds \quad ; \quad G(s) = f(s)\, g(s_0,s) \tag{5.1}$$

where $f(s)$ and $g(s_0,s)$ represent the boundary values and the kernel respectively. The arc length s is measured from the singular point of the kernel with $s = s_0 = 0$.

The evaluation procedure of the integrals along an interval with bounded kernel will be given in Section 5.1.2. Expressions for singular integrals involving Kelvin and Williams' auxiliaries are given in Sections 5.1.2.2 and 5.1.2.3. Finally the estimation of errors is discussed in Section 5.1.3.

5.1.2 Approximation of the Integrals

5.1.2.1 Non-Singular Intervals

As mentioned in the previous section, the boundary is divided into N_L segments with N_L nodal points. The length of the j-th interval is denoted by

$$h_j = s_{j+1} - s_j \tag{5.2}$$

The arc length s_j is measured from the m-th point (point P in Fig. 12), at which the auxiliary solution is unbounded. Let us evaluate the Eq (5.1) in the interval $[s_{j-1}, s_{j+1}]$,

$$I_j = \int_{s_{j-1}}^{s_{j+1}} G(s)ds \quad ; \quad s \notin [s_{m-1}, s_{m+1}] \tag{5.3}$$

Since G(s) is analytic in this interval, it can be expanded in a Taylor series about point J

$$G = G_j + \left(\frac{\partial G}{\partial s}\right)_j s + \frac{1}{2}\left(\frac{\partial^2 G}{\partial s^2}\right) s^2 + O(s^3) \tag{5.4}$$

Now substituting for $\left(\frac{\partial G}{\partial s}\right)_j$ and $\left(\frac{\partial^2 G}{\partial s^2}\right)_j$ their central differences and performing the integration we get

$$I_j = \frac{h_{j-1}}{6}\{[2 + \alpha - \alpha^2](fg)_{j-1} + [\frac{1}{\alpha} + 3 + 3\alpha + \alpha^2](fg)_j + [-\frac{1}{\alpha} + 1 + 2\alpha](fg)_{j+1}\} + O(h_{j-1}^{\beta}) \tag{5.5}$$

where the lower case subscripts indicate the point at which the functions are evaluated. Here $\alpha = \frac{h_j}{h_{j-1}}$ and $\beta = 4$ for $h_j \neq h_{j-1}$, $\beta = 5$ for $h_{j-1} = h_j$. The equation (5.5) reduces to Simpson's rule for $h_{j-1} = h_j$.

For approximation of Eq. (5.1) in the interval adjacent to the singular point where there is a rapid change of the kernel, a method of subdivision is used by first representing the density function as

$$f(s) = a + bs + cs^2 \tag{5.6}$$

and then using Simpson's rule for pairs of adjacent sub-intervals.

In the intervals where the density function is represented by either the proper or the extended Williams' solutions, the kernels are approximated by a p-th order polynomial. Integration of Eq. (5.1) can then be performed directly.

A more detailed discussion of the approximation of the boundary curves and the integrals involving Kelvin concentrated forces was given by Forbes[6].

5.1.2.2 Intervals Containing the Kelvin Singularity

The value of the integrals at the singularity involving the Kelvin field was given in Section 2.2.2. In the interval containing the singularity, the integrals are evaluated by expressing the boundary values and the kernels in power series with respect to the arc length s measured from the singular point. It is assumed that the density functions are expressible in the form given by Eq. (5.6). The Kelvin kernel can be expressed as [1]

$$g(s) = \frac{\alpha_{-1}}{s} + \beta_0 \text{Ln } |s| + \sum_{n=0}^{N} \alpha_n s^n \tag{5.7}$$

it is then possible to substitute f(s) and g(s) into

$$I_m = \int_{h_{m-1}}^{h_{m+1}} f(s)g(s)ds \tag{5.8}$$

which is to be evaluated in the Cauchy principal value sense.

5.1.2.3 Intervals Containing the Williams' Singularity

The singular integrals containing the Williams' solution forms can be evaluated using the orthogonality conditions discussed in Appendix C. As an example let us evaluate a singular integral along the boundary of a sharp notch (see Fig. 12) with the n-th Williams' solution form as the f functions and the m-th improper Williams' solution as the kernel. We get

$$I(\varepsilon) = -F_{mn}\, \varepsilon^{\lambda_n + \lambda_m^*} - H(\phi = 0) \int_{-\varepsilon}^{h} \rho^{\lambda_n + \lambda_m^* - 1}\, d\rho + H(\phi = \theta_0) \int_{\varepsilon}^{h} \rho^{\lambda_n + \lambda_m^* - 1}\, d\rho \tag{5.9}$$

---

[1] See Appendix F.

where the first term is the value of the integral on the circular boundary L_ε (see Fig. 12). This piece is taken out before application of the Betti's law to the whole body. The integrals F_{mn} and H_{mn} are given Eqs. (C.5) and (C.8). Here h is the length of the interval between the irregular point and the transition points. We evaluate $I(\varepsilon)$ by performing the integration and taking the limit $\varepsilon \to 0$. For example, if both solutions have zero traction on the boundary then $H(\phi = 0) = H(\phi = \theta_0) = 0$ and

$$\lim_{\varepsilon \to 0} I(\varepsilon) = \begin{cases} -F_{mn} & \text{for} \quad \lambda_n + \lambda_m^* = 0 \\ 0 & \text{for} \quad \lambda_n + \lambda_m^* \neq 0 \end{cases} \tag{5.10}$$

The other integrals which arise involving the Williams' logarithmic solutions can also be evaluated using the orthogonality conditions of Appendix C.

5.1.3 Errors in the Approximate Solutions

The errors of the numerical solutions of the boundary value problems considered in this study come from the following sources.

i. Discretization error due to replacement of the integrals by finite sums,

ii. Truncation error of the series representing the extended Williams' solutions; and

iii. Round-off errors arising from evaluation of the auxiliary fields and the solution of the final linear equations for the unknowns.

Experience has shown that the errors of the first kind, the discretization errors, are larger than the other two. No attempt will be made to give quantitative estimate of the errors other than comparing the result with exact solution when one is available. In fact, in all the problems solved the final equations are strongly diagonal and the solutions are very stable. The solutions do not change appreciably by changing either the quadrature formula used or the number of the nodal points. The discussion of the results and, in particular, of these points will be given in Section 5.3.

5.1.4 Numerical Implementation of the Proposed Method of the Boundary Value Problems with Tractions Prescribed

We have seen that the solution of a given problem involves two types of integral equations. One of these types is written for the regular boundary points and the other type for the part of the boundary where the solution is represented either by the proper or the extended Williams' solutions. The integral equations are then approximated by a set of linear algebraic equations. The system can be presented in matrix form

$$[A]\{u\} = \{B\} \tag{5.11}$$

where [A] is the coefficient matrix. The entries of the column vector u are all the unknowns of the problem, the generalized displacements, the unknown boundary displacements at regular points and any unknown tractions along the cut (in the case of the crack problem). The vector B is known.

Before solving Eq. (5.11) for the unknowns, the rigid body displacements must be specified, otherwise the matrix [A] is singular. This is done by setting three unknown displacements equal to zero and eliminating their corresponding equations from the Eq. (5.11). These constraints must be such that they prevent rigid body motions without inhibiting any strains due to loading.

Once the unknowns are found, the displacements at any point of the body can be determined using Eq. (2.5). The determination of stresses is discussed in Appendix F. The field inside the annular region can be found using Eq. (3.7). The displacements and stresses at any point inside the inner piece can be determined either by applying the BIE method to the body with known boundary values or by superposing the previously found unit fields in case of boundary points.

5.2 Solution of Some Sample Problems

5.2.1 General Remarks

Results of approximate solution of several problems using the integral equation method developed in this study are given in the next sections of this Chapter. In all problems, Poisson's ratio taken to be $\nu = 0.25$.

Before calculations can be carried out, a scale must be chosen for the eigenfunctions and other extended Williams' solutions. In the problems under consideration, the magnitude of the vector displacement for each extended Williams' solutions is set equal to r_0 at $\theta = 0$ and $\rho = r_0$ where r_0 is shown in each figure of the respective problem.

The results presented in the following sections include the displacements at certain boundary points and stresses at several interior points. Some of the generalized displacements are also tabulated. All the values are given in terms of the applied load σ_0 and r_0.

Except for the second part of the first problem, no exact analytical solution exist for the problems solved in this study. However, the results of the second problem are compared with Barone's [18] solution. For the other problems the result are checked by comparing the solution with a sharp notch or infinitesimal crack. General discussion on the results will be given in Section 5.3.

5.2.2 A Cracked Disk Under Constant Radial Tension (Problem No. 1)

As discussed in Section 2.3 the main object of this example is to demonstrate how an arbitrary self-equilibrated load on the disk can be expanded using proper Williams' solutions. The disk as shown in Fig. 16 is loaded with radial traction of constant magnitude T_ρ = const. Equations (2.15) are used for the expansion of the load. The improper Williams' solutions corresponding to the infinitesimal crack (Eqs. 2.16) are taken as auxiliaries. Applying the reciprocal theorm to the body in which the singular point P is excluded by a disk of small radius ε and then taking the limit $\varepsilon \to 0$, we get

$$\begin{aligned}
&\sum_{\substack{m=4 \\ m\neq j}}^{M} \alpha_m r_0^{\lambda_m+\lambda_j^*} \int_{\phi=0}^{\phi=2\pi} [A_m(\phi)\, P_j^*(\phi) + B_m(\phi)\, R_j^*(\phi)]d\phi \\
&+\alpha_j \int_{\phi=0}^{\phi=2\pi} [P_j(\phi)\, A_j^*(\phi) + R_j(\phi)\, B_j^*(\phi)]d\phi \qquad (5.11) \\
&= r_0^{\lambda_j^*+1} \int_{\phi=0}^{\phi=2\pi} [T_\rho\, A_j^*(\phi) + T_\phi B_j^*(\phi)]d\phi
\end{aligned}$$

where the α's are the unknown expansion coefficients, r_0 is the radius of the of the disk, and M is total number of expansion function including the three rigid body motions (supressed in this problem).

The left hand sides of the integral equations were computed directly and the right hand sides were approximated by Simpson's rule. Table 1 gives the expansion coefficients for three different numbers of eigenfunctions used as terms in the expansion. It can be seen that the values of the coefficients stabilize as the number of functions increases. This is especially true for the first coefficient which is proportional to the stress intensity factor. Table 2 gives the computed value of tractions on the boundary. Convergence to the exact answers depends on the character of the applied tractions. For example, this same problem was solved with loading not uniform but corresponding to the Griffith problem (Fig. 17). The results are given in Tables 1 and 2 along with those of constant radial loading. It can be seen that convergence is much better than for the first loading case. This is expected because the first few Williams' solutions do represent the field in the vicinity of the crack. This will be the case in all actual calculations in real stress concentration problems provided that the circle is reasonably small with the body diameter and greater than the fillet radius.

As was mentioned the first coefficient of the expansions in Table 1 is proportional to the stress intensity factor. For example, for the Griffith load [33] and M = 17 this value is to within 0.04 percent of the exact value.

5.2.3 Uniformly Loaded Plate with a Straight Edge Crack (Problem No. 2)

This problem (Figs. 18 and 19) is solved by "splitting" the body as described in Appendix A. In this method, the crack is extended by an imaginary cut (the dashed line AB in Fig. 18); then the Barone and Robinson solution technique is applied to both pieces of the body simultaneously.

The generalized displacements for the irregular point A (point 1 in Fig. 19) are given in Table 3. The displacements for some boundary points are given in Table 4, along with the values from Barone's [18] solution. As can be seen they are in good agreement. The stress distribution along the cut AB is given in Fig. 20. Although the stresses resulting from the Barone solution are not given here, they also match.

It should be mentioned that the introduction of the Williams' solution at point 25 at the end of the cut (Fig. 19) is for computational ease and reduction of the number of unknowns; this point could have been treated as a regular point.

5.2.4 Uniformly Loaded Plate with a Curved Edge Crack (Problem No. 3)

This problem (see Figs. 21, 22 and 23) is solved to show the versatility of the "splitting" method described in Appendix A. The solution procedure is essentially the same as that for the straight edge crack (Problem No. 2). The generalized displacements for the tip of the crack is given in Table 3 along with those of problem 2 (straight edge crack). Here, the generalized displacements of mode 5 and 6 can be used for the determination of the stress intensity factor for normal and shearing mode.

The displacements for some boundary points are given in Table 5. The distribution of the normal and radial stresses on the cut are given in Fig.

24. Curiously enough, the normal stress distribution on the particular cut chosen is the same as for the straight edge crack[1] and is not a function of the shape and orientation of the cut so long as the crack remains inside the left hand side edge of the body.

5.2.5 Uniformly Loaded Body with a Notch Having a Fillet of Small Radius (Problem No. 4)

This problem as shown in Figs. 25, 26 and 27 is solved using the method described in Chapter 3. The field in the annular region is represented by four real[2] and four complex modified Williams' solutions. Since each complex solution gives two independent real solutions [Ref. 18], we have twelve generalized displacements as unknowns for the annular region.

Table 6 gives the expansion coefficients for the first three modified Williams' solutions using nine proper and three improper eigenfunctions. As described in Section 3.4 these solutions are derived from the expansion of the unit fields. Table 7 gives one component of displacements and tractions of the first two unit fields along with their corresponding values from the modified Williams' solutions. It can be seen from the table they are remarkably close. Table 8 gives the generalized displacements of the modified Williams' solutions for the annular region (see Fig. 4).

The displacements for some boundary points are given in Table 9. The same table gives the results from the solution of the fillet problem using

---

[1] From the geomentry and the loading of the two problems, the integral as well as the first moment of the normal stress along the cut should match for obvious statical reasons, but it is interesting that their distributions also match.

[2] Including two rigid body translations and one rotation.

the ordinary BIE method with 50 boundary points. The stresses and displacements for certain points of the inner piece are given in Table 10. Finally, the stress distribution along the axis of symmetry is given in Fig. 28.

5.2.6 Uniformly Loaded Body with a Wide Edge Crack (Problem No. 5)

A uniformly loaded body with a parallel-sided crack of finite but small width (wide crack) as shown in Figs. 29, 30 and 31 is solved by the method described in Chapter 4.

As discussed in Section 4.2, the first step of the solution is determination of the perturbed Williams' solutions. Tables 11 and 12 give the stresses and displacement of the perturbed and unperturbed Williams' solution for two points at the boundary of the inner piece. As can be seen from the tables, the perturbation alters the magnitude of the displacement field of the unperturbed solution by less than 5 percent (for the first solution). The effect of perturbation on the stress field is less pronounced for points inside the body and away from the boundary. Table 13 gives expansion coefficients for 3 modified perturbed solutions and Table 14 gives one component of traction and displacement to two unit fields and their matching values from the expansion (the modified perturbed solutions). The results are not as good as in the corresponding expansion for the fillet problem (Section 3.3), especially for the traction in x-direction.

The generalized displacements for the annulus are given in Table 15 and displacements for a selection of boundary points are shown in Table 16 and finally the stress distribution along the cut is given in Fig. 32. Comparison of the stress distribution with that of the infinitesimal crack (Fig. 20) shows that except for the region in the vicinity of the crack they almost coincide, which is expected.

5.3 Discussion of the Results

The solutions presented in the previous sections were found to be stable with respect to the number of boundary points and the number of extended Williams' solutions used in the expansion expressions. This is also the general conclusion reached by Barone [18] for the infinitesimal crack and sharp notch problems. This stability reflects the fact that the proposed integral equation approach leads to a strongly diagonal system of linear algebraic equations. The accuracy of the integral approximation is also an important factor. Certain numerical refinements such as subdividing the boundary intervals and including the boundary curvature in the evaluation of the singular integrals played a particularly important part in achieving accurate results.

In the case of the wide crack problem, the expansion of the first unit field is not as accurate as was expected. It seems that for more accurate expansion, several more perturbed Williams' solutions would be needed. However, each additional Williams' solution involves traction that vary rapidly with ϕ on the circular boundary. Stresses at the curved tip of the crack have been found applying such variation to the boundary the stress which arise are very small (less than 0.25 percent of the stress applied to the boundary). In addition, calculation was done applying the difference between the applied traction of the unit field and the traction found from the truncated series. Again no significant stress is found at the roots of the crack. It is therefore unnecessary to refine the expansion for the annulus because the stress pattern does not change where it is of interest.

6. SUMMARY, CONCLUSIONS AND RECOMMENDATIONS FOR FURTHER STUDIES

6.1 Summary

A boundary integral equation technique has been described for the analysis of homogeneous elastic bodies for which small displacement theory is assumed to hold. Major emphasis is placed on treatment of bodies with high stress concentrations. Examples of such problems are bodies with notches having a fillet of small radius and bodies with parallel-sided cracks of small but finite width. The formulation of the solution technique is based on the reciprocal theorem. The boundary integral equation technique uses only the boundary values not the interior field for the solution of a given problem.

The method of solution for the notch with a fillet of small radius is developed from the method introduced by Barone and Robinson [18], for the solution of a sharp notch. At moderate distance from the fillet, the intermediate field in the body is expressible in terms of solutions of Williams' type [16]. Unlike the case of the sharp notch, decaying as well as the growing solutions are present. An inner region containing the fillet is separated out and analyzed under load systems corresponding to the intermediate fields of Williams' type. It is then possible to match the displacements and stresses on the boundary between the inner and intermediate bodies. It is in this way that the details of the boundary configurations of the fillet are reflected in a set of generalized coordinates which characterize

the intermediate field. The remainder of the problem, for the intermediate and the distant field, is solved in essentially the same way as Barone and Robinson [18] handled the sharp notch.

The solution of the wide crack problem is similar except that it is necessary to alter the Williams' solution applicable to the infinitesimal crack. Perturbed Williams' solution are developed for this purpose. Finally, a modified version of the Barone and Robinson solution technique is used to avoid certain numerical difficulties. The modification, incidentally, is very useful for the infinitesimal crack problem as well.

6.2 Conclusions

The general conclusion of this study is that the method developed gives accurate and numerically stable results with rather small computational effort. The solution of the problems is fairly insensitive to the number of extended Williams' solutions used for the region with high concentration of stresses. The solution also is not affected very much by the number of boundary points used. Instead, it depends more on the method of approximation used for the evaluation of the integrals. In particular, a larger interval length can be used provided there is finer subdivision for the evaluation of the integrals. However, no quantitative analysis has been carried out to determine the optimum interval length and minimum computing time.

The methods of this study can be used very effectively for determination of the stress intensity or stress concentration factor. For example, the stress intensity factor for the Griffith problem [33] was computed to within 0.3 per cent of the exact solution using the splitting method of

Appendix A. In this computation there were 30 boundary points with 51 unknowns (taking advantage of the symmetry).

6.3 Recommendations for Further Studies

One important extension of the methods developed in this study would be an analysis in which the material is treated as elastic-plastic rather than elastic. The application of load to bodies with sharp notches will often cause formation of a plastic region limited to the vicinity of the singular point. This is also true for bodies with high stress concentration such as those considered in this study. A method similar to that used for the solution of the fillet problem could be used for this case. The body would be divided into three regions, an inner piece containing the fillet and the entire plastic region, an annular region for which a modified Williams' solution with non-linear coefficients would be developed, and the larger body which is tied to the annulus by the usual integral equation technique.

Another problem that deserves consideration is the solution of piecewise non-homogeneous bodies with a crack. This problem, as well as the problem of non-homogeneous bodies with a V-notch may be solved with no apparent difficulty using the "splitting" technique discussed in Appendix A. The stress and displacement field in the vicinity of the crack tip that would be needed for the solution of the problem by this method, is given by O.K. Aksentian (24).

A third problem of interest is the improvement of the perturbed Williams' solutions developed in Chapter 4 for the solution of the wide crack problem. The perturbation procedure developed seems to have an asymptotic rather than a convergent character. If the opening angle of the inner piece (angle DFB in Fig. 11) is sizable, the accuracy by this

perturbation method may be limited to the degree where it is unsatisfactory. The development of a convergent procedure would be very desirable. Several unsuccessful attempts were made to find a simple procedure in the course of analysis.

Another extension would be to develop a numerical method for evaluating the effect of the plate thickness on the singular stress distribution. Analysis of thick plates shows that the stress state is essentially three-dimensional near the edge [34-36]. However, the fact that this boundary layer disturbance is local suggests the possibility of applying a local correction to the two-dimensional solution.

LIST OF REFERENCES

1. Love, A. E. H., A Treatise on the Mathematical Theory of Elasticity, Fourth Edition, Dover, New York, 1944.

2. Pearson, C. E., Theoretical Elasticity, Harvard University, 1959.

3. Jaswon, M. A., "Integral Equation Methods in Potential Theory. I," Proc. Roy. Soc., Ser. A, 275, 1963.

4. Symm, G. T., "Integral Equation Methods in Potential Theory. II," Proc. Roy. Soc., Ser. A, 275, 1963.

5. Rizzo, F. J., "An Integral Equation Approach to Boundary Value Problems of Classical Elastostatics," Quarterly of Applied Math., Vol. 25, April 1967, pp. 83-95.

6. Forbes, D. J., "Numerical Analysis of Elastic Plates and Shallow Shells by an Integral Equation Method," Civil Engineering Studies, SRS 345, University of Illinois, July, 1969.

7. Cruse, T. A., "Numerical Solutions in Three Dimensional Elastostatics," Computers and Structures, Vol. 5, 1969, pp. 1259-1274.

8. Massonnet, C. E., "Numerical Use of Integral Procedures," Stress Analysis, Edited by D. C. Zienkiewicz and G. S. Holister, Wiley, 1965.

9. Mendelson, A., "Boundary-Integral Methods in Elasticity and Plasticity," NASA TND 7418, 1973.

10. Swedlow, J. L. and Cruse, T. A., "Formulation of Boundary Integral Equations for Three-Dimensional Elasto-Plastic Flow," Computers and Structures, Vol. 7, 1971, pp. 1673-1683.

11. Snyder, M. D. and Cruse, T. A., "Boundary-Integral Equation Analysis of Cracked Anisotropic Plates," International Journal of Fracture, Vol. 11, No. 2, April, 1975.

12. Cruse, T. A., "Boundary-Integral Equation Fracture Mechanics Analaysis," Boundary-Integral Equation Method: Computational Applications in Applied Mechanics, Edited by T. A. Cruse and F. J. Rizzo.

13. Snyder, M. D. and Cruse, T. A., "Crack Tip Stress Intensity Factors in Finite Anisotropic Plates," Air Force Material Laboratory Technical Report AFML-TR-73-209 (1973).

14. Cruse, T. A., "Numerical Evaluation of Elastic Stress Intensity Factors by the boundary Integral Equation Method," in The Surface Crack: Physical Problems and Computational Solutions, American Society of Mechanical Engineers, New York (1972).

15. Bowie, O. L., "Rectangular Tensile Sheet with Symmetric Edge Cracks," Journal of Applied Mechanics, Vol. 31, June, 1964, pp. 208-212.

16. Cross, B., Srawley, J. E., Brown, Jr., W. F., "Stress Intensity Factors for a Single-Edge Notch Tension Specimen by Boundary Collocation of a Stress Function," NASA E-2488, 1964.

17. Creager, M. and Paris, C. P., "Elastic Field Equations for Blunt Crack with Reference to Stress Corrosion Cracking," International Journal of Fracture Mechanics, Vol. 3, No. 4, December 1967, pp. 247-251.

18. Barone, M. R. and Robinson, A. R., "Approximate Determination of Stresses Near Notches and Corners in Elastic Media by an Integral Equation Method," Civil Engineering Studies, SRS 374, March, 1971.

19. Williams, M. L., "Stress Singularities Resulting from Various Boundary Conditions in Angular Corners of Plates in Extension," Journal of Applied Mechanics, Vol. 19, December, 1952, pp. 526-528.

20. Williams, M. L., "The Complex-Variable Approach to Stress Singularities," Journal of Applied Mechanics, Vol. 23, September 1956, pp. 477-478.

21. Besuner, P. M. and Snow, D. W., "Application of the Two-Dimensional Integral Equation Method to Engineering Problems," Boundary-Integral Equation Method: Computational Applications in Applied Mechanics, Edited by T. A. Cruse and F. J. Rizzo, ASME, AMD - Vol. 11, 1975, pp. 101-117.

22. Shaw, R. P., "Boundary Integral Equation Methods Applied to Water Waves," ASME, AMD - Vol. 11, 1975, pp. 7-12.[1]

23. Shippy, D. J., "Application of the Boundary-Integral Equation Method to Transient Phenomena in Solids," ASME, AMD - Vol. 11, 1975, pp. 15-30.[1]

24. Aksentian, O. K., "Singularities of the Stress-Strain State of a Plate in the Neighborhood of an Edge," PMM, Applied Mathematics and Mechanics, Vol. 31, No. 1, August, 1967, pp. 193-202.

25. Wilson, W. K., "Analytic Determination of Stress Intensity Factors for the Manjoine Brittle Fracture Test Specimen," Westinghouse Research Report for AEC, WERL 0029-3, August, 1965.

26. Westergaard, H. M., "Bearing Pressures and Cracks," Trans., A.S.M.E., Ser. A, Vol. 61, 1939.

27. Crandall, S. H., Engineering Analysis, McGraw-Hill Book Company, 1956.

---

[1] In the collection cited in Ref. 21.

28. Morse, P. M. and Feshbach, H., Method of Theoretical Physics, McGraw-Hill Book Company, 1953.

29. Courant, R. and Hilbert, D., Method of Mathematical Physics, Vol. II, Wiley and Sons, 1962.

30. Dettman, J. W., Mathematical Methods in Physics and Engineering, Second Edition, McGraw-Hill Book Company.

31. Budak, B. M. and S. V. Fomin, Multiple Integrals, Field Theory and Series, Translated from Russian by V. M. Volosov, Mir Publisher, Moscow, 1973.

32. Hadamard, J., Lectures on Cauchy's Problem in Linear Partial Differential Equations, New Haven, Yale University Press, 1920.

33. Sneddon, I. N. and Lowengrub, M., Crack Problems in the Classical Theory of Elasticity, John Wiley and Sons, New York, 1969.

34. Hartranft, R. J. and Sih, C. C., "The Use of Eigenfunction Expansions in General Solution of Three-Dimensional Crack Problems," Journal of Applied Math. and Mech., Vol. 19, No. 2, August 1969, pp. 123-138.

35. Hartranft, R. J. and Sih, C. C., "Stress Singularity for a Crack with an Arbitrary Curved Front," Engineering Fracture Mechanics, 1977, Vol. 9, pp. 709-718.

36. Varovich, I. I. and Malkina, O. S., "The State of Stress in a Thick Plate," PMM, Applied Mathematics and Mechanics, Vol. 31, No. 2, 1967, pp. 252-263.

37. Kellogg, O. D., Foundations of Potential Theory, Dover Publication Inc., New York, 1954.

TABLE 1

COEFFICENTS OF EXPANSION FOR PROBLEM 1

Mode No.	Eigen-value λ	(Radial Loading)/α[1]			(Griffith Loading)/α		
		Solution 1 M=9[3]	Solution 2 M=13	Solution 3 M=17	Solution 1 M=9	Solution 2 M=13	Solution 3 M=17
4[2]	0.50	8.4286	8.4137	8.4119	2.6554	2.6530	2.6527
5	1.00	-1.7861	-1.7788	-1.7779	-0.0117	-0.0008	-0.0006
6	1.50	4.6084	4.5942	4.5923	-0.6403	-0.6614	-0.6618
7	2.00	0.3332	0.3337	0.3339	-0.0015	-0.0002	-0.0002
8	2.50	-0.0986	-0.0889	-0.0891	-0.0959	-0.0827	-0.0827
9	3.00	0.0155	0.0382	0.0382	-0.0334	-0.0002	-0.0002
10	3.50	-0.0139	-0.0275	-0.0271	0.0015	-0.0207	-0.0206
11	4.00	-0.0039	0.0100	0.0097	-0.0161	-0.0002	-0.0002
12	4.50	0.0165	-0.0144	-0.0112	0.0337	-0.0069	-0.0064
13-16	5.00-6.00	-	<0.003	<0.003	-	<0.0012	<0.0005
17-20	6.50-8.50	-	-	<0.001	-	-	<0.0002

[1] $\alpha = \sigma_0/E$ where σ_0 is the applied load and E is Young modulus of elasticity.

[2] Modes corresponding to rigid body motions are excluded

[3] M = Number of eigenfunctions used.

TABLE 2

EXACT AND COMPUTED TRACTIONS FOR PROBLEM 1

Loading	B. Points	Tractions/σ_0[1]							
		Exact		Solution 1 with M=9[2]		Solution 2 with M=13		Solution 3 with M=17	
		T_ρ	T_ϕ	T_ρ	T_ϕ	T_ρ	T_ϕ	T_ρ	T_ϕ
Radial Tension	1	1.00	0.0	1.161	0.000	1.046	0.000	1.016	0.000
	4	1.00	0.0	0.992	0.065	1.022	-0.014	1.002	-0.011
	7	1.00	0.0	0.976	-0.092	0.996	0.034	1.010	-0.014
	10	1.00	0.0	1.037	0.086	0.978	-0.015	1.014	-0.002
	13	1.00	0.0	0.956	-0.051	1.007	-0.012	1.010	0.006
Griffith Load	1	0.000	0.000	0.191	0.000	0.015	0.000	0.008	0.000
	4	0.729	0.315	0.704	0.151	0.736	0.305	0.731	0.312
	7	0.877	0.756	0.852	0.858	0.877	0.754	0.878	0.754
	10	1.015	0.994	1.065	0.933	1.011	1.000	1.015	0.994
	13	1.117	1.116	1.053	1.097	1.117	1.115	1.117	1.116

[1] σ_0 is applied traction.

[2] M = number of eigenfunctions used in the expansion.

TABLE 3

GENERALIZED DISPLACEMENTS FOR BOUNDARY POINT 1 (Problems 2 and 3)

Mode No.	Eigenvalues λ	(Generalized Displacements)/α[1]	
		Problem No. 2	Problem No. 3
1[2]	0.00	-47.620	-47.860
2	0.00	0.000	1.387
3	1.00	0.000	1.380
4[3]	1.00	-0.615	-1.473
5	0.50	19.482	16.578
6	0.50	0.000	5.455
7	1.50	1.570	1.648
8	1.50	0.000	0.056
9	2.00	0.000	-0.108
10	2.00	0.039	0.024
11	2.50	0.090	-0.008
12	2.50	0.000	0.015

[1] $\alpha = \frac{\sigma_0}{E}$ where σ_0 is the applied load and E is the modulus of elasticity.

[2] The first three modes correspond to rigid body motions

[3] Simple extension.

TABLE 4

SELECTED BOUNDARY DISPLACEMENTS
FOR PROBLEM 2

Boundary Points	Splitting Method (Appendix A)		Barone's Solution (Ref. 18)	
	U_x/α[1]	U_y/α	U_x/α	U_y/α
1	-47.67	0.00	-47.62	0.00
2	-48.22	-21.11	-48.18	-21.10
3	-48.65	-31.86	-48.60	-31.87
4	-48.85	-41.63	-48.80	-41.60
5	-48.89	-50.85	-48.83	-50.81
6	-48.83	-59.70	-48.76	-59.61
7	-48.83	-68.42	-48.76	-68.30
8	-40.14	-68.42	-40.07	-68.30
10	-23.44	-68.59	-23.43	-68.48
18	-10.97	-11.07	-10.97	-11.06
21	-16.20	3.65	-16.22	3.60
23	-28.10	5.10	-26.76[2]	5.13
25	-35.15	0.00	-35.06	0.00

[1] $\alpha = \frac{\sigma_0}{E} r_0$ where σ_0 is the applied load, E is the modulus of elasticity and r_0 is given in Fig. 19.

[2] There may be a typographical error in Ref 18.

TABLE 5

SOME BOUNDARY DISPLACEMENTS
FOR PROBLEM 3

Boundary Points	U_x/α [1]	U_y/α
1	-47.86	- 1.39
3	-62.00	-32.13
5	-69.31	-42.68
7	-69.96	-52.44
9	-69.80	-71.40
11	-50.78	-71.25
14	-24.14	-70.91
17	1.40	-73.13
20	- 2.28	-34.14
23	-14.53	- 5.13
25	-16.27	4.13
27	-28.89	5.50
29	-30.82	0.60
33	-19.59	- 3.21

$\alpha = \frac{\sigma_0}{E} r_0$ where σ_0 is the applied traction, E is the modulus of elasticity and r_0 is given in Fig. 23.

TABLE 6

EXPANSION COEFFICIENTS FOR CERTAIN MODIFIED WILLIAMS' SOLUTIONS (Problem 4)

Mode No.	Eigenvalue λ	Expansion Coefficients		
		Solution No. 4 $\lambda_0^2 = 0.54448$	Solution No. 5 $\lambda_0 = 1.62926+i0.23125$	Solution No. 6
4[1]	0.54448	0.769900	-0.000666	-0.000431
5	1.62926+i0.23125	-0.708000	0.978813	-0.002572
6		-0.002695	-0.001012	0.997131
7	2.97184+i0.37393	0.343755	0.007658	-0.007378
8		0.185256	0.006627	0.002075
9	4.31038+i0.45549	0.527339	0.020260	0.005180
10		-0.035010	0.001954	0.009042
11	5.64712+i0.54368	0.809780	0.041734	0.037121
12		-0.463231	0.014679	0.006847
13	-0.54448	-0.013316	-0.000374	0.000024
14	-1.62926-i0.23125	-0.000028	-0.000008	0.000004
15		0.000199	0.000082	0.000002

[1]The first three modes corresponding to rigid body motions are not included in the expansion.

[2]λ_0 is corresponding eigenvalue of the applied traction used to develop the unit field.

TABLE 7

COMPARISON OF BOUNDARY DATA OF SELECTED UNIT FIELDS AND THE MODIFIED WILLIAMS' SOLUTIONS (Problem 4)

Boundary Points[1]	Solution No. 4 λ_0[2] = 0.54448				Solution No. 5 λ_0 = 1.62926+i0.23125			
	Traction t_x/t_{x2}[3]		Displ. u_x/α[4]		Traction t_x/t_{x2}		Displ. u_x/α	
	Unit Field	Expansion	Unit Field	Expansion	Unit Field	Expansion	Unit Field	Expansion
2	1.0000	1.0082	0.63523	0.63548	1.0000	1.0054	2.64236	2.64218
4	1.2116	1.2103	0.59563	0.59612	2.9468	2.9355	1.70988	1.71063
6	1.3990	1.4033	0.55616	0.55640	4.6293	4.6330	0.79091	0.79091
8	1.5556	1.5524	0.52125	0.51845	5.9625	5.9800	0.06009	0.06084
10	1.6676	1.6710	0.48374	0.48322	6.8963	6.8888	0.79654	0.79616
12	1.7239	1.7350	0.44910	0.44893	7.4083	7.3890	1.38089	1.38052
14	1.7165	1.7179	0.41260	0.41252	7.5045	7.5075	1.78761	1.78799
18	1.4966	1.4940	0.32539	0.32576	6.5596	6.5583	2.02872	2.02834
24	0.7079	0.7071	0.14479	0.14489	3.0482	3.0520	1.11313	1.11313

[1] See Fig. 26.

[2] λ_0 is the eigenvalue of the traction of the unit field.

[3] t_{x2} is traction at point 2.

[4] $\alpha = \frac{t_{x2}}{E} r_0$ where E is Young modulus of elasticity and r_0 is shown in Fig. 27.

TABLE 8

GENERALIZED DISPLACEMENTS FOR PROBLEM 4

Mode No.	Eignevalue λ[1]	(Generalized Displacements)/α[2]
1	0.00	0.000
2	0.00	6.719
3	1.00	0.000
4	0.54448	6.140
5	1.6293+i0.2313	4.767
6		-0.274
7	2.9718+i0.3739	-2.169
8		-1.169
9	4.3104+i0.4555	-0.338
10		-0.029
11	5.64712+i0.5137	-0.535
12		0.326

[1] λ corresponds to the applied traction of the unit field.

[2] $\alpha = \frac{\sigma_0}{E}$ where σ_0 is the applied load and E is the modulus of elasticity.

TABLE 9

SELECTED BOUNDARY DISPLACEMENTS

FOR PROBLEM 4

Point No.[2]	(Displacements)/α[1]			
	Method of Chapter 3		Ordinary BIE Method	
	U_x	U_y	U_x	U_y
1	0.000	6.331	0.000	6.330
2	-3.015	5.664	-3.018	5.635
3	-4.658	4.897	-4.656	4.887
4	-5.827	4.153	-5.829	4.149
5	-6.578	3.516	-6.581	3.510
9	-8.996	-0.699	-8.999	-0.700
11	-6.533	0.000	-6.533	0.000
13	-4.214	0.778	-4.214	0.776
17	-0.593	4.726	-0.592	4.718
19	0.000	6.025	0.000	6.017

[1] $\alpha = \frac{\sigma_0}{E} r_0$ where σ_0 is the applied load, E is Young modulus of elasticity and r_0 is shown in Fig. 27.

[2] See Fig. 27.

TABLE 10

STRESSES AND DISPLACEMENTS AT SELECTED POINTS

OF THE INNER PIECE (Problem 4)

Point[1] No.	Values from: 1. Method of Chapter 3 2. Ordinary BIE Method				
	Stresses			Displacements	
	σ_{xx}/σ_0[2]	σ_{yy}/σ_0	σ_{xy}/σ_0	U_x/α[3]	U_y/α
1	1.363	1.363	1.363	-1.962	6.002
	1.372	1.374	1.363	-1.960	5.998
10	3.464	0.520	-0.764	-1.123	5.823
	3.459	0.526	-0.772	-1.120	5.820
28	2.842	1.632	0.000	0.000	6.181
	2.842	1.628	0.000	0.000	6.180
64	13.522	0.002	0.000	0.000	6.265
	13.425	0.144	0.000	0.000	6.259
73	7.430	2.219	0.000	0.000	6.331
	7.408	2.206	0.000	0.000	6.330

[1] See Fig. 26.

[2] σ_0 is the applied load.

[3] $\alpha = \frac{\sigma_0}{E} r_0$ where E is modulus of elasticity and r_0 is shown in Fig. 27.

TABLE 11

VALUES OF THE PERTURBED AND UNPERTURBED WILLIAMS' SOLUTIONS AT

POINT 1 (Problem 5, Fig. 30)

Mode No.	Eigenvalue λ[1]	σ_{yx}/σ_{yx4}[2]		σ_{yy}/σ_{yx4}		U_x/α[3]	
		Unperturbed	Perturbed	Unperturbed	Perturbed	Unperturbed	Perturbed
4	0.50	1.000	0.021	0.104	0.046	-8.136	-8.218
5	1.00	0.000	0.000	0.000	0.000	82.15	82.15
6	1.50	0.405	0.004	-0.006	9.833	9.833	9.802
7	2.00	22.081	-0.007	0.000	0.133	-31.921	-28.650
8	2.50	0.731	-0.001	-0.012	0.001	-9.129	-9.171
9	3.00	-26.497	-0.355	-1.656	-0.038	11.800	12.276
10	3.50	-2.293	0.000	-0.048	0.001	3.581	3.768
11	4.00	20.977	0.016	2.650	0.219	4.140	5.651
12	4.50	2.744	0.000	0.172	0.001	1.780	2.008

[1] λ corresponds to the eigenfunctions of the infinitesimal crack (unperturbed solution).

[2] σ_{yx4} is the value of σxy for the eigenfunction number 4.

[3] $\alpha = \frac{\sigma_{xy4}}{E} \cdot r_0$ where E is Young modulus of elasticity and r_0 shown in Fig. 31.

TABLE 12

VALUES OF THE PERTURBED AND UNPERTURBED WILLIAMS' SOLUTION

AT POINT 26 (Problem 5, Fig. 30)

Mode No.	Eigenvalue λ[1]	σ_{xx}/σ_{xx4}		σ_{yy}/σ_{xx4}		U_x/α^3	
		Unperturbed	Perturbed	Unperturbed	Perturbed	Unperturbed	Perturbed
4	0.50	1.000	1.014	1.000	0.988	0.500	0.496
5	1.00	2.530	2.530	0.000	0.000	3.030	3.030
6	1.50	1.195	1.200	1.195	1.205	0.200	0.205
7	2.00	2.024	1.999	0.000	0.009	0.380	0.441
8	2.50	0.800	0.810	0.800	0.791	0.080	0.089
9	3.00	1.214	1.281	0.000	0.015	0.152	0.173
10	3.50	0.448	0.475	0.448	0.422	0.032	0.041
11	4.00	0.648	0.683	0.000	0.027	0.061	0.061
12	4.50	0.230	0.262	0.230	0.198	0.013	0.019

[1] λ corresponds to the eigenfunction of the infinitesimal crack (unperturbed solution).

[2] σ_{xx4} is stress of solution number 4 with $\lambda = 0.50$.

[3] $\alpha = \frac{\sigma_{xx4}}{E} r_0$ where E is Young modulus of elasticity and r_0 shown in Fig. 27.

TABLE 13

COEFFICIENTS OF EXPANSION FOR SELECTED MODIFIED PERTURBED SOLUTIONS (Problem 5)

Mode No.	Eigenvalues λ[1]	Coeff. of Expansion		
		λ = 0.5	λ = 1.50	λ = 2.00
4	0.050	1.06473	-0.02285	-0.01272
5	1.00	0.04392	-0.00507	-0.00960
6	1.50	-0.13221	1.04189	0.02557
7	2.00	0.01062	-0.01259	1.00871
8	2.50	0.04513	0.01923	-0.01630
9	3.00	-0.03285	-0.00215	0.00092
10	3.50	0.04673	-0.00964	0.02006
11	4.00	-0.01040	0.01021	-0.02406
12	4.50	-0.03833	-0.00669	0.01315
13[2]	0.00	-0.00039	0.00004	0.00123
14	-0.50	-0.00715	0.00158	0.00231
15	-1.00	0.00122	0.00000	-0.00019
16	-1.50	-0.00086	-0.00001	-0.00008

[1] λ corresponds to eigenfunctions of infinitesimal crack.

[2] This is the concentrated force solution which is used to satisfy the equilibrium in x-direction.

TABLE 14

COMPARISON OF BOUNDARY DATA OF SELECTED UNIT FIELDS

AND MODIFIED PERTURBED SOLUTIONS (Problem 5)

Boundary Points[1]	Solution No. 4 $\lambda_0^2 = 0.50$				Solution No. 6 $\lambda_0 = 1.50$			
	Traction t_y/t_{y3}		Displ. U_x/α		Traction t_y/t_{y3}		Displ. Uy/α^4	
	Unit Field	Expansion	Unit Field	Expansion	Unit Field	Expansion	Unit Field	Expansion
3	1.0000	1.071	18.859	18.887	1.000	1.012	18.322	18.308
5	2.825	2.811	17.502	17.537	2.954	2.941	15.738	15.734
7	5.256	5.121	15.643	15.634	5.460	5.451	12.246	12.261
9	7.963	7.886	13.372	13.349	8.211	8.210	8.233	8.257
11	10.504	10.586	10.976	10.904	10.791	10.799	4.141	4.147
13	12.427	12.581	8.622	8.554	12.794	12.796	0.421	0.424
15	13.388	13.463	6.467	6.456	13.859	13.827	2.525	2.533
17	13.448	13.455	5.502	5.525	13.959	13.950	3.614	3.633
19	12.695	12.541	3.899	3.899	13.216	13.235	4.913	4.914

[1] See Fig. 30.

[2] λ_0 is the eigenvalue of the corresponding infinitesimal crack.

[3] t_{y3} is traction at boundary point 3.

[4] $\alpha = \frac{t_{y3}}{E} r_0$ where E is modulus of elasticity and r_0 is shown in Fig. 31.

TABLE 15

GENERALIZED DISPLACEMENTS FOR PROBLEM 5

Mode No.	λ[1]	(Generalized Displ.)/α[2]
1	0.00	0.000
2	0.00	-47.420
3	1.00	0.000
4	0.50	-18.167
5	1.00	0.041
6	1.50	-0.753
7	2.00	0.109
8	2.50	0.703
9	3.00	-0.308
10	3.50	0.422
11	4.00	-0.276
12	4.50	-0.281

[1] λ corresponds to the tractions used for the development of the unit field.

[2] $\alpha = \frac{\sigma_0}{E}$ where σ_0 is the applied load and E modulus of elasticity.

TABLE 16

SELECTED BOUNDARY DISPLACEMENTS FOR PROBLEM 5

Boundary Points	(Displacements)/α[1]	
	U_x	U_y
1	-47.42	0.00
2	-47.97	-21.32
3	-49.03	-32.29
4	-49.30	-42.28
5	-49.38	-51.64
6	-49.29	-60.69'
7	-49.29	-69.52
8	-40.46	-69.52
10	-23.88	-69.70
18	-11.19	-11.27
21	-16.52	3.68
23	-28.57	5.06
25	-35.69	0.00

1 $\alpha = \frac{\sigma_0}{E} r0$ where σ_0 is the applied traction, E is the Young modulus of elasticity and r_0 is shown in Fig. 31.

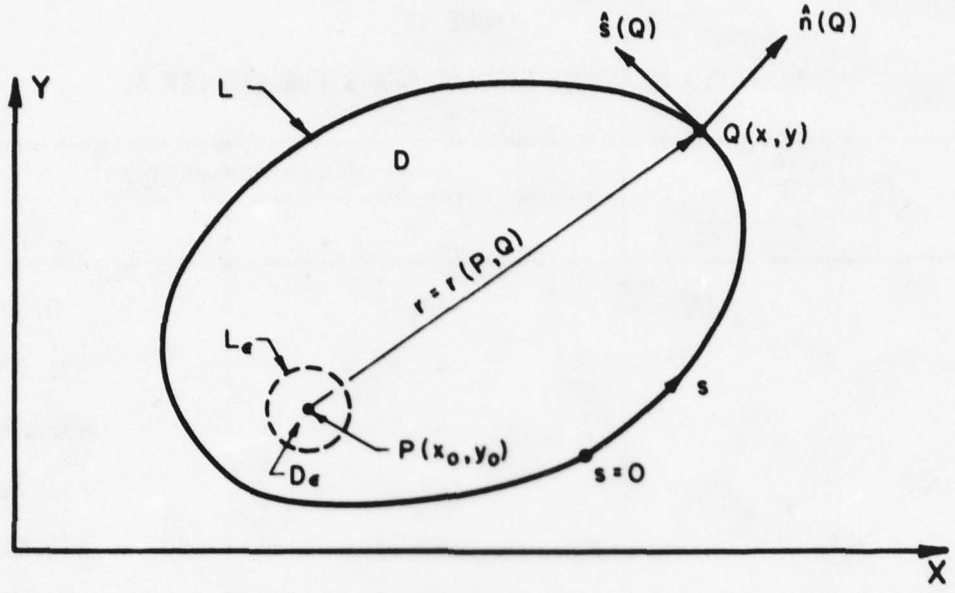

FIG. 1. RECTANGULAR COORDINATE SYSTEM

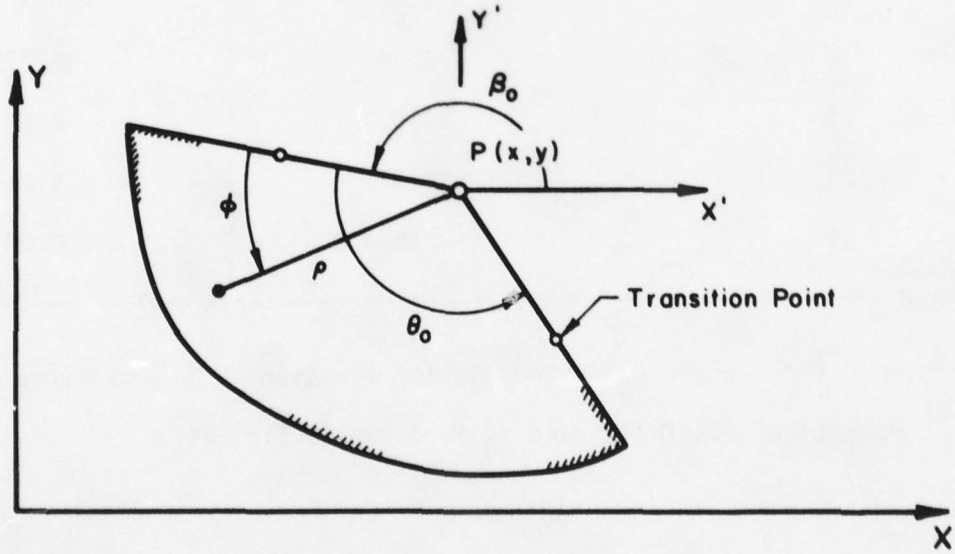

FIG. 2. LOCAL COORDINATE SYSTEM AT A CORNER

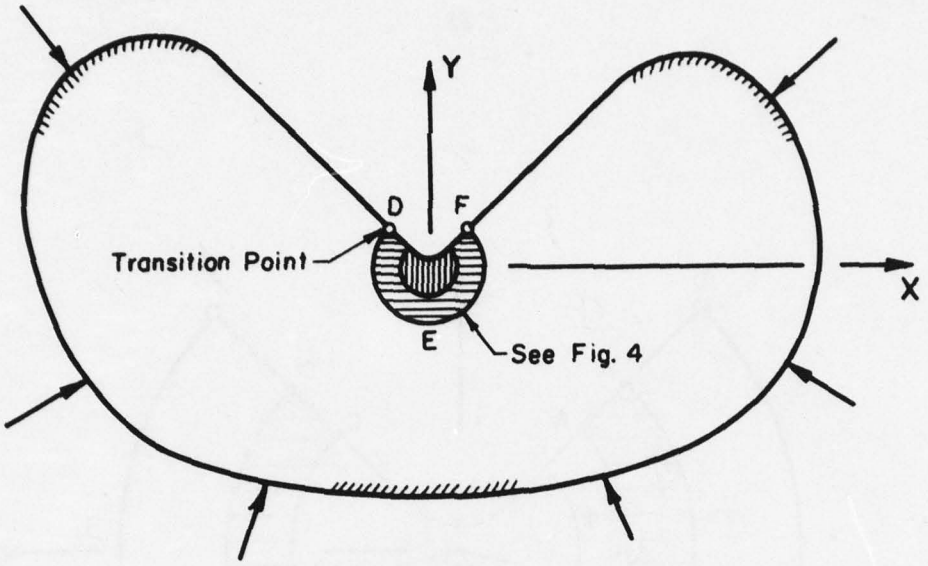

FIG. 3. A BODY WITH A NOTCH HAVING A FILLET OF SMALL RADIUS

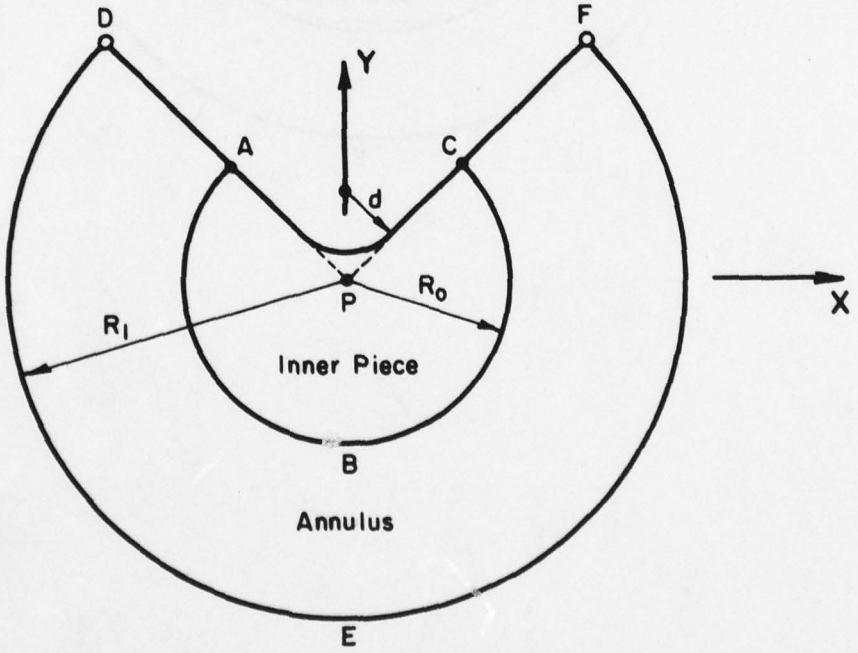

FIG. 4. DETAIL OF THE FILLET REGION

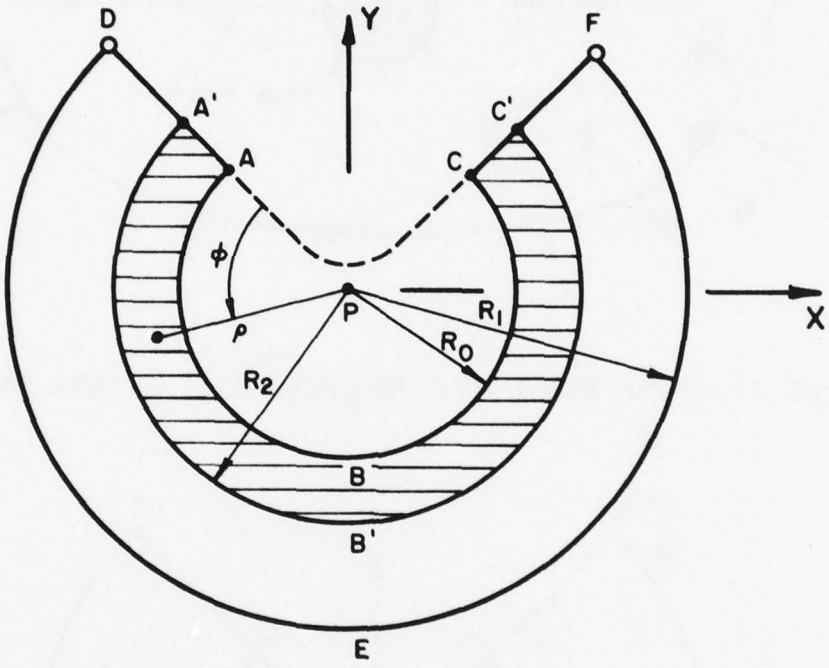

FIG. 5. AN ANNULAR SUB-REGION OF THE ANNULUS

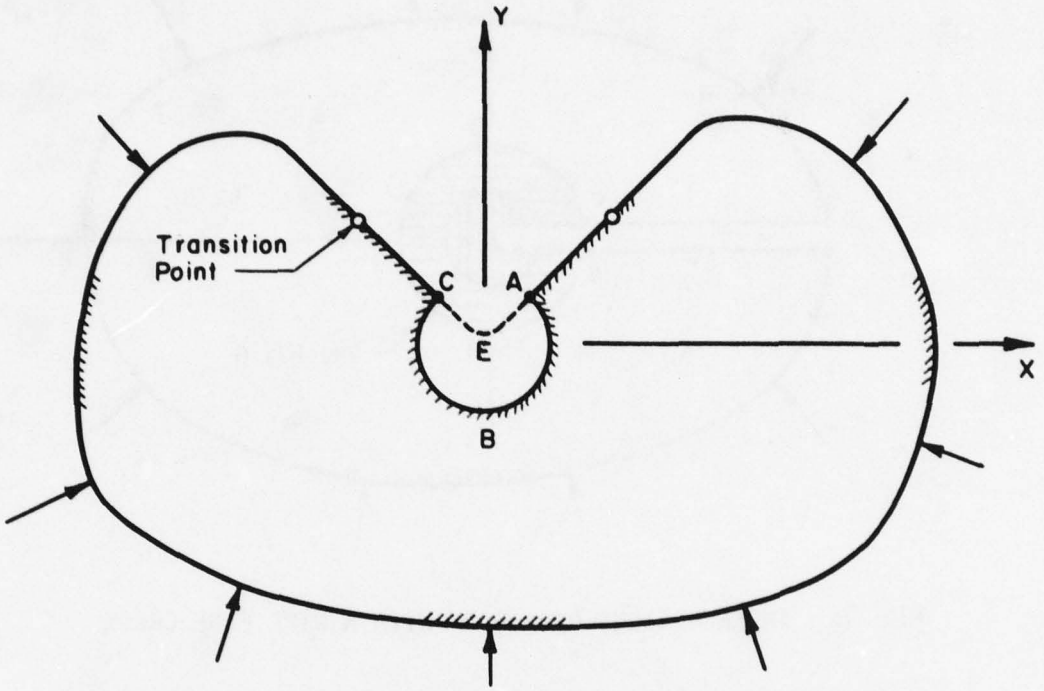

FIG. 6. BODY FORMED BY THE REMOVAL OF THE INNER PIECE

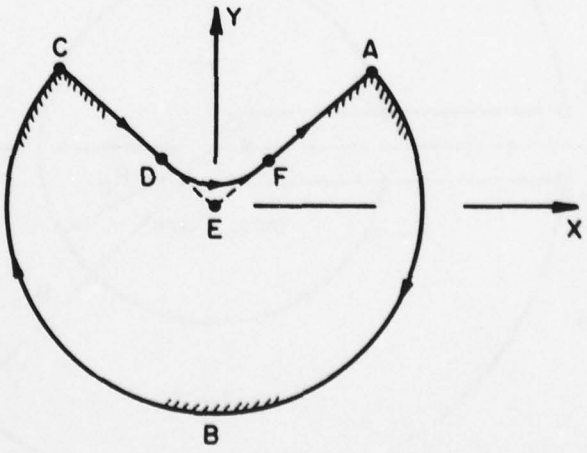

FIG. 7. AN EQUIVALENT PATH OF INTEGRATION FOR THE BOUNDARY OF THE INNER PIECE

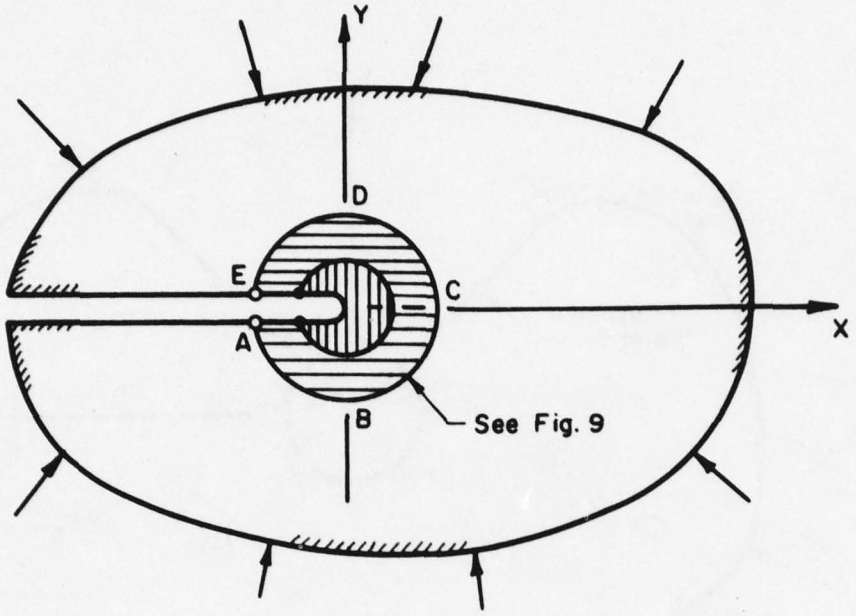

FIG. 8. THREE REGIONS OF A BODY WITH A WIDE EDGE CRACK

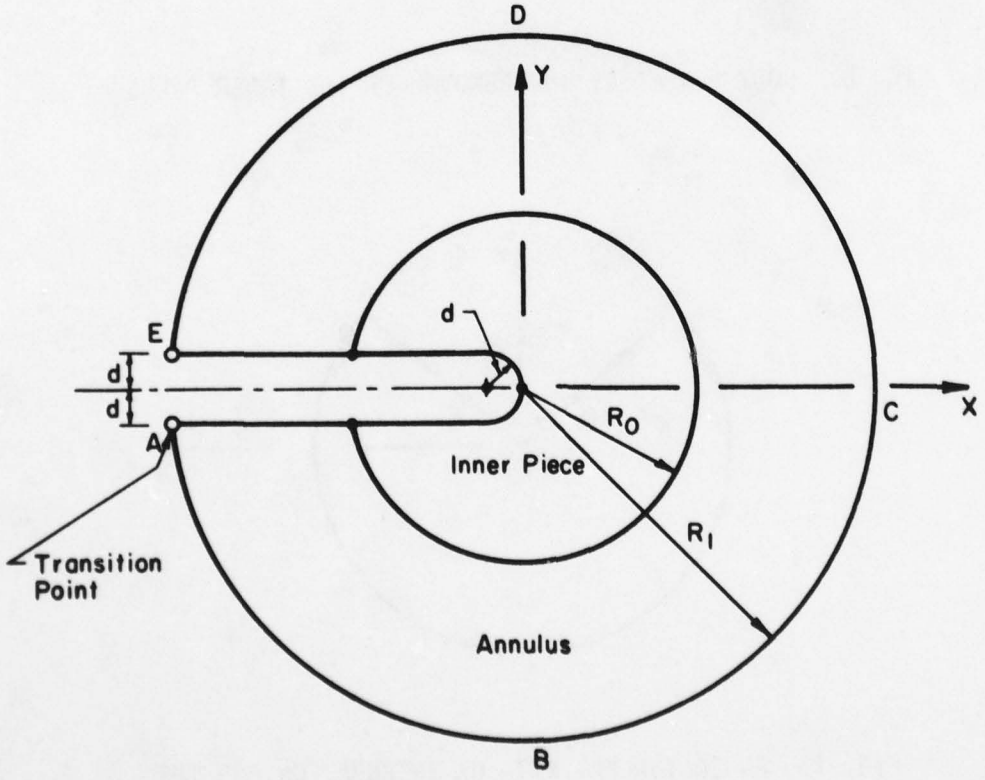

FIG. 9. DETAIL OF THE INNER PIECE AND THE ANNULUS OF THE WIDE CRACK

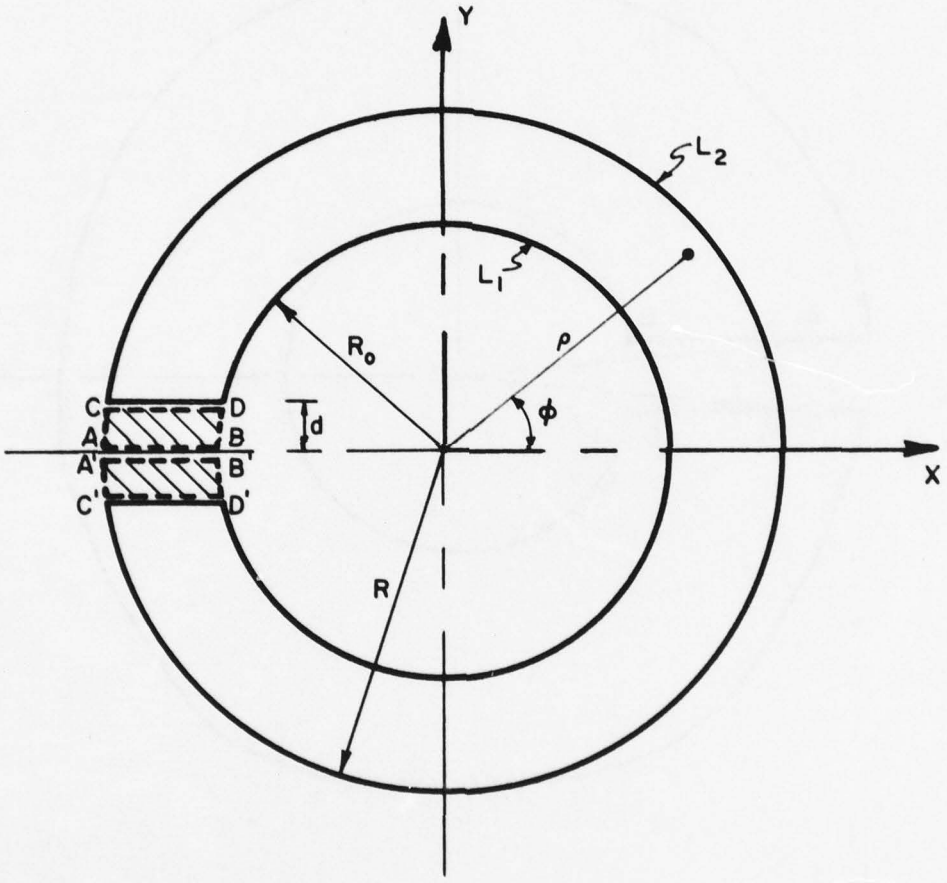

FIG. 10. AN ANNULAR SUB-REGION FOR A BODY WITH A WIDE CRACK

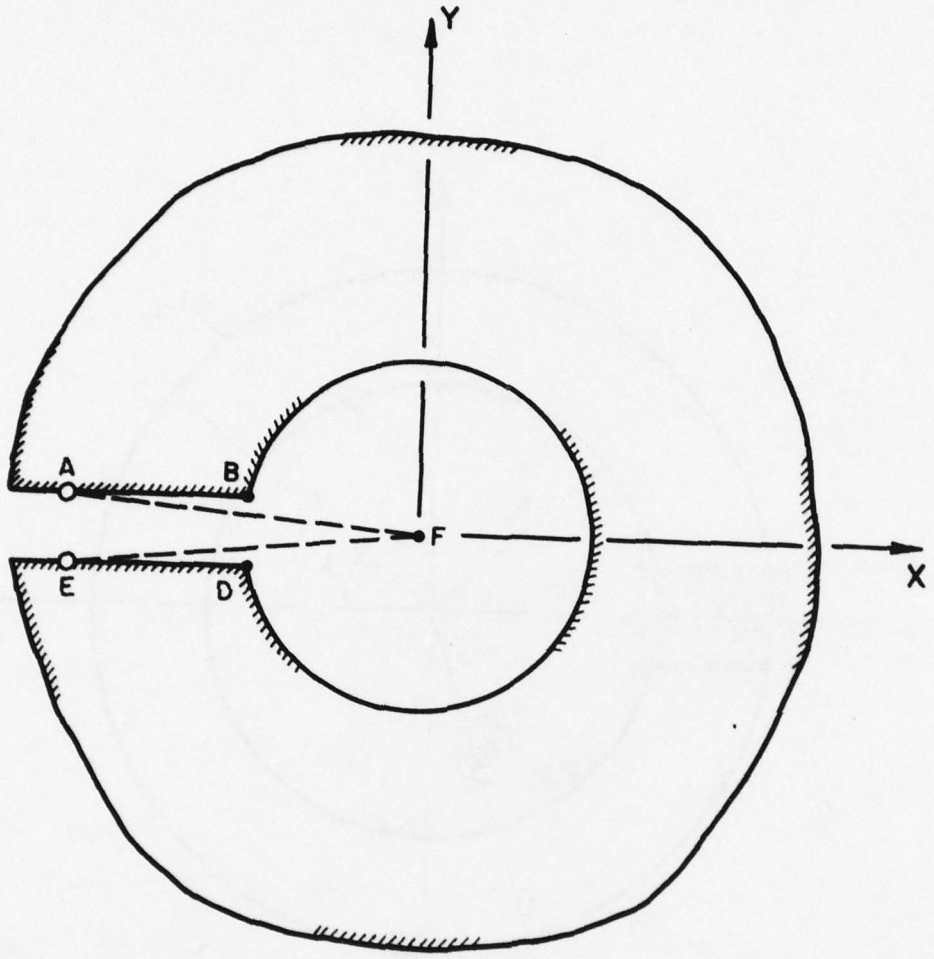

FIG. 11. AN EQUIVALENT PATH OF INTEGRATION FOR THE INNER PIECE OF THE WIDE CRACK PROBLEM

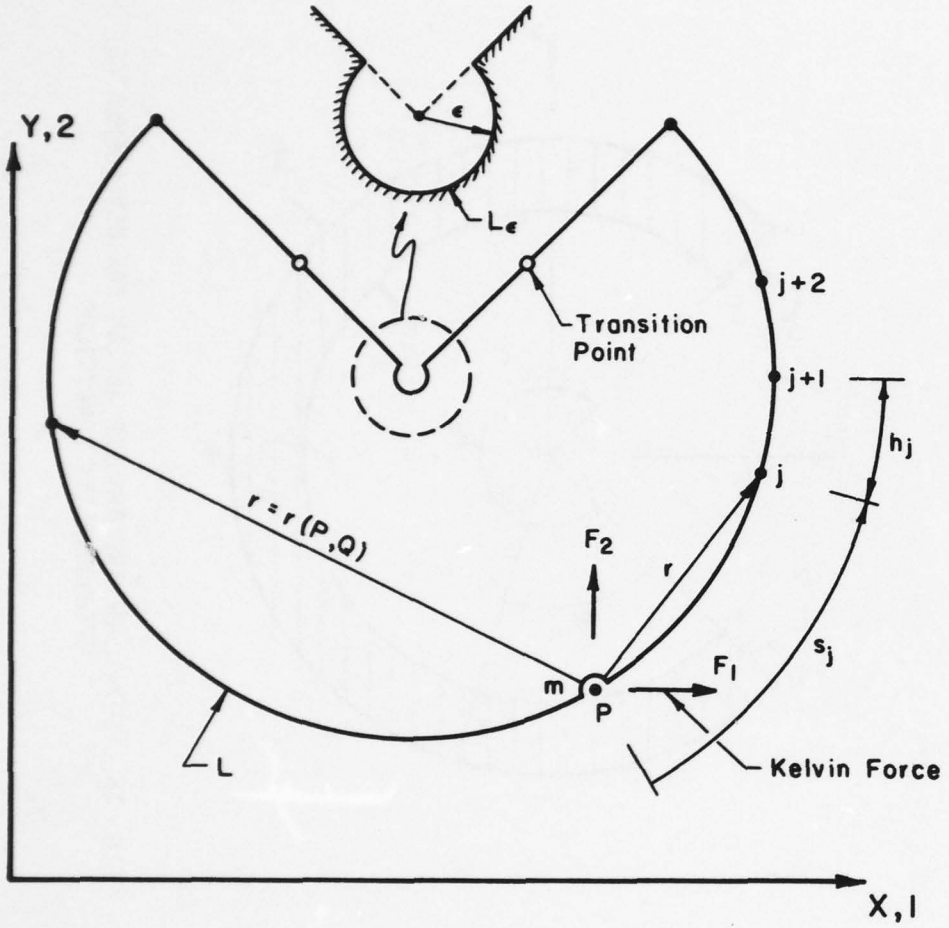

FIG. 12. DETAIL OF THE BOUNDARY CURVE

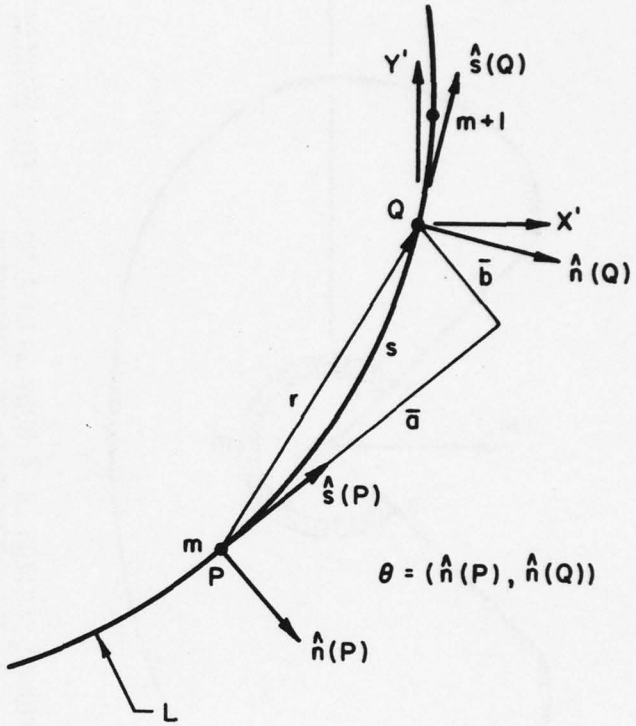

FIG. 13. A SEGMENT OF THE BOUNDARY CURVE

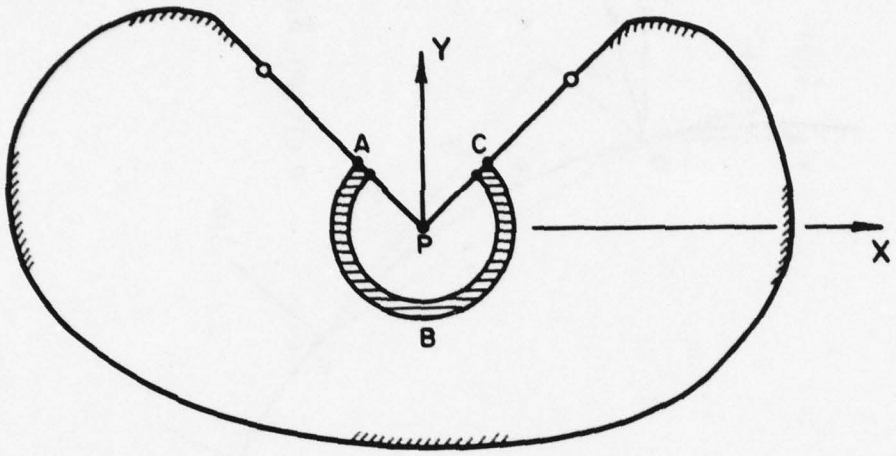

FIG. 14. AN ANNULAR SECTION OF A BODY WITH A NOTCH FOR DEVELOPMENT OF THE ORTHOGONALITY CONDITIONS

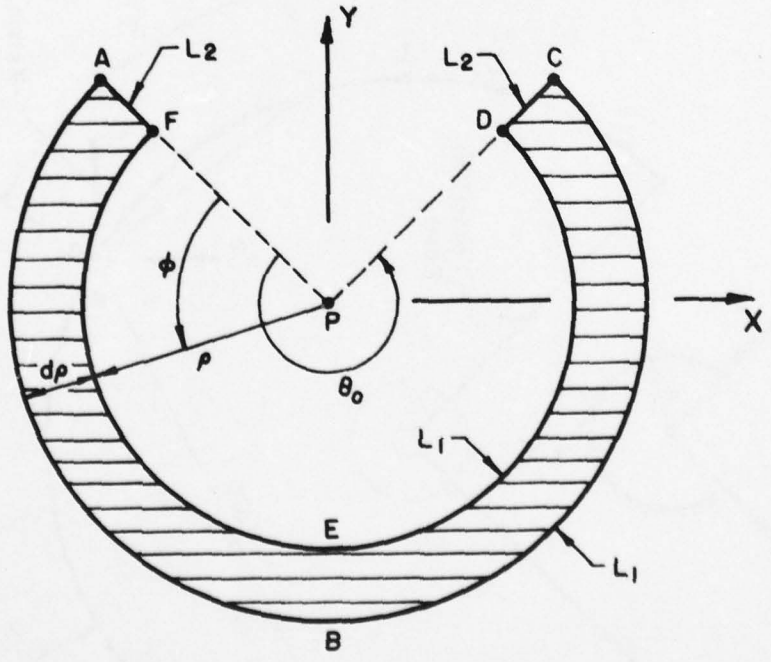

FIG. 15. DETAIL OF THE ANNULAR REGION FOR DEVELOPMENT OF ORTHOGONALITY CONDITIONS

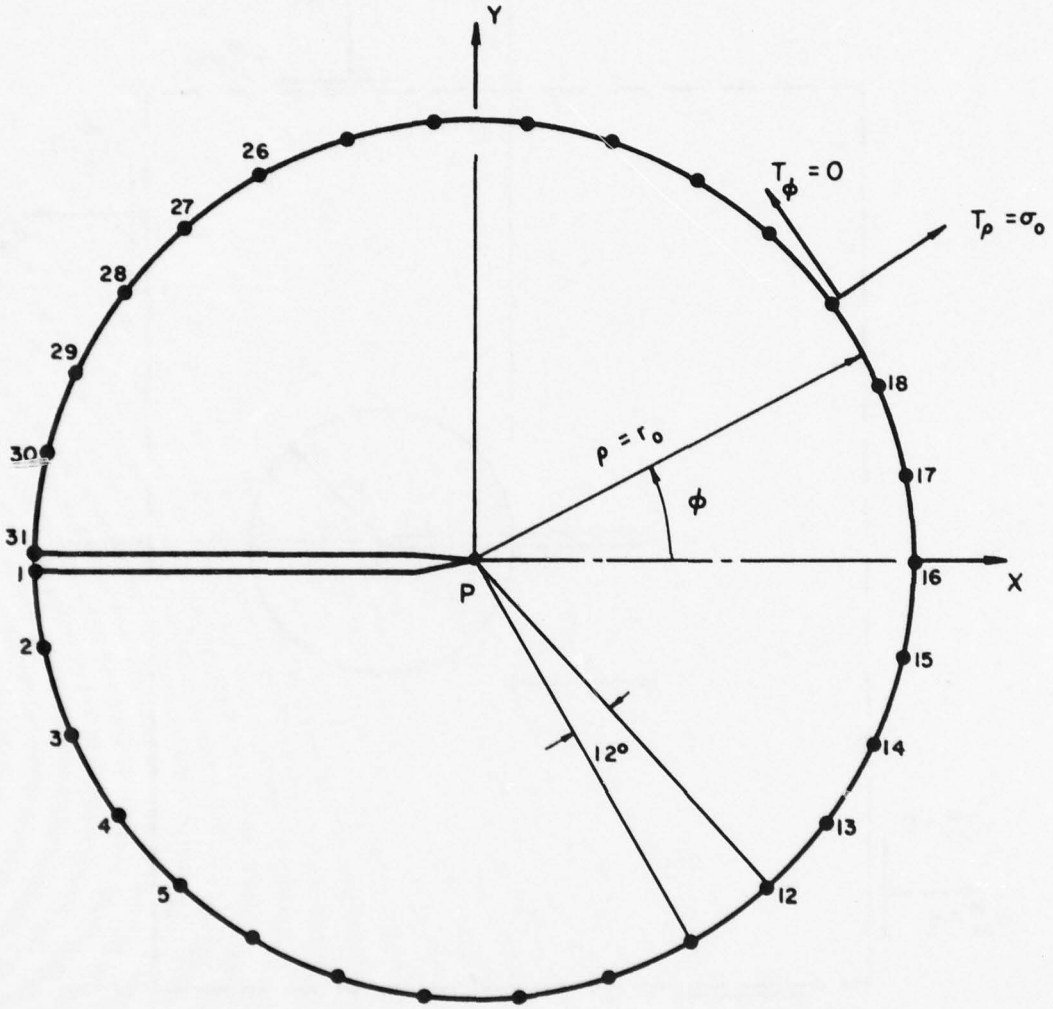

FIG. 16. A CRACKED DISK UNDER CONSTANT RADIAL TENSION (Problem 1)

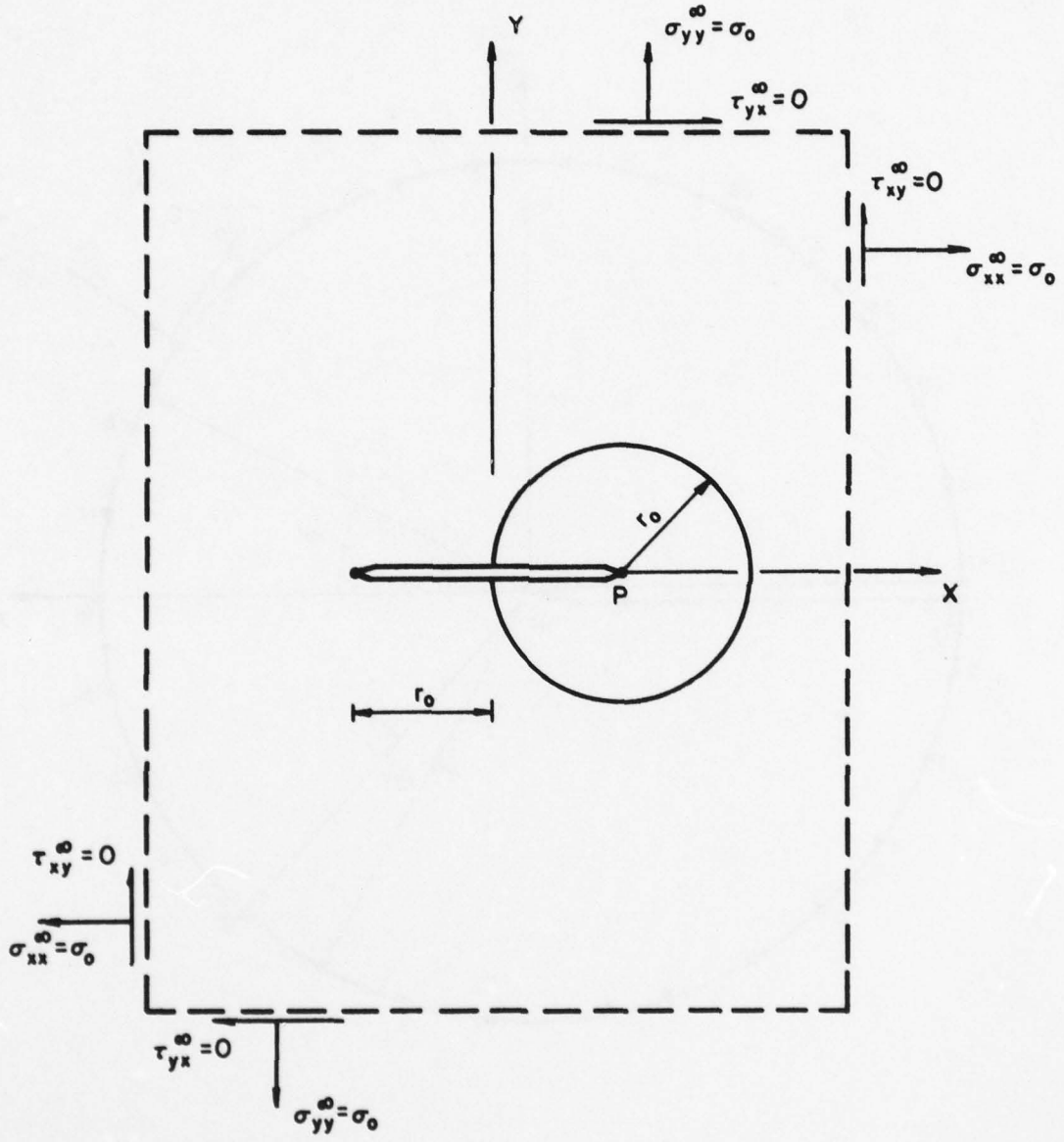

FIG. 17. PROBLEM 1 EMBEDDED IN THE GRIFFITH CONFIGURATION

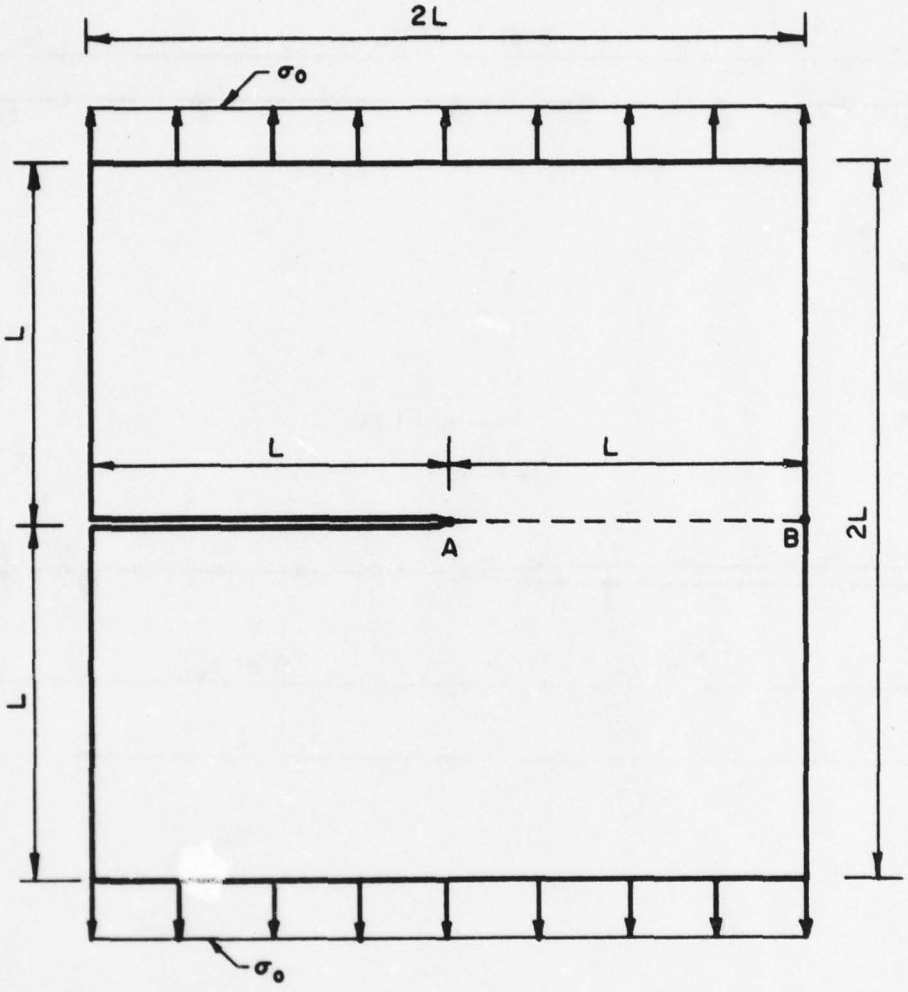

FIG. 18. A UNIFORMLY LOADED PLATE WITH A STRAIGHT EDGE CRACK
(Problem 2)

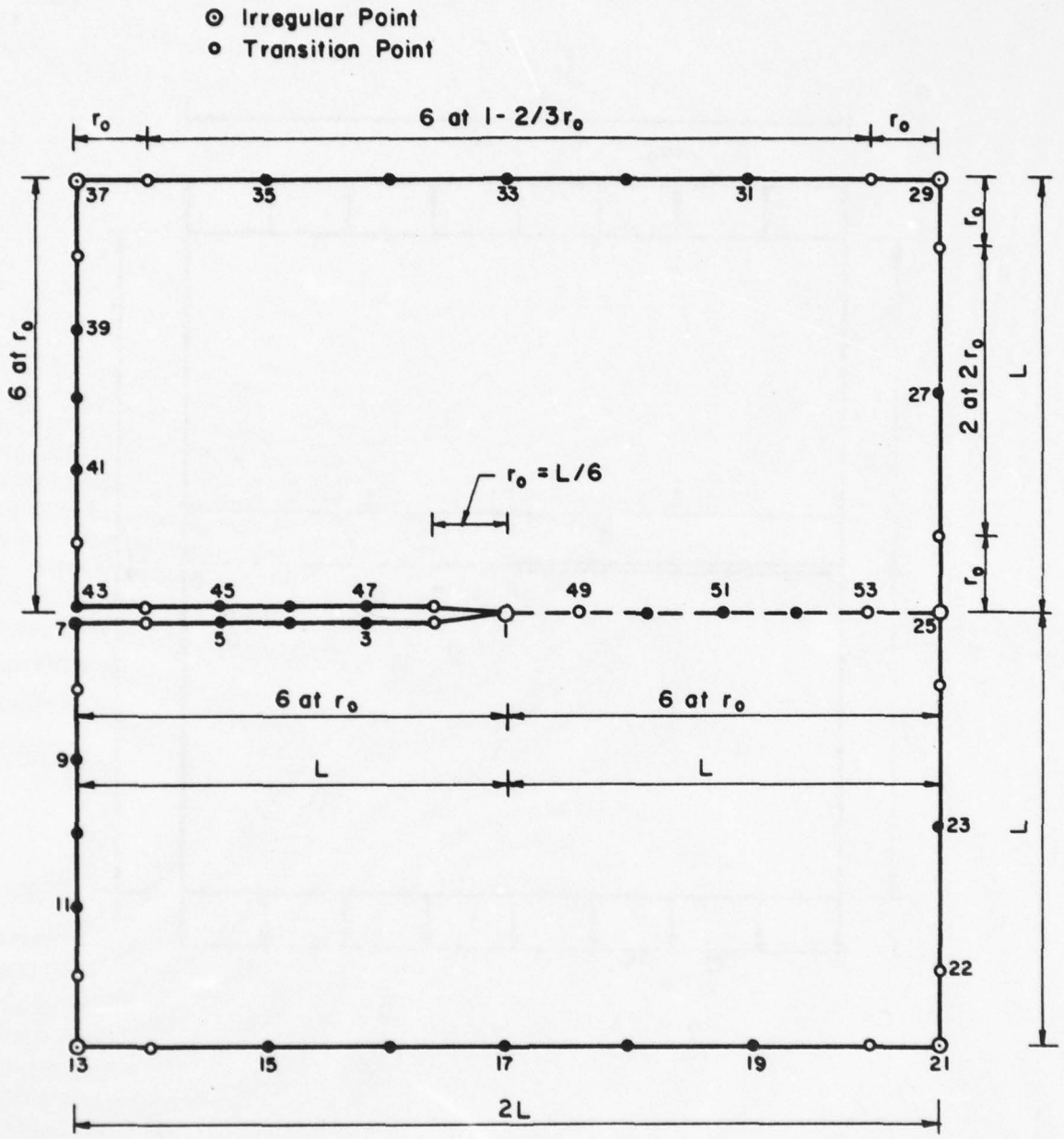

FIG. 19. DATA FOR PROBLEM 2

AD-A069 113 ILLINOIS UNIV AT URBANA-CHAMPAIGN DEPT OF CIVIL ENGIN--ETC F/G 13/13
BOUNDARY INTEGRAL EQUATION SOLUTION OF PLANE ELASTICITY PROBLEM--ETC(U)
APR 79 H NIKOOYEH, A R ROBINSON N00014-75-C-0164

UNCLASSIFIED UILU-ENG-79-2005 NL

2 OF 2
AD A069113

END
DATE FILMED
6-79
DDC

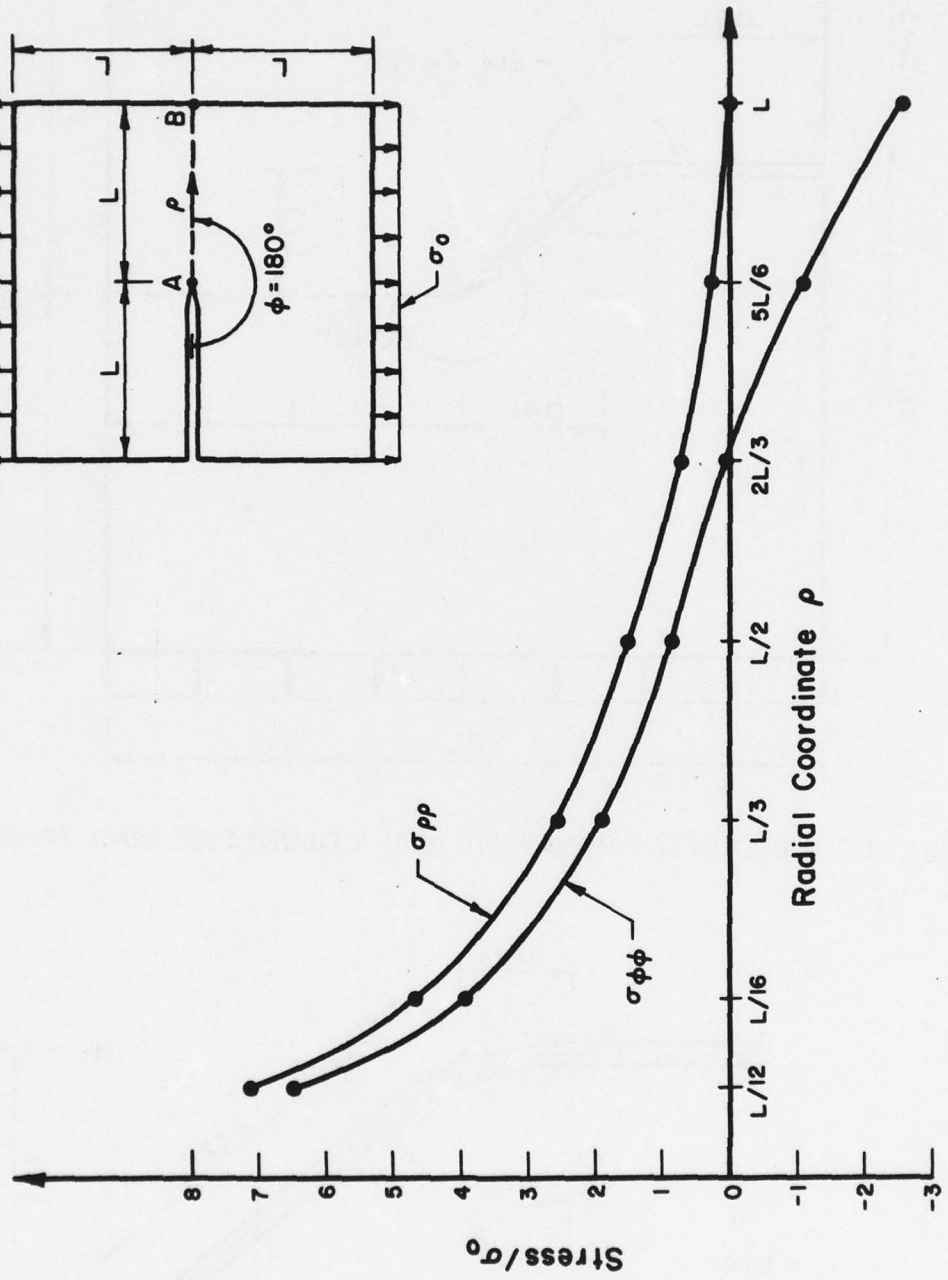

FIG. 20. COMPUTED STRESSES FOR SECTION AB (Problem 2)

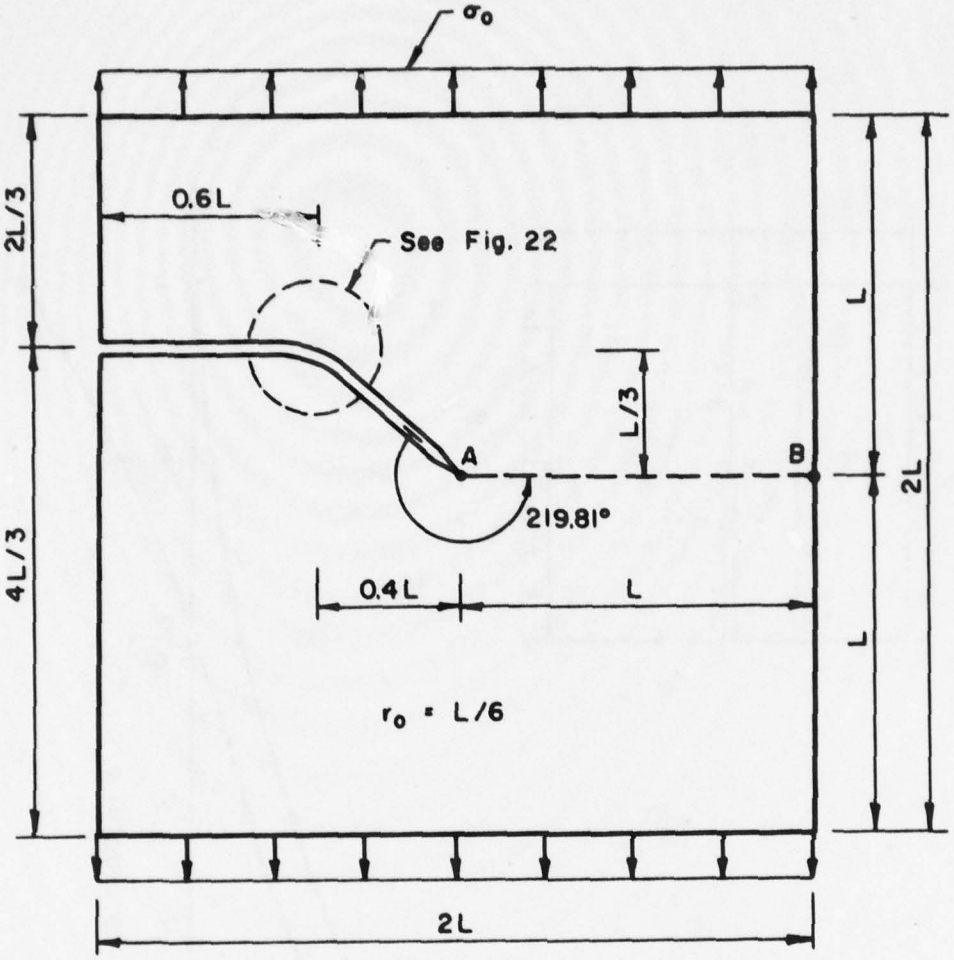

FIG. 21. A UNIFORMLY LOADED PLATE WITH A CURVED EDGE CRACK (Problem 3)

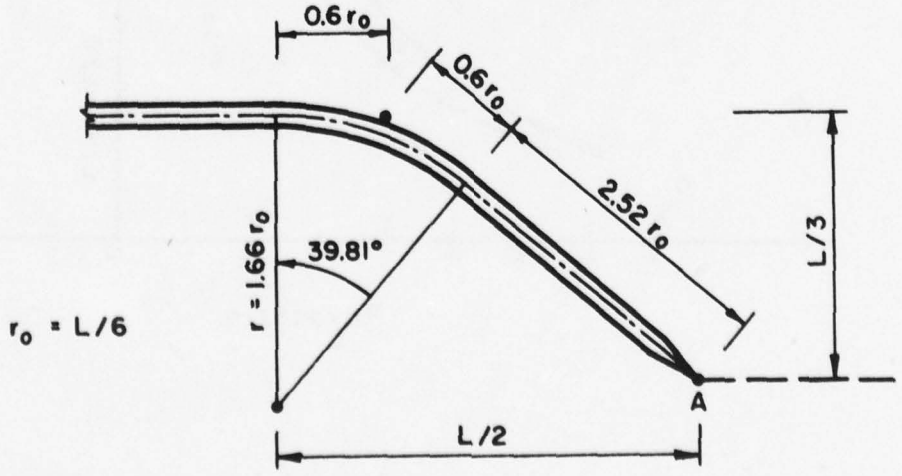

FIG. 22. DETAIL OF THE CURVED PART OF THE CRACK (Problem 3)

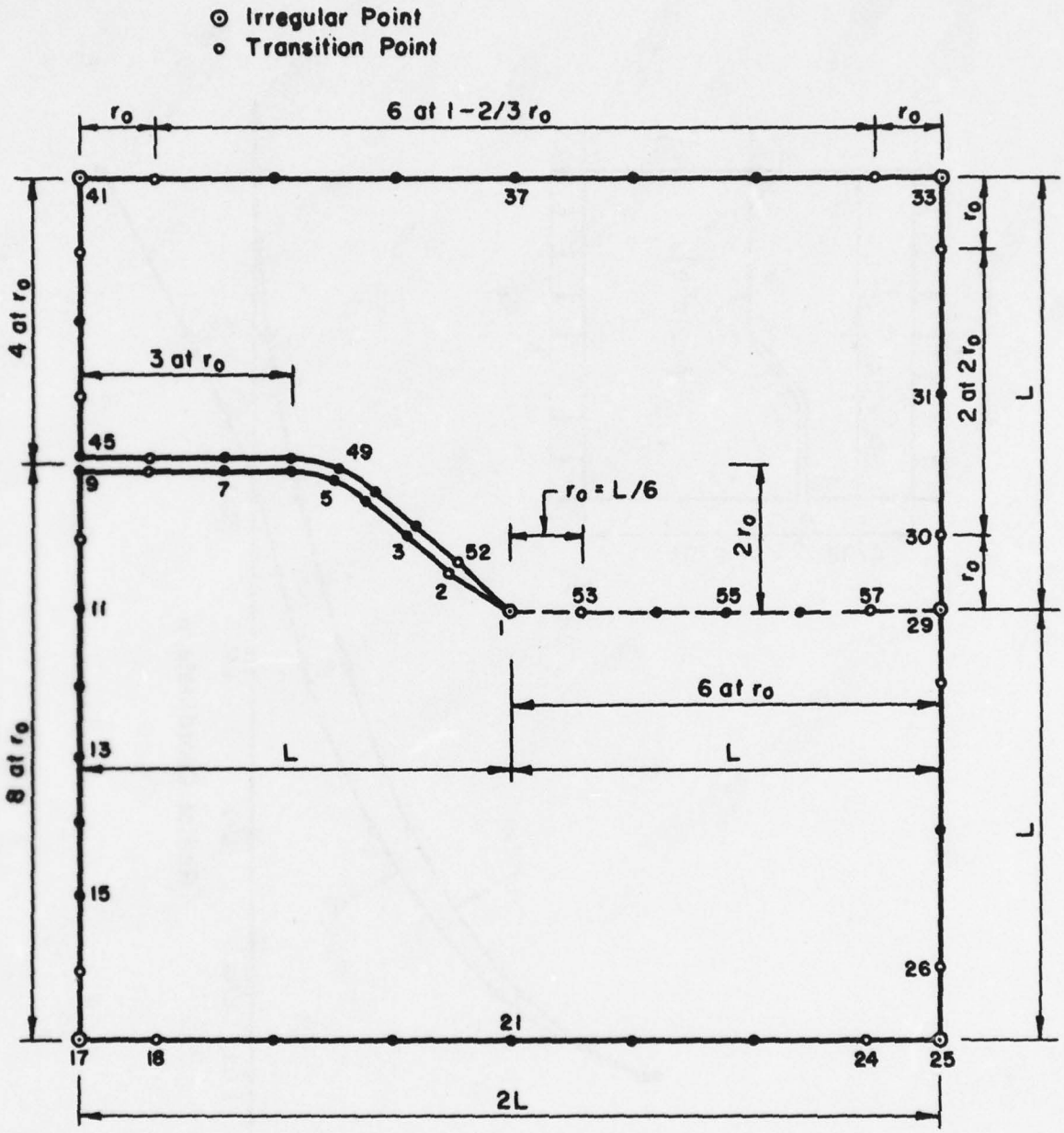

FIG. 23. DATA FOR PROBLEM 3

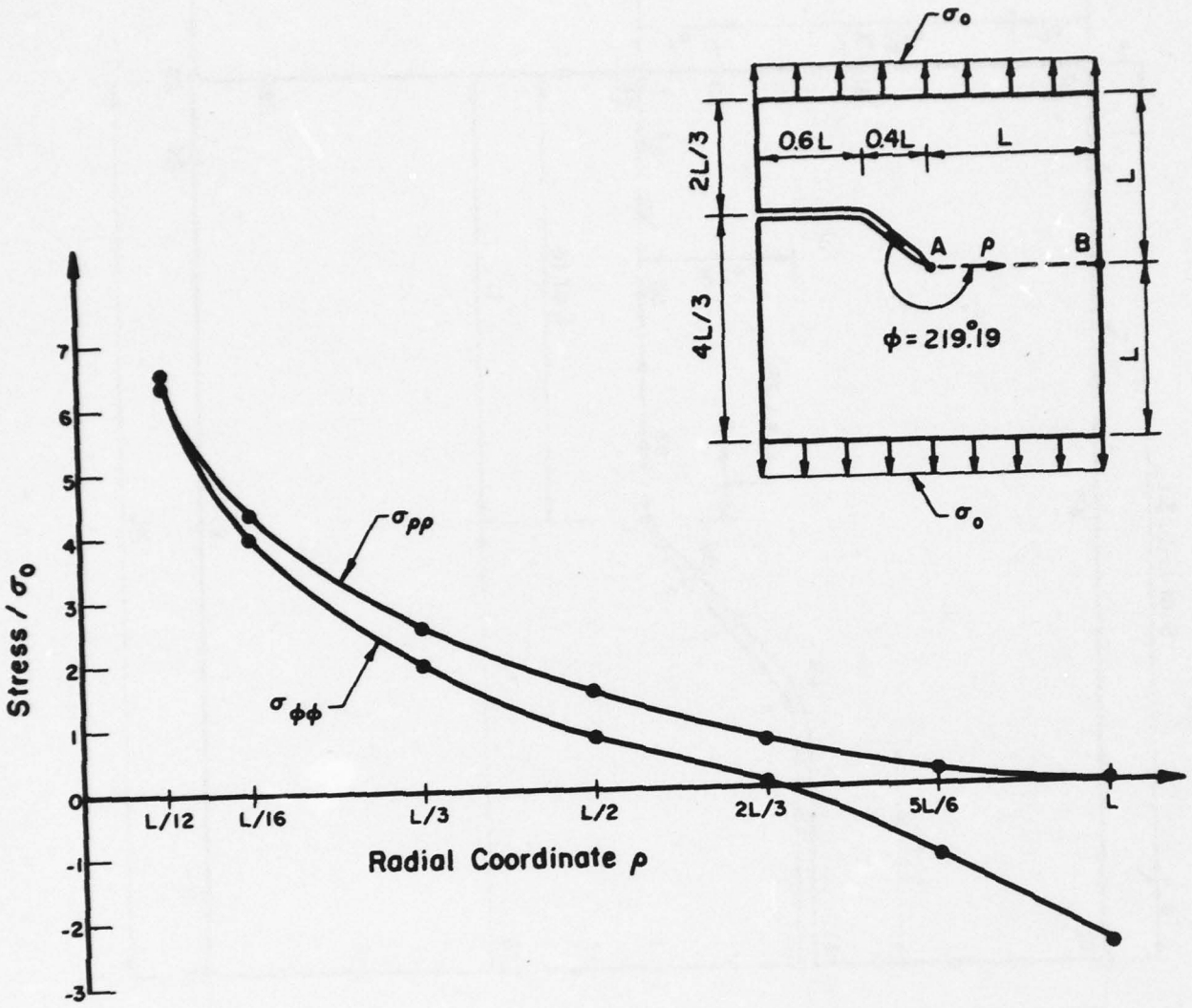

FIG. 24. COMPUTED STRESSES ALONG THE CUT AB (Problem 3)

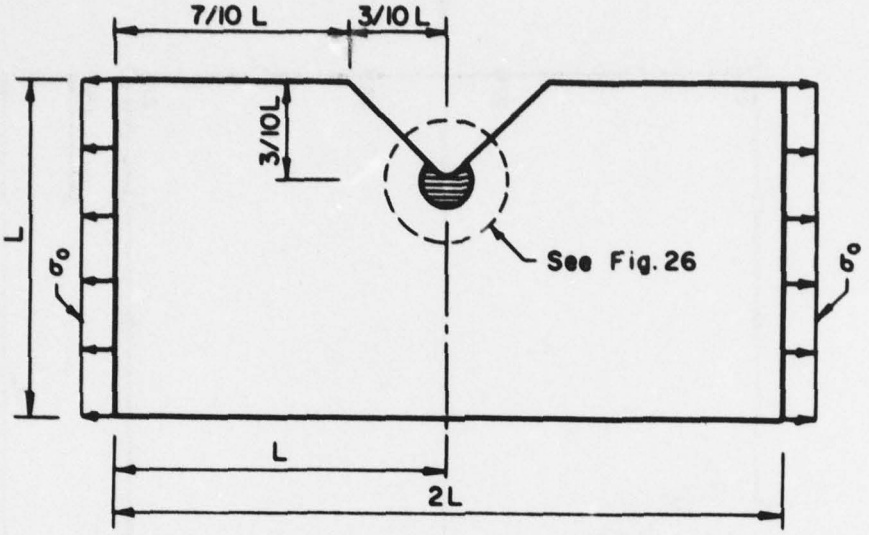

FIG. 25. A UNIFORMLY LOADED PLATE WITH A NOTCH HAVING A FILLET OF SMALL RADIUS (Problem 4)

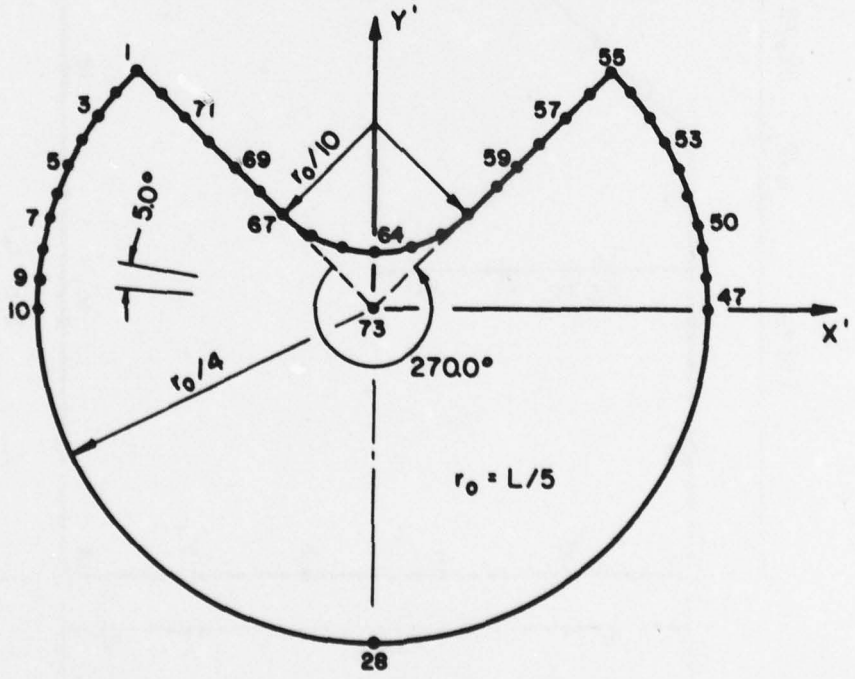

FIG. 26. DETAIL OF THE INNER PIECE (Problem 4)

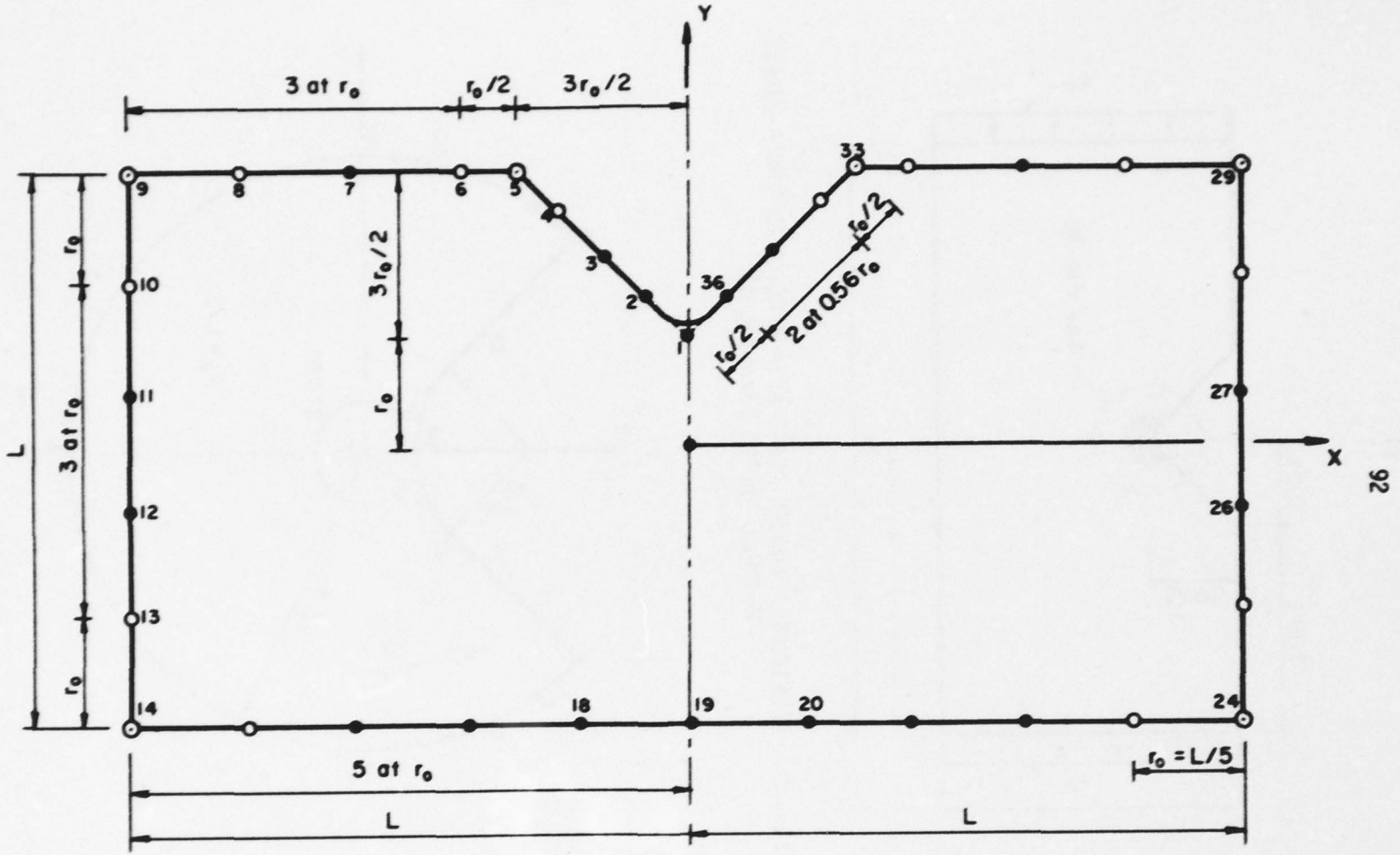

FIG. 27. DATA FOR PROBLEM 4

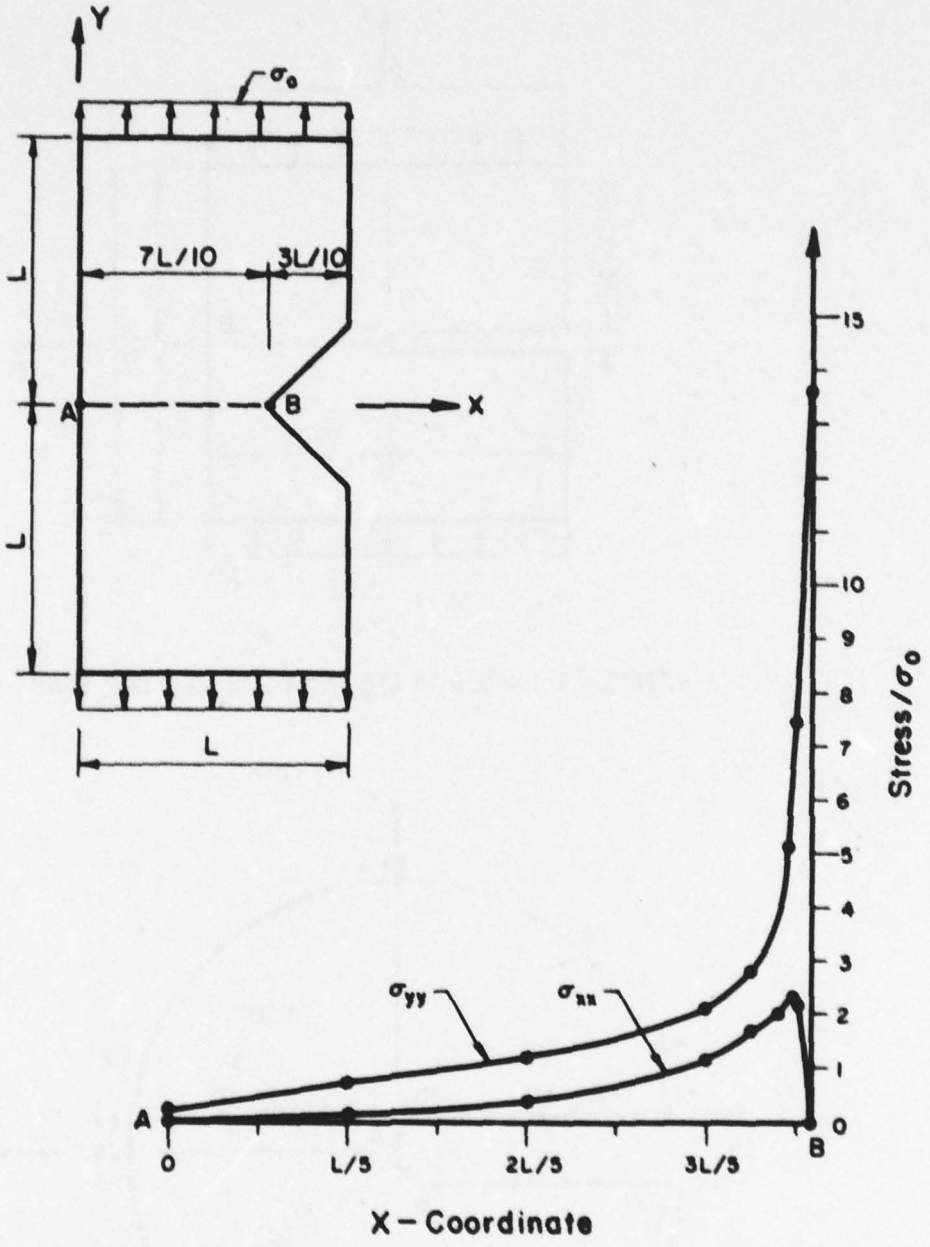

FIG. 28. COMPUTED STRESSES FOR SECTION AB (Problem 4)

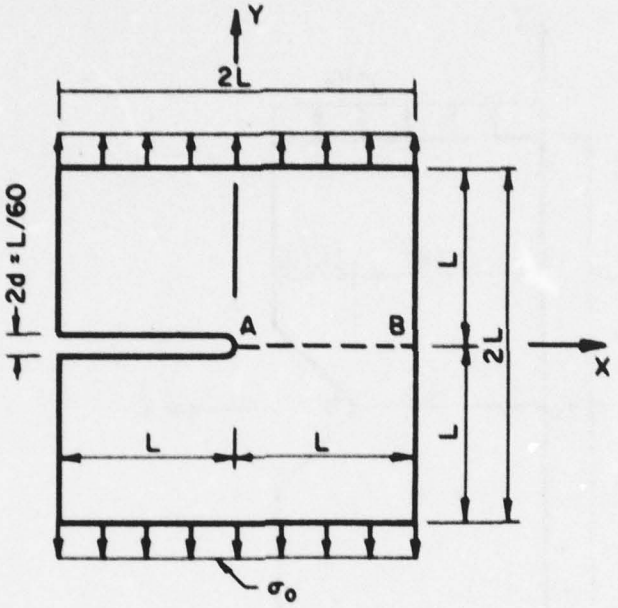

FIG. 29. A UNIFORMLY LOADED PLATE WITH A WIDE EDGE CRACK (Problem 5)

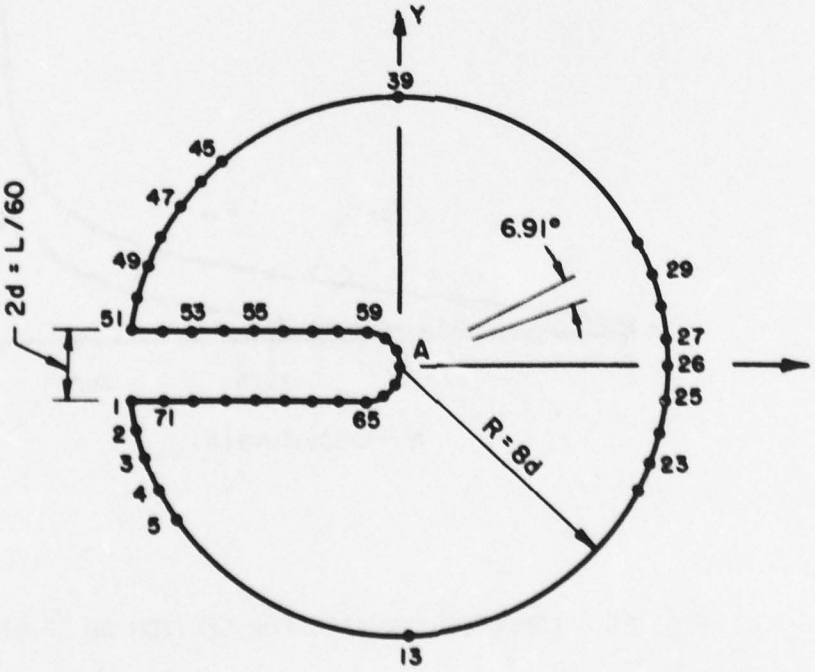

FIG. 30. DETAIL OF THE INNER PIECE (Problem 5)

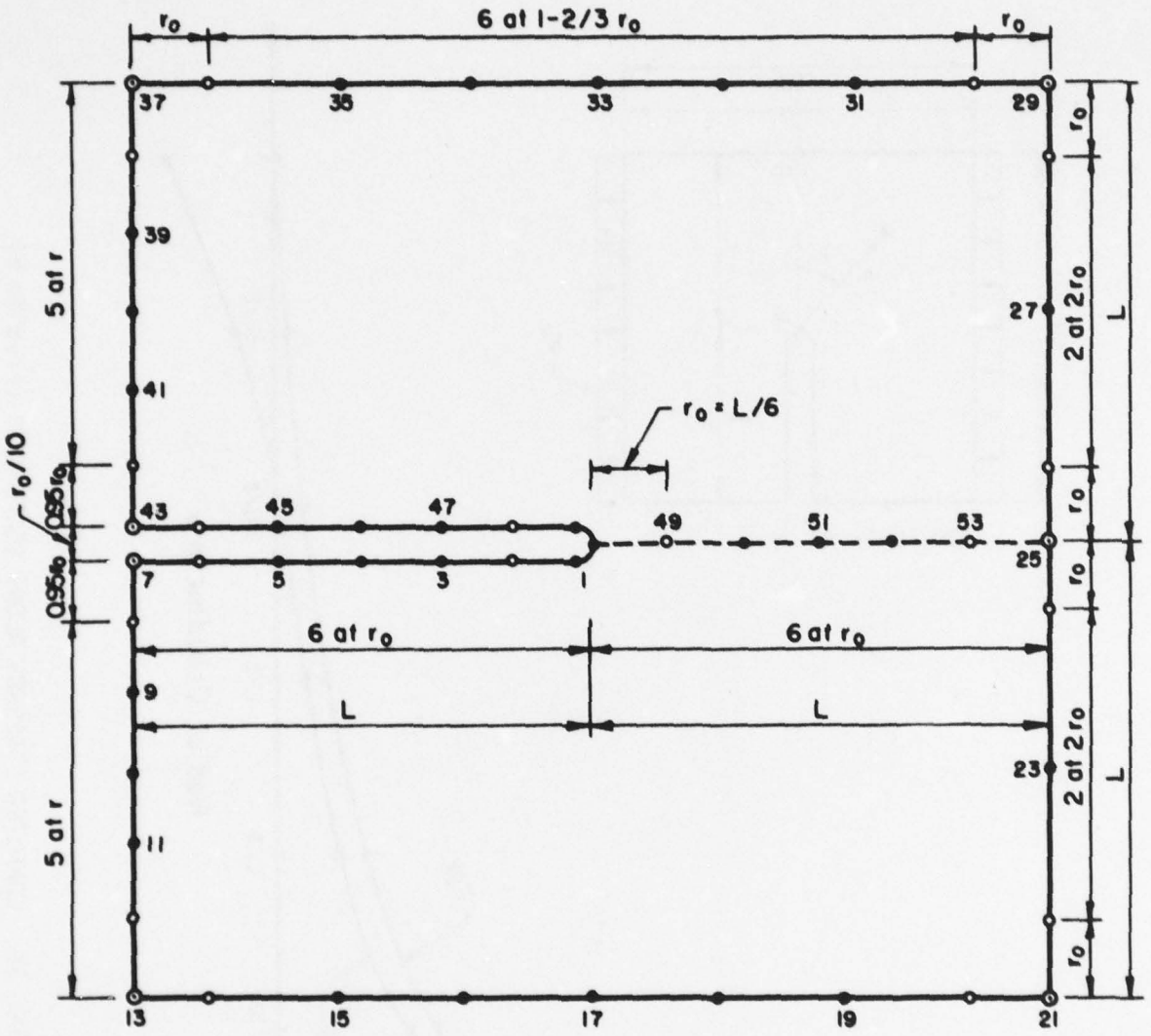

FIG. 31. DATA FOR PROBLEM 5

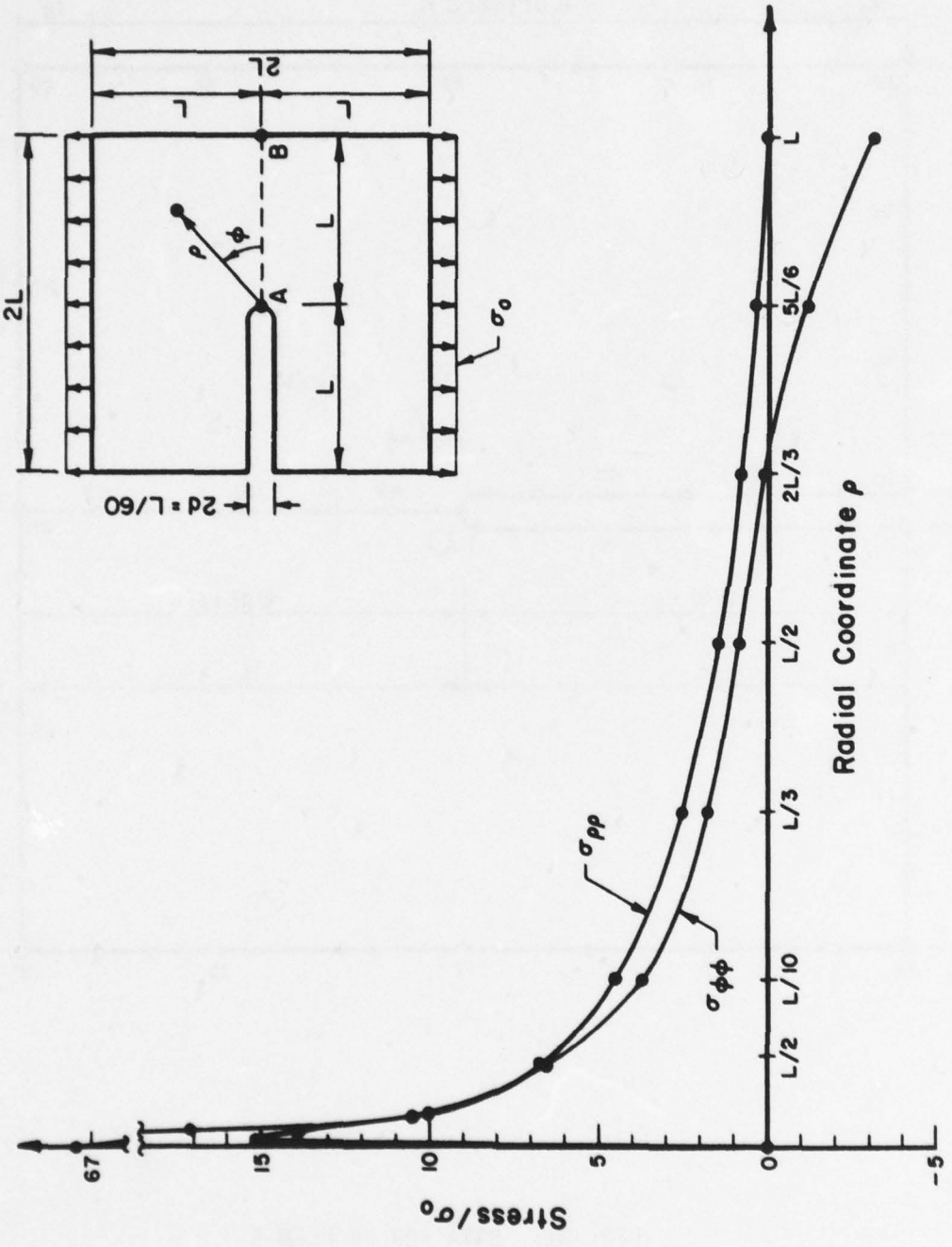

FIG. 32. COMPUTED STRESSES ALONG SECTION AB (Problem 5)

APPENDIX A

SOLUTION OF A CRACK PROBLEM BY SPLITTING THE BODY

A.1 Introduction

Some difficulties arise when solving a crack problem using the straightforward Barone and Robinson method. The source of the problem can be explained as follows: Application of the Kelvin concentrated force solution as an auxiliary at points along the crack boundary (beyond transition points), leads to an indeterminate integral equation, because this force picks out only two independent combination of four displacements, namely, the sum of them at the top and bottom of the crack. In the Barone and Robinson solution technique [18], in order to pick out the difference of the displacements, Westergaard's solutions [26] were used as an auxiliary. This solution corresponds to equal and opposite prying forces acting at some point along a semi-infinite crack in an infinite body. However, this solution is applicable only for a straight crack. Moreover, the use of this solution represents a very special technique which does not fit comfortably in the framework of the general procedure.

In some other investigations the problem has been resolved by either developing a Green's type function to fit the entire physical problem [13], or replacing the crack by an open notch [14]. The first method is naturally limited to very special types of crack problems. The second approach, which actually changes the geometry of the body, may provide a fairly accurate value of the stress intensity factor, but does not give accurate value of stress field near the crack tip.

A.2 Splitting the Body

In order to overcome the above mentioned difficulty, it is convenient to cut the cracked body by extending the crack in some arbitrary fashion. The Barone and Robinson solution technique may then be applied to each piece of the body. The resultant equations can be solved simultaneously along with constraint equations which must be introduced to insure compatibility of displacements and tractions along the imaginary cut.

The solution to two sample problems using the method are given in Section 5.2. It is worth mentioning that the proper Williams' solutions are used to represent the stress state along the interval extending from the irregular point up to the so-called transition points. Therefore, in order to reflect the actual nature of the singularity in the vicinity of the irregular point, the interior angle from boundary to boundary (wedge angle) must be taken as 2π. Even though each of the pieces of the cut body has an angle less than 2π, the cut is wholly fictitious and the stress field of interest is that for the uncut body.

APPENDIX B

DERIVATION OF NEW SOLUTIONS FROM THE WILLIAMS' DISPLACEMENT FIELD (WILLIAMS' LOGARITHMIC SOLUTIONS)

A new solution can be derived by differentiating the Williams' displacement field with respect to the parameter λ, the exponent of ρ in Eqs. (2.10). To show this, we rewrite Eqs. (2.1)

$$\begin{aligned} u_\rho &= A(\phi)\rho^\lambda \\ u_\phi &= B(\phi)\rho^\lambda \end{aligned} \tag{B.1}$$

This displacement field satisfies the equilibrium equations for all values of λ, so does any linear combination of these fields for different values of λ. In particular

$$\begin{aligned} u_\rho^{(1)} &= \frac{u_\rho(\lambda_2) - u_\rho(\lambda_1)}{\lambda_2 - \lambda_1} \\ u_\phi^{(1)} &= \frac{u_\phi(\lambda_2) - u_\phi(\lambda_1)}{\lambda_2 - \lambda_1} \end{aligned} \tag{B.2}$$

also satisfy the equilibrium equations. Taking the limit as $\lambda_2 \to \lambda_1$ we get a new solution of the elasticity equations:

$$\begin{aligned} u_\rho^{(1)} &= \frac{\partial u_\rho}{\partial \lambda} = \left[\frac{\partial A(\phi)}{\partial \lambda} + A(\phi)\,\mathrm{Ln}(\rho)\right]\rho^\lambda \\ u_\phi^{(1)} &= \frac{\partial u_\phi}{\partial \lambda} = \left[\frac{\partial B(\phi)}{\partial \lambda} + B(\phi)\,\mathrm{Ln}(\rho)\right]\rho^\lambda \end{aligned} \tag{B.3}$$

where

$$\frac{\partial A(\phi)}{\partial \lambda} = [\cos(\lambda-1)\phi - (\lambda-3+4\nu)\phi \sin(\lambda-1)\phi]C_1 + [\sin(\lambda-1)\phi + (\lambda-3+4\nu)\phi \cos(\lambda-1)\phi]C_2 + [-\phi \sin(\lambda+1)\phi]C_3 + [\phi \cos(\lambda+1)\phi]C_4 , \tag{B.4}$$

$$\frac{\partial B(\phi)}{\partial \lambda} = [-\sin(\lambda-1)\phi - (\lambda+3-4\nu)\phi \cos(\lambda-1)\phi]C_1 + [\cos(\lambda-1)\phi - (\lambda+3-4\nu)\phi \sin(\lambda-1)\phi]C_2 + [-\phi \cos(\lambda+1)\phi]C_3 + [-\phi \sin(\lambda+1)\phi]C_4 \tag{B.5}$$

The corresponding stresses are

$$\sigma^{(1)}_{\rho\rho} = \frac{\partial \sigma_{\rho\rho}}{\partial \lambda} = \left[\frac{\partial P(\phi)}{\partial \lambda} + P(\phi) \, \mathrm{Ln}(\rho) \right] \rho^{\lambda-1}$$

$$\sigma^{(1)}_{\phi\phi} = \frac{\partial \sigma_{\rho\phi}}{\partial \lambda} = \left[\frac{\partial Q(\phi)}{\partial \lambda} + Q(\phi) \, \mathrm{Ln}(\rho) \right] \rho^{\lambda-1} \tag{B.6}$$

$$\sigma^{(1)}_{\rho\phi} = \frac{\partial \sigma_{\rho\phi}}{\partial \lambda} = \left[\frac{\partial R(\phi)}{\partial \lambda} + R(\phi) \, \mathrm{Ln}(\rho) \right] \rho^{\lambda-1}$$

where $P(\phi)$, $Q(\phi)$ and $R(\phi)$ are given in Eq. (2.13).

Other new solutions can be found by taking higher derivatives of the Williams' displacement fields with respect to λ. The general form of the n-th solution is given in Appendix D using complex fields and complex variables.

APPENDIX C

ORTHOGONALITY CONDITIONS FOR THE WILLIAMS' SOLUTION FORMS

C.1 Orthogonality Conditions for the Extended Willaims' Solutions

Consider a body with a sharp notch of interior angle θ_0 (see Fig. 14, 15). We remove the annulus ABCDEF from the body as shown. Let us write Betti's law for the piece using two different Williams' solution forms.

$$W = W_{L_1} + W_{L_2} = 0; \tag{C.1}$$

$$W_{L_i} = \int_{L_i} [t_j^* u_j - u_j^* t_j] ds \qquad i = 1,2 \quad ; \quad J = 1,2 \tag{C.2}$$

In Equation (C.2) the summation convention is used for the lower-case indices. The L_1 is the curved part of the boundary and L_2 consists of the two straight edges shown in Fig. 15.

Substituting for the tractions and displacement in Eq. (C.2) from Eqs. (2.15), we get

$$W_{L_1} = F_{mn}[(\rho + d\rho)^{\lambda_m + \lambda_n^*} - \rho^{\lambda_m + \lambda_n^*}] \tag{C.3}$$

or

$$W_{L_1} = F_{mn}[(\lambda_m + \lambda_n^*)\rho^{\lambda_m + \lambda_n^* - 1} d\rho]; \tag{C.4}$$

$$F_{mn} = \int_{\phi=0}^{\phi=\theta_0} \{ [A_m(\phi)\, P_n^*(\phi) + B_m(\phi)\, R_n^*(\phi)] \tag{C.5}$$

$$-[A_n^*(\phi)\, P_m(\phi) + B_n^*(\phi)\, R_n(\phi)]\} d\phi$$

and,

$$W_{L_2} = G_{mn} \rho^{\lambda_m + \lambda_n^* - 1} d\rho \quad ; \tag{C.6}$$

$$G_{mn} = H_{mn}(\phi = \theta_0) - H_{mn}(\phi = 0) \tag{C.7}$$

Here

$$H(\phi) = [A_m(\phi) R_n^*(\phi) + B_m(\phi) Q_n^*(\phi)] \tag{C.8}$$

$$- [A_n^*(\phi) R_m(\phi) + B_n^*(\phi) Q_m(\phi)]$$

Substituting for W_{L_1} and W_{L_2} in Eq. (C.1) we obtain

$$[(\lambda_m + \lambda_n^*) F_{mn} + G_{mn}] \rho^{\lambda_m + \lambda_n^* - 1} d\rho = 0 \tag{C.9}$$

Since Equation (C.9) must be true for all values of ρ we have

$$(\lambda_m + \lambda_n^*) F_{mn} + G_{mn} = 0 \tag{C.10}$$

We consider the two possible cases:

a) $G_{mn} = 0$ then $F_{mn} = 0$ if $\lambda_m + \lambda_n^* \neq 0$ (C.11)

and for $\lambda_m + \lambda_n^* = 0$ Eq. (C.10) does not give any information about F_{mn}. Conversely, if the first term in Eq. (C.10) is zero then $G_{mn} = 0$.

b) $G_{mn} \neq 0$ Then $F_{mn} = -\frac{G_{mn}}{\lambda_m + \lambda_n^*}$ for $\lambda_m + \lambda_n^* \neq 0$ (C.12)

which shows that the integrals around the curved boundary can be evaluated by finding the work terms at the two end points and divide it by $\lambda_m + \lambda_n^*$.

C.2 Orthogonality Conditions for the Williams' Logarithmic Solutions

Just as in the previous case, we write Betti's law for the annulus (Fig. 15) using two solutions, where one of them is a Williams' logarithmic solution and the other one is an ordinary Williams' solution. We have

$$W^{(1)} = W_{L_1}^{(1)} + W_{L_2}^{(1)} = 0 \tag{C.13}$$

where the superscript indicates that the Williams' logarithmic solution used is the first derivative of the Williams' solution with respect to the exponent of ρ. Evaluating $W_{L_1}^{(1)}$ using Eq. (C.2), we get

$$\begin{aligned} W_{L_1}^{(1)} = {} & F_{mn}^{(1)} \left[(\rho + d\rho)^{\lambda_m + \lambda_n^*} - \rho^{\lambda_m + \lambda_n^*}\right] \\ & + F_{mn} \left[\mathrm{Ln}(\rho + d\rho)\,(\rho + d\rho)^{\lambda_m + \lambda_n^*} - \mathrm{Ln}(\rho)\,\rho^{\lambda_m + \lambda_n^*}\right] \end{aligned} \tag{C.14}$$

or

$$\begin{aligned} W_{L_1}^{(1)} = {} & F_{mn}\,(\lambda_m + \lambda_n^*)\,\rho^{\lambda_m + \lambda_n^* - 1}\,d\rho \\ & + F_{mn}\left[1 + (\lambda_m + \lambda_n^*)\,\mathrm{Ln}(\rho)\right]\rho^{\lambda_m + \lambda_n^* - 1}\,d\rho \end{aligned} \tag{C.15}$$

where F_{mn} is given by Eq. (C.5) and

$$F^{(1)}_{mn} = \int_{\phi=0}^{\phi=\theta_0} \{[A^{(1)}_m(\phi)\, P^*_n(\phi) + B^{(1)}_m(\phi)\, R_n(\phi)] - [A^*_n(\phi)\, P^{(1)}_m(\phi) + B^*_n(\phi)\, R^{(1)}_m(\phi)]\}d\phi \tag{C.16}$$

The $W^{(1)}_{L_2}$ is also evaluated using Eq. (C.2):

$$W^{(1)}_{L_2} = G_{mn}\, \rho^{\lambda_m + \lambda^*_n - 1}\, d\rho + G^{(1)}_{mn}\, \rho^{\lambda_m + \lambda^*_n - 1}\, \mathrm{Ln}(\rho)d\rho \tag{C.17}$$

where G_{mn} is given by Eq. (C.7) and

$$G^{(1)}_{mn} = H^{(1)}_{mn}(\phi = \theta_0) - H^{(1)}_{mn}(\phi = 0); \tag{C.18}$$

$$H^{(1)}_{mn}(\phi) = [A^{(1)}_m(\phi)\, R^*_n(\phi) + B^{(1)}_m(\phi)\, Q^*_n(\phi)] - [A^*_n(\phi)\, R^{(1)}_m(\phi) + B^*_n(\phi)\, Q^{(1)}_m(\phi)] \tag{C.19}$$

Substituting for $W^{(1)}_{L_1}$ and $W^{(1)}_{L_2}$ in Eq. (C.19), we get

$$\{[(\lambda_m + \lambda^*_n)\, F^{(1)}_{mn} + F_{mn} + G^{(1)}_{mn}] + [(\lambda_m + \lambda^*_n)\, F_{mn} + G_{mn}]\, \mathrm{Ln}(\rho)\}\, \rho^{\lambda_m + \lambda^*_n - 1}\, d\rho = 0 \tag{C.20}$$

Since Eq. (C.20) must be true for all values of ρ, we obtain

$$(\lambda_m + \lambda_n^*)\, F_{mn} + G_{mn} = 0 \tag{C.21}$$

$$(\lambda_m + \lambda_n^*)\, F_{mn}^{(1)} + F_{mn} + G_{mn}^{(1)} = 0 \tag{C.22}$$

Equation (C.21) has been discussed in Section C.1. For the case $\lambda_m + \lambda_n^* \neq 0$ we have

$$F_{mn} = -\frac{G_{mn}}{\lambda_m + \lambda_n^*} \tag{C.23}$$

and from Eq. (C.22) we obtain

$$F_{mn}^{(1)} = -\frac{G_{mn}}{(\lambda_m + \lambda_n^*)^2} - \frac{G_{mn}^{(1)}}{(\lambda_m \quad \lambda_n)} \tag{C.24}$$

which, just as in the previous case, simplifies the evaluation of $F_{mn}^{(1)}$.

APPENDIX D

THE WILLIAMS' SOLUTIONS IN COMPLEX FORM

Most calculations using Williams' solutions are carried out in the natural polar coordinates. However, for the wide crack problem, it is much more convenient to work in Cartesian coordinates. The expressions are simplified considerably by using complex fields and complex variables. By transformation of Eqs. (2.10) and (2.11), we find for the displacements.

$$u_x - iu_y = \lambda \bar{D}_1 \bar{Z} Z^{\lambda-1} + \bar{D}_2 Z^{\lambda} - (3 - 4\nu)\, D_1 \bar{Z}^{\lambda} \tag{D.1}$$

The stresses are of the form

$$\sigma_{yy} + i\sigma_{yx} = -2\mu\lambda \left[D_1 \bar{Z}^{\lambda-1} + (\bar{D}_1 + \bar{D}_2) Z^{\lambda-1} + (\lambda-1)\bar{D}_1 \bar{Z} Z^{\lambda-2}\right] = \psi(Z, \bar{Z}) \tag{D.2}$$

$$\sigma_{xx} = 2\mu\lambda \text{ Real } [-2D_1 \bar{Z}^{\lambda-1} + \bar{D}_2 Z^{\lambda-1} + (\lambda - 1)\bar{D}_1 \bar{Z} Z^{\lambda-2}] \tag{D.3}$$

where $Z = x + iy$, and the superior bar indicates the complex conjugate, here

$$D_1 = C_1 + iC_2 \tag{D.5}$$

$$D_2 = C_3 + iC_4$$

where the C's are the unknown real constants of integration, given in Eqs. (2.11).

Referring to Eq. (D.2), we see that the condition of no traction on a crack $(x, y_0 = 0)$, $x < 0$ is $\psi(x + iy_0\ x - iy_0) = 0$, $x < 0$.

In the derivation of the perturbed Williams' solutions for the wide crack, extensive use will be made of the derivatives

$$\frac{\partial^n \psi}{\partial y^n} = (i)^n \left[\prod_{\ell=0}^{n} (\lambda - \ell)\right] \{(-1)^n D_1 \bar{Z}^{\lambda-n-1} + (\bar{D}_1 + \bar{D}_2 - n\bar{D}_1) Z^{\lambda-n-1} + \bar{D}_1(\lambda-n-1)\bar{Z}Z^{\lambda-n-2}\} \tag{D.6}$$

for the expansion of the ψ function in a Taylor series.

In addition to the ordinary Williams' solutions, Williams' logarithmic solutions are also used as perturbation functions. The n-th logarithmic solution can be written of the form:

$$u_x^{(n)} - iu_y^{(n)} = n\bar{D}_1 \bar{Z} Z^{\lambda-1}\ Ln^{n-1}(Z) + [\lambda \bar{D}_1 \bar{Z} Z^{\lambda-1} + \bar{D}_2 Z^{\lambda}]\ Ln^n(Z) - (3 - 4\nu) D_1 \bar{Z}^{\lambda}\ Ln^n(\bar{Z}) \tag{D.7}$$

$$\psi^{(n)} = \sigma_{yy}^{(n)} + i\sigma_{yx}^{(n)} = -2\mu\lambda \{D_1 [n\ Ln^{n-1}(\bar{Z}) + \lambda Ln^n(\bar{Z})]\bar{Z}^{\lambda-1} + (\bar{D}_1 + \bar{D}_2)[n\ Ln^{n-1}(Z) + \lambda Ln^n(Z)]Z^{\lambda-1} + \bar{D}_1 [n(n-1)\ Ln^{n-2}(Z) + n(2\lambda - 1)\ Ln^{n-1}(Z) + \lambda^2\ Ln^n(Z)]\bar{Z}Z^{\lambda-2}\} \tag{D.8}$$

$$\sigma_{xx}^{(n)} = 2\mu \text{ Real } \{-2D_1 [n\, Ln^{n-1}(\bar{Z}) + Ln^n(\bar{Z})]\bar{Z}^{\lambda-1}$$

$$+ D_2 [n\, Ln^{n-1}(Z) + \lambda Ln^n(Z)]Z^{\lambda-1} \qquad (D.9)$$

$$+ D_1 [n(n-1)\, Ln^{n-2}(Z) + n(2\lambda - 1)\, Ln^{n-1}(Z) + \lambda^2\, Ln^n(Z)]\bar{Z}Z^{\lambda-2}\}$$

APPENDIX E

GENERAL FORMS OF PERTURBATION FUNCTIONS AND THEIR DETERMINATION FROM BOUNDARY CONDITIONS

E.1 General Forms of the Perturbation Functions

As mentioned in Section 4.2, for the determination of the perturbed solutions in the wide crack problem we start from the eigenfunctions corresponding to the infinitesimal crack (zeroth perturbation), with the eigenvalues

$$\lambda_m = \pm \frac{m}{2} \qquad m = 0, 1, 2, 3 \ldots \tag{E.1}$$

which occur as double roots. The general form of these solutions is given in polar coordinates by Eqs. (2.10) through Eqs. (2.13) and in complex form by Eqs. (D.1) through Eqs. (D.3). These solutions are divided into symmetric and anti-symmetric forms. For example, for the half-integer eigenvalues

$$\lambda_m = \pm 0.50, \pm 1.50, \pm 2.50, \pm \ldots . \tag{E.2}$$

The relations

$$C_{2m} = C_{4m} = 0 \tag{E.3}$$

must hold in order that the solutions be symmetric about the x-axis. A relation of the form

$$C_{3m} = -(\lambda_m - 1)C_{1m} \tag{E.4}$$

between the other two components of the vector guarantees homogeneous traction boundary conditions along the half line $x < 0$, $y = 0$, or guarantees that we have an eigensolution.

Similarly the eigenvectors for the anti-symmetric eigenfunctions corresponding to eigenvalues given by Eq. (E.2), are of the form

$$C_{1m} = C_{3m} = 0 \tag{E.5}$$

The half line $x < 0$, $y = 0$ is freed of traction if

$$C_{4m} = -(\lambda_m + 1)\, C_{2m} \tag{E.6}$$

It can be seen that the half integers are double eigenvalues for the slit plane. The integers also correspond to double eigenvalues and may be split into symmetric and anti-symmetric solutions. These eigenvalues are treated much the same way as the half integer ones.

For the λ's given by Eq. (E.2), one other independent symmetric solution can be derived; this solution will, of course, not be an eigenfunction. A simple choice of the C's for this solution is given by Eq. (E.3) and

$$C_{3m} \neq 0 \quad ; \quad C_{1m} = 0 \tag{E.7}$$

which gives $\sigma_{yx}(x < 0, y = 0) = 0$, $\sigma_{yy}(x < 0, y = 0) \neq 0$.

The Williams' logarithmic solutions are other solution forms used in the perturbation process. Here again, two independent symmetric solutions can be derived by properly choosing the constants of integration. For example, for λ_m given by Eq. (E.2), if the c's taken in proportion given by Eqs. (E.3) and (E.4) the solution will be symmetric and the tractions of the logarithmic term will satisfy the homogeneous boundary condition along the half line $x < 0$, $y = 0$. If the C's are chosen of the form given by Eq. (E.7), the solution will give non-zero tractions varying logarithmically along the boundary edges of the corresponding infinitesimal crack.

E.2 Determination of the Perturbation Functions from the Boundary Conditions

The Φ_k functions (Eq. 4.1) have to be determined subject to the boundary conditions given by Eqs. (4.4). As an example let us take a symmetric case and find Φ_k for the first perturbation ($k = 1$). We have

$$\Phi = \beta_1\psi_1 + \beta_2\psi_2 \tag{E.8}$$

Here the indices indicating the perturbation number are dropped for brevity. The β's are unknown coefficients yet to be determined, and the ψ's are the

solution functions to be found to satisfy the boundary conditions given by

$$\Phi \Big|_{\substack{x < 0 \\ y = 0}} = \frac{\partial \Phi_0}{\partial y} \Big|_{\substack{x < 0 \\ y = 0}} \tag{E.9}$$

In Eq. (E.9) the Φ_0 (zeroth perturbation function) is known. It is the eigenfunction corresponding to the infinitesimal crack with the eigenvalue given by Eq. (E.2) and the eigenvector given by Eqs. (E.3) and (E.4). For a particular eigenvalue say λ_0, the right hand side of Eq. (E.9) can be evaluated using Eq. (D.6). We obtain

$$\Phi \Big|_{\substack{x < 0 \\ y = 0}} = (f_0 + ig_0)\rho^{\lambda_0 - 2} \tag{E.10}$$

In Eq. (E.10) one or both of the values f_0 and g_0 may be zero depending upon the eigenvalue and the symmetric or anti-symmetric nature of the eigenfunction.

As discussed in Section 4.2, one of the functions in the Eq. (E.9) will be of non-eigenfunction type with coefficients given by Eq. (E.4) and the other of the form of the Williams' logarthmic type with the C's proportional to the eigenvector of the zeroth eigenfunction. Evaluating these functions using Eq. (D.4) and (D.7) and substituting in Eq. (D.8), we obtain

$$\begin{aligned} &\beta_1(f_1 + ig_1)\rho^{\lambda_1 - 1} + \beta_2[(f_2 + ig_2) + (f_3 + ig_3)\,\mathrm{Ln}(\rho)]\rho^{\lambda_2 - 1} \\ &\qquad = (f_0 + ig_0)\rho^{\lambda_0 - 2} \end{aligned} \tag{E.11}$$

The C's of the ψ_2 function are taken proportional to those of Φ_0 which, according to Section E.1, will give

$$f_3 + ig_3 = 0 \quad ; \tag{E.12}$$

$$\beta_1(f_1 + ig_1)\rho^{\lambda_1-1} + \beta_2(f_2 + ig_2)\rho^{\lambda_2-1} = (f_0 + ig_0)\rho^{\lambda_0-2} \tag{E.13}$$

Since the solution function must satisfy the boundary conditions all along the ($x < 0$, $\rho = |x|$) we should choose

$$\begin{aligned} \lambda_1 - 1 &= \lambda_0 - 2 \quad ; \quad \lambda_1 = \lambda_0 - 1 \\ \lambda_2 - 1 &= \lambda_0 - 2 \quad ; \quad \lambda_2 = \lambda_0 - 1 \end{aligned} \tag{E.14}$$

and finally Eq. (E.13) must be true for all values of ρ which give

$$\begin{aligned} \beta_1 f_1 + \beta_2 f_2 &= f_0 \\ \beta_1 f_1 + \beta_2 g_2 &= g_0 \end{aligned} \tag{E.15}$$

for the determination of β_1 and β_2.

APPENDIX F

DETERMINATION OF DISPLACEMENTS AND STRESSES FOR AN ARBITRARY POINT IN THE BODY

F.1 Formulation of the Problem

As mentioned in Section 2.1.2, once the unknown boundary values are determined, the displacements at any point of the boundary can be found using Eq. (2.5). The strain and eventually the stresses are evaluated by differentiation of Eq. (2.4) or Eq. (2.5) with respect to x_0 and y_0 under the integral sign.[1] We obtain

$$\alpha_{ij} \frac{\partial u_j}{\partial x_0}(P) = \int_L [t_j(Q) \frac{\partial u^*_{ij}}{\partial x_0}(P,Q) - u_j(Q) \frac{\partial t^*_{ij}}{\partial x_0}(P,Q)]ds \tag{F.1}$$

$$\alpha_{ij} \frac{\partial u_j}{\partial y_0}(P) = \int_L [t_j(Q) \frac{\partial u^*_{ij}}{\partial y_0}(P,Q) - u_j(Q) \frac{\partial t^*_{ij}}{\partial y_0}(P,Q)]ds \tag{F.2}$$

---

[1] The x_0 and y_0 are cartesian coordinate of point P where the Kelvin load is applied. The integration under the integral sign for the singular integral is permissible [31].

All the terms in Eqs. (F.1) and (F.2) are defined in Sections 2.2.1 and 2.2.2. The final expressions for the Kelvin kernels involve the chord length r connecting P and Q and its derivatives with respect to x, y, n, s coordinates at point Q. We have

$$r^2 = (x - x_0)^2 + (y - y_0)^2$$

$$r_n = \ell r_x + m r_y \quad , \quad r_s = \ell r_y - m r_x \tag{F.3}$$

$$r_x = \frac{x-x_0}{r} \quad , \quad r_y = \frac{y-y_0}{r}$$

where ℓ and m are the direction cosine of the normal to the boundary at point Q. Furthermore

$$\frac{\partial r}{\partial x_0} = -r_x \quad ; \quad \frac{\partial r}{\partial y_0} = -r_y$$

$$\frac{\partial}{\partial x_0} \mathrm{Ln}(r) = -\frac{r_x}{r} \quad ; \quad \frac{\partial}{\partial y_0} \mathrm{Ln}(r) = -\frac{r_y}{r} \tag{F.4}$$

$$\frac{\partial r_n}{\partial x_0} = \frac{r_y}{r}(-\ell r_y + m r_x) \quad ; \quad \frac{\partial r_n}{\partial y_0} = -\frac{r_x}{r}(-\ell r_y + m r_x)$$

$$\frac{\partial r_s}{\partial x_0} = \frac{r_y}{r}(\ell r_x + m r_y) \quad ; \quad \frac{\partial r_s}{\partial y_0} = -\frac{r_x}{r}(\ell r_x - m r_y)$$

Using Eqs. (F.3) and (F.4) we obtain for the Kelvin kernels.

$$\frac{\partial u^*_{11}}{\partial x_0} = -\frac{r_x}{r}(1 + 2Cr_y^2) \quad ; \quad \frac{\partial u^*_{11}}{\partial y_0} = \frac{r_y}{r}(-1 + 2Cr_x^2)$$

$$\frac{\partial u^*_{12}}{\partial x_0} = C\frac{r_y}{r}(r_x^2 - r_y^2) \quad ; \quad \frac{\partial u^*_{12}}{\partial y_0} = -C\frac{r_x}{r}(r_x^2 - r_y^2) \qquad \text{(F.5)}$$

$$\frac{\partial u^*_{22}}{\partial x_0} = \frac{r_x}{r}(-1 + 2Cr_y^2) \quad ; \quad \frac{\partial u^*_{22}}{\partial y_0} = -\frac{r_y}{r}(1 + 2Cr_x^2)$$

and

$$\frac{\partial t^*_{11}}{\partial x_0} = \frac{A}{r^2}[-2r_x r_y^2 r_n + (B + r_x^2) R_x]$$

$$\frac{\partial t^*_{11}}{\partial y_0} = \frac{A}{r^2}[-2r_x^2 r_y r_n + (B + r_y^2) R_y]$$

$$\frac{\partial t^*_{12}}{\partial x_0} = \frac{A}{r^2}[(1 - 2r_x^2) r_y r_n + r_x r_y R_x + BR_y]$$

(F.6)

$$\frac{\partial t^*_{12}}{\partial y_0} = \frac{A}{r^2}[(1 - 2r_y^2) r_x r_n + r_x r_y R_x - BR_y]$$

$$\frac{\partial t^*_{22}}{\partial x_0} = \frac{A}{r^2}[-2r_x r_y^2 r_n - (B + r_y^2) R_x]$$

$$\frac{\partial t^*_{22}}{\partial y_0} = \frac{A}{r^2}[-2r_x^2 r_y r_n + (B + r_y^2) R_y]$$

where

$$R_x = 2r_x r_n - \ell$$
$$R_y = 2r_y r_n - m \qquad (F.7)$$

F.2. Evaluation of Integrals in the Singular Case

For the evaluation of the integrals of Eqs. (2.5), (F.1) and (F.2) along the intervals in which the kernels are unbounded, the density function is represented by a second order polynomial given by Eq. (5.1) and the kernel is expressed in terms of the curvature of the boundary and its derivatives with respect to the arc length in the neighborhood of the singular points. The expression for the curvature can be written as

$$k = k_0 + k's + \frac{k''}{2!} s^2 + \frac{k'''}{2!} s^3 + \ldots\ldots\ldots \qquad (F.8)$$

where $k' = \frac{\partial k}{\partial s}$ and $k'' = \frac{\partial^2 k}{\partial s^2}$. Using the relation $\frac{\partial \theta}{\partial s} = k$, we get

$$\theta = \int_0^s k\, ds = k_0 s + \frac{k'}{2} s^2 + \frac{k''}{6} s^3 + \ldots \qquad (F.9)$$

where the angle θ is shown in Fig. 13. Furthermore, the chord length r and its derivative with respect to x, y, n, s coordinate (see Fig. 13) can be expanded using Eqs. (F.7) and F.8). We obtain[1]

---

[1] See Forbes [6] for more detail.

$$\cos\theta(s) = 1 - \frac{k^2 s^2}{2} - \frac{kk'}{2} s^3 + \left[\frac{k^4}{24} - \frac{k'^2}{8} - \frac{kk''}{6}\right] s^4 + \ldots . \qquad (F.10)$$

$$\sin\theta(s) = ks + \frac{k's^2}{2} + [k'' - k^3]\frac{s^3}{6} - \frac{k^2 k'}{4} s^4 + \ldots . \qquad (F.11)$$

$$\bar{a}(s) = s - \frac{k^2 s^3}{6} - \frac{kk'}{8} s^4 + \left[\frac{k^4}{120} - \frac{k'^2}{40} - \frac{kk''}{30}\right] s^5 + \ldots . \qquad (F.12)$$

$$\bar{b}(s) = \frac{ks^2}{2} + \frac{k's^3}{6} + [k'' - k^3]\frac{s^4}{24} - \frac{k^2 k'}{20} s^5 + \ldots . \qquad (F.13)$$

$$r^2(s) = (\bar{a}^2 + \bar{b}^2) = s^2\left[1 - \frac{k^2 s^2}{12} - \frac{kk's^3}{12} + \left(\frac{k^4}{360} - \frac{k'^2}{45} - \frac{kk''}{40}\right) s^4\right] \qquad (F.14)$$

$$\mathrm{Ln}(r) = \mathrm{Ln}|s| - \left(\frac{k^2 s^2}{24} + \frac{kk'}{24} s^3 + \ldots .\right) \qquad (F.15)$$

$$\begin{aligned} r_x = {} & -m_0 + s\left[-\frac{\ell_0 k}{2}\right] + s^2\left[\frac{m_0 k^2}{8} - \frac{\ell_0 k'}{6}\right] \\ & + s^3\left[\frac{\ell_0 k^3}{48} + \frac{m_0 kk'}{12} - \frac{\ell_0 k''}{24}\right] \\ & + s^4\left[\frac{\ell_0 k^2 k'}{45} - \frac{m_0 k^4}{48.8} + \frac{m_0 kk''}{48} + \frac{m_0 k'^2}{72}\right] \end{aligned} \qquad (F.16)$$

$$\begin{aligned} r_y = {} & \ell_0 + s\left[-\frac{m_0 k}{2}\right] + s^2\left[-\frac{\ell_0 k^2}{2} - \frac{m_0 k'}{6}\right] \\ & + s^3\left[\frac{m_0 k^3}{48} - \frac{\ell_0 kk''}{12} - \frac{m_0 k''}{24}\right] \\ & + s^4\left[\frac{m_0 k^2 k'}{45} + \frac{\ell_0 k^4}{48\times 8} - \frac{\ell_0 kk''}{48} - \frac{\ell_0 k'^2}{72}\right] \end{aligned} \qquad (F.17)$$

$$r_s = 1 + s^2\left[-\frac{k^2}{8}\right] + s^3\left[-\frac{kk'}{6}\right] + s^4\left[\frac{k^4}{48x8} - \frac{k'^2}{18} - \frac{kk''}{16}\right] \tag{F.18}$$

$$r_n = s\left[\frac{k}{2}\right] + s^2\left[\frac{k'}{3}\right] + s^3\left[\frac{k''}{8} - \frac{k^3}{48}\right] + s^4\left[\frac{-29k^2k'}{45 \times 16}\right] \tag{F.19}$$

$$\begin{aligned} \ell(s) = \ell_0 &+ s\left[-m_0k\right] + s^2\left[\frac{-\ell_0k^2}{2} - \frac{m_0k'}{2}\right] \\ &+ s^3\left[\frac{-\ell_0kk'}{2} + \frac{m_0k^3}{6} - \frac{m_0k''}{6}\right] \\ &+ s^4\left[\ell_0\left(\frac{k^4}{24} - \frac{k'^2}{8} - \frac{kk''}{6}\right) + \frac{m_0k^2k'}{4}\right] \end{aligned} \tag{F.20}$$

$$\begin{aligned} m(s) = m_0 &+ s\left[\ell_0k\right] + s^2\left[-\frac{m_0k^2}{2} = \frac{\ell_0k'}{2}\right] \\ &+ s^3\left[-\frac{m_0kk'}{2} - \frac{\ell_0k^3}{6} + \frac{\ell_0k''}{6}\right] \\ &+ s^4\left[m_0\left(\frac{k^4}{24} - \frac{k'^2}{8} - \frac{kk''}{6}\right) - \frac{\ell_0k^2k'}{4}\right] \end{aligned} \tag{F.21}$$

$$\begin{aligned} \frac{1}{r} = \frac{1}{s} &+ s\left[\frac{k^2}{24}\right] + s^2\left[+\frac{kk'}{24}\right] + s^3\left[\frac{k'^2}{90} + \frac{kk''}{80} = \frac{7k^4}{120.48}\right] \\ &+ s^4\left[\frac{7k^3k'}{360x8}\right] \end{aligned} \tag{F.22}$$

$$\frac{1}{r^2} = \frac{1}{s^2} + \frac{k^2}{12} + s\left[\frac{kk'}{12}\right] + s^2\left[\frac{k^4}{240} + \frac{k'^2}{45} + \frac{kk''}{40}\right] \tag{F.23}$$

In the singular interval, the displacements and tractions of the Kelvin forces can be represented as a truncated laurant series with respect to arc lengths using Eqs. (F.14) through (F.23). The general form of the kernels can be written of the form (see Ref. 6).

$$g(s) = \frac{\alpha_{-1}}{s} + \alpha_0 + \alpha_1 s + \alpha_2 s^2 + \ldots\ldots \qquad \text{(F.24)}$$

Similarly for evaluation of the integrals of Eqs. (F.1) and (F.2) in the interval where the kernels are unbounded, the relations given by Eqs. (F.5) and (F.6) are also expanded using Eqs. (F.14) through (F.23), the expansions are lengthy only few will be given here

$$\frac{\partial u^*_{11}}{\partial x_0} = \frac{m_0(1+2C\ell_0^2)}{s} + \left[\frac{\ell_0 k}{2} + \ell_0 kC(\ell_0^2 - 2m_0^2)\right] \qquad \text{(F.25)}$$

$$- \left[\frac{m_0 k^2}{12} - \frac{\ell_0 k'}{6} + 2C\left(\frac{-m_0^3 k'}{4} - \frac{\ell_0^3 k'}{6} + \frac{m_0^2 \ell_0 k'}{3} + \frac{5m_0 \ell_0^2 k^2}{6}\right)\right] s$$

$$- \left[\left(\frac{m_0 kk'}{24} - \frac{\ell_0 k''}{24}\right) + 2C\left(-\frac{m_0^3 kk'}{6} - \frac{\ell_0^3 k''}{24} + \frac{\ell_0^3 k^3}{8} + \frac{m_0^2 \ell_0 k''}{12}\right.\right.$$

$$\left.\left. - \frac{3m_0^2 \ell_0 k^3}{8} + \frac{13m_0 \ell_0^2 kk'}{24}\right)\right] s^2$$

$$\frac{\partial u_{12}^{*}}{\partial x_0} = \frac{C\ell_0(-1 + 2m_0^2)}{s} + C[\frac{m_0 k}{2} + m_0 k(2\ell_0^2 - m_0^2)] \qquad (F.26)$$

$$+ C[\frac{\ell_0 k^2}{12} + \frac{m_0 k'}{6} + \frac{\ell_0^3 k^2}{2} - \frac{m_0^3 k'}{3} + \frac{2m_0\ell_0^2 k'}{3} - \frac{5m_0^2\ell_0 k^2}{3}]s$$

$$+ C[\frac{\ell_0 kk'}{24} + \frac{m_0 k''}{24} + \frac{\ell_0^3 kk'}{3} + \frac{m_0^3 k^3}{4} - \frac{m_0^3 k''}{12} + \frac{m_0\ell_0^2 k''}{6}$$

$$- \frac{13m_0^2\ell_0 kk'}{12} - \frac{3m_0\ell_0^2 k^3}{4}]s^2$$

$$\frac{\partial t_{11}^{*}(Q)}{\partial x_0} = \frac{A\ell_0(B + m_0^2)}{s^2} + A[\ell_0 k^2(-\frac{5m_0^2}{6} + \frac{\ell_0^2}{4} - \frac{B}{12}) + m_0 k'(\frac{\ell_0^2}{3} - \frac{m_0^2}{6} - \frac{B}{6})]$$

$$+ A[m_0 k^3(\frac{5m_0^2}{24} - \frac{3\ell_0^2}{4} - \frac{B}{24}) + \ell_0 kk'(-\frac{13m_0^2}{12} + \frac{\ell_0^2}{3} - \frac{B}{12})$$

$$+ m_0 k''(\frac{\ell_0^2}{4} - \frac{1}{12} - \frac{B}{12})]s \qquad (F.27)$$

$$+ A[\ell_0 k^4(\frac{79m_0^2}{240} - \frac{\ell_0^2}{8} - \frac{B}{240}) + m_0 k^2 k'(\frac{31m_0^2}{90} - \frac{131\ell_0^2}{120} - \frac{B}{60})$$

$$+ \ell_0 kk''(\frac{-2m_0^2}{5} + \frac{\ell_0^2}{8} - \frac{B}{40}) + \ell_0 k'^2(\frac{-31m_0^2}{120} + \frac{\ell_0^2}{12} - \frac{B}{120})]s^2$$

$$\frac{\partial t^{*}_{12}(Q)}{\partial x_0} = \frac{Am_0(\ell_0^2 - B)}{s^2} + A[m_0k^2(\frac{7\ell_0^2}{12} - \frac{m_0^2}{2} - \frac{1}{4} - \frac{B}{12})$$

$$+ \ell_0k'(\frac{2m_0^2}{3} + \frac{\ell_0^2}{6} - \frac{1}{3} + \frac{B}{6})] \qquad (F.28)$$

$$+ A[\ell_0k^3(\frac{\ell_0^2}{6} - \frac{19m_0^2}{24} + \frac{1}{12} + \frac{B}{24}) + \ell_0k''(\frac{7m_0^2}{24} + \frac{\ell_0^2}{24} - \frac{1}{8} + \frac{B}{12})$$

$$+ m_0kk'(-\frac{7m_0^2}{12} + \frac{5\ell_0^2}{6} + \frac{1}{4} - \frac{B}{12})]s$$

$$+ A[m_0k^4(\frac{-7\ell_0^2}{20} + \frac{5m_0^2}{48} - \frac{B}{240}) + \ell_0k^2k'(\frac{567\ell_0^2}{72 \times 30} - \frac{2298m_0^2}{45 \times 48} + \frac{69}{45 \times 16} + \frac{B}{60})$$

$$+ m_0kk''(\frac{19\ell_0^2}{60} - \frac{5m_0^2}{24} + \frac{1}{12} - \frac{B}{210}) + m_0k'^2(\frac{219\ell_0^2}{45 \times 24} - \frac{5m_0^2}{36} + \frac{1}{18} - \frac{B}{120})]s^2$$

The other relations given by Eqs. (F.5) and (F.6) can be evaluated in like manner. The kernels for the strain equations can now be written in the form

$$g(s) = \frac{\alpha_{-2}}{s^2} + \frac{\alpha_{-1}}{s} + \alpha_0 + \alpha_1 s + \alpha_2 s^2 \qquad (F.29)$$

Using Eq. (5.6) the density function f(s) and the kernel, Eq. (F.24) or (F.27) in Eq. (5.1) we can easily evaluate the integrals in the singular intervals for determination of displacements or strains.

PART 1 - Government

Administrative and Liaison Activities

Office of Naval Research
Department of the Navy
Arlington, VA 22217
Attn: Code 474 (2)
Code 471
Code 200

Director
Office of Naval Research
Branch Office
666 Summer Street
Boston, MA 02210

Director
Office of Naval Research
Branch Office
536 South Clark Street
Chicago, IL 60605

Director
Office of Naval Research
New York Area Office
715 Broadway - 5th Floor
New York, NY 10003

Director
Office of Naval Research
Branch Office
1030 East Green Street
Pasadena, CA 91106

Naval Research Laboratory (6)
Code 2627
Washington, DC 20375

Defense Documentation Center (12)
Cameron Station
Alexandria, VA 22314

Navy

Undersea Explosion Research Division
Naval Ship Research and Development Center
Norfolk Naval Shipyard
Portsmouth, VA 23709
Attn: Dr. E. Palmer, Code 177

Navy (Con't.)

Naval Research Laboratory
Washington, DC 20375
Attn: Code 8400
8410
8430
8440
6300
6390
6380

David W. Taylor Naval Ship Research and Development Center
Annapolis, MD 21402
Attn: Code 2740
28
281

U.S. Naval Weapons Center
China Lake, CA 93555
Attn: Code 4062
4520

Commanding Officer
U.S. Naval Civil Engineering Laboratory
Code L31
Port Hueneme, CA 93041

Naval Surface Weapons Center
White Oak
Silver Spring, MD 20910
Attn: Code R-10
G-402
K-82

Technical Director
Naval Ocean Systems Center
San Diego, CA 92152

Supervisor of Shipbuilding
U.S. Navy
Newport News, VA 23607

U.S. Navy Underwater Sound Reference Division
Naval Research Laboratory
P.O. Box 8337
Orlando, FL 32806

Navy (Con't.)

Chief of Naval Operations
Department of the Navy
Washington, DC 20350
Attn: Code OP-098

Strategic Systems Project Office
Department of the Navy
Washington, DC 20376
Attn: NSP-200

Naval Air Systems Command
Department of the Navy
Washington, DC 20361
Attn: Code 5302 (Aerospace and Structures)
604 (Technical Library)
320B (Structures)

Naval Air Development Center
Director, Aerospace Mechanics
Warminster, PA 18974

U.S. Naval Academy
Engineering Department
Annapolis, MD 21402

Naval Facilities Engineering Command
200 Stovall Street
Alexandria, VA 22332
Attn: Code 03 (Research and Development)
04B
045
14114 (Technical Library)

Naval Sea Systems Command
Department of the Navy
Washington, DC 20362
Attn: Code 03 (Research and Technology)
037 (Ship Silencing Division)
035 (Mechanics and Materials)

Naval Ship Engineering Center
Department of the Navy
Washington, DC 20362
Attn: Code 6105G
6114
6120D
6128
6129

Commanding Officer and Director
David W. Taylor Naval Ship
Research and Development Center
Bethesda, MD 20084
Attn: Code 042
17
172
173
174
1800
1844
1102.1
1900
1901
1945
1960
1962

Naval Underwater Systems Center
Newport, RI 02840
Attn: Dr. R. Trainor

Naval Surface Weapons Center
Dahlgren Laboratory
Dahlgren, VA 22448
Attn: Code G04
G20

Technical Director
Mare Island Naval Shipyard
Vallejo, CA 94592

U.S. Naval Postgraduate School
Library
Code 0384
Monterey, CA 93940

Webb Institute of Naval Architecture
Attn: Librarian
Crescent Beach Road, Glen Cove
Long Island, NY 11542

Army

Commanding Officer (2)
U.S. Army Research Office
P.O. Box 12211
Research Triangle Park, NC 27709
Attn: Mr. J. J. Murray,
CRD-AA-IP

Watervliet Arsenal
MAGGS Research Center
Watervliet, NY 12189
Attn: Director of Research

U.S. Army Materials and Mechanics
Research Center
Watertown, MA 02172
Attn: Dr. R. Shea, DRXMR-T

U.S. Army Missile Research and
Development Center
Redstone Scientific Information
Center
Chief, Document Section
Redstone Arsenal, AL 35809

Army Research and Development
Center
Fort Belvoir, VA 22060

Air Force

Commander WADD
Wright-Patterson Air Force Base
Dayton, OH 45433
Attn: Code WWRMDD
AFFDL (FDDS)
Structures Division
AFLC (MCEEA)

Chief Applied Mechanics Group
U.S. Air Force Institute of Technology
Wright-Patterson Air Force Base
Dayton, OH 45433

Chief, Civil Engineering Branch
WLRC, Research Division
Air Force Weapons Laboratory
Kirtland Air Force Base
Albuquerque, NM 87117

Air Force Office of Scientific Research
Bolling Air Force Base
Washington, DC 20332
Attn: Mechanics Division

Department of the Air Force
Air University Library
Maxwell Air Force Base
Montgomery, AL 36112

NASA

National Aeronautics and Space Administration
Structures Research Division
Langley Research Center
Langley Station
Hampton, VA 23365

National Aeronautics and Space Administration
Associate Administrator for Advanced
Research and Technology
Washington, DC 20546

Scientific and Technical Information Facility
NASA Representative (S-AK/DL)
P.O. Box 5700
Bethesda, MD 20014

Other Government Activities

Commandant
Chief, Testing and Development Division
U.S. Coast Guard
1300 E Street, NW
Washington, DC 20226

Technical Director
Marine Corps Development
and Education Command
Quantico, VA 22134

Director Defense Research
and Engineering
Technical Library
Room 3C128
The Pentagon
Washington, DC 20301

Director
National Bureau of Standards
Washington, DC 20034
Attn: Mr. B. L. Wilson, EM 219

Dr. M. Gaus
National Science Foundation
Environmental Research Division
Washington, DC 20550

Library of Congress
Science and Technology Division
Washington, DC 20540

Director
Defense Nuclear Agency
Washington, DC 20305
Attn: SPSS

Mr. Jerome Persh
Staff Specialist for Materials
and Structures
OUSDR&E, The Pentagon
Room 3D1089
Washington, DC 20301

Chief, Airframe and Equipment Branch
FS-120
Office of Flight Standards
Federal Aviation Agency
Washington, DC 20553

National Academy of Sciences
National Research Council
Ship Hull Research Committee
2101 Constitution Avenue
Washington, DC 20418
Attn: Mr. A. R. Lytle

National Science Foundation
Engineering Mechanics Section
Division of Engineering
Washington, DC 20550

Picatinny Arsenal
Plastics Technical Evaluation Center
Attn: Technical Information Section
Dover, NJ 07801

Maritime Administration
Office of Maritime Technology
14th and Constitution Ave., NW
Washington, DC 20230

Maritime Administration
Office of Ship Construction
14th and Constitution Ave., NW
Washington, DC 20230

PART 2 - Contractors and Other Technical Collaborators

Universities

Dr. J. Tinsley Oden
University of Texas at Austin
345 Engineering Science Building
Austin, TX 78712

Professor Julius Miklowitz
California Institute of Technology
Division of Engineering
and Applied Sciences
Pasadena, CA 91109

Dr. Harold Liebowitz, Dean
School of Engineering and
Applied Science
George Washington University

Professor Eli Sternberg
California Institute of Technology
Division of Engineering and
Applied Sciences
Pasadena, CA 91109

Professor Paul M. Naghdi
University of California
Department of Mechanical Engineering
Berkeley, CA 94720

Professor A. J. Durelli
Oakland University
School of Engineering
Rochester, MI 48063

Professor F. L. DiMaggio
Columbia University
Department of Civil Engineering
New York, NY 10027

Professor Norman Jones
Massachusetts Institute of Technology
Department of Ocean Engineering
Cambridge, MA 02139

Professor E. J. Skudrzyk
Pennsylvania State University
Applied Research Laboratory
Department of Physics
State College, PA 16801

Professor J. Kempner
Polytechnic Institute of New York
Department of Aerospace Engineering and
Applied Mechanics
333 Jay Street
Brooklyn, NY 11201

Professor J. Klosner
Polytechnic Institute of New York
Department of Aerospace Engineering and
Applied Mechanics
333 Jay Street
Brooklyn, NY 11201

Professor R. A. Schapery
Texas A&M University
Department of Civil Engineering
College Station, TX 77843

Professor Walter D. Pilkey
University of Virginia
Research Laboratories for the
Engineering Sciences
School of Engineering and
Applied Sciences
Charlottesville, VA 22901

Professor K. D. Willmert
Clarkson College of Technology
Department of Mechanical Engineering
Potsdam, NY 13676

Dr. Walter E. Haisler
Texas A&M University
Aerospace Engineering Department
College Station, TX 77843

Dr. Hussein A. Kamel
University of Arizona
Department of Aerospace and
Mechanical Engineering
Tucson, AZ 85721

Dr. S. J. Fenves
Carnegie-Mellon University
Department of Civil Engineering
Schenley Park
Pittsburgh, PA 15213

Universities (Con't.)

Dr. Ronald L. Huston
Department of Engineering Analysis
University of Cincinnati
Cincinnati, OH 45221

Professor G. C. M. Sih
Lehigh University
Institute of Fracture and
Solid Mechanics
Bethlehem, PA 18015

Professor Albert S. Kobayashi
University of Washington
Department of Mechanical Engineering
Seattle, WA 98105

Professor Daniel Frederick
Virginia Polytechnic Institute and
State University
Department of Engineering Mechanics
Blacksburg, VA 24061

Professor A. C. Eringen
Princeton University
Department of Aerospace and
Mechanical Sciences
Princeton, NJ 08540

Professor E. H. Lee
Stanford University
Division of Engineering Mechanics
Stanford, CA 94305

Professor Albert I. King
Wayne State University
Biomechanics Research Center
Detroit, MI 48202

Dr. V. R. Hodgson
Wayne State University
School of Medicine
Detroit, MI 48202

Dean B. A. Boley
Northwestern University
Department of Civil Engineering
Evanston, IL 60201

Professor P. G. Hodge, Jr.
University of Minnesota
Department of Aerospace Engineering
and Mechanics
Minneapolis, MN 55455

Dr. D. C. Drucker
University of Illinois
Dean of Engineering
Urbana, IL 61801

Professor N. M. Newmark
University of Illinois
Department of Civil Engineering
Urbana, IL 61803

Professor E. Reissner
University of California, San Diego
Department of Applied Mechanics
La Jolla, CA 92037

Professor William A. Nash
University of Massachusetts
Department of Mechanics and
Aerospace Engineering
Amherst, MA 01002

Professor G. Herrmann
Stanford University
Department of Applied Mechanics
Stanford, CA 94305

Professor J. D. Achenbach
Northwestern University
Department of Civil Engineering
Evanston, IL 60201

Professor S. B. Dong
University of California
Department of Mechanics
Los Angeles, CA 90024

Professor Burt Paul
University of Pennsylvania
Towne School of Civil and
Mechanical Engineering
Philadelphia, PA 19104

Universities (Con't.)

Professor H. W. Liu
Syracuse University
Department of Chemical Engineering
and Metallurgy
Syracuse, NY 13210

Professor S. Bodner
Technion R&D Foundation
Haifa, Israel

Professor Werner Goldsmith
University of California
Department of Mechanical Engineering
Berkeley, CA 94720

Professor R. S. Rivlin
Lehigh University
Center for the Application
of Mathematics
Bethlehem, PA 18015

Professor F. A. Cozzarelli
State University of New York at Buffalo
Division of Interdisciplinary Studies
Karr Parker Engineering Building
Chemistry Road
Buffalo, NY 14214

Professor Joseph L. Rose
Drexel University
Department of Mechanical Engineering
and Mechanics
Philadelphia, PA 19104

Professor B. K. Donaldson
University of Maryland
Aerospace Engineering Department
College Park, MD 20742

Professor Joseph A. Clark
Catholic University of America
Department of Mechanical Engineering
Washington, DC 20064

Professor T. C. Huang
University of Wisconsin-Madison
Department of Engineering Mechanics
Madison, WI 53706

Dr. Samuel B. Batdorf
University of California
School of Engineering
and Applied Science
Los Angeles, CA 90024

Professor Isaac Fried
Boston University
Department of Mathematics
Boston, MA 02215

Professor Michael Pappas
New Jersey Institute of Technology
Newark College of Engineering
323 High Street
Newark, NJ 07102

Professor E. Krempl
Rensselaer Polytechnic Institute
Division of Engineering
Engineering Mechanics
Troy, NY 12181

Dr. Jack R. Vinson
University of Delaware
Department of Mechanical and Aerospace
Engineering and the Center for
Composite Materials
Newark, DL 19711

Dr. Dennis A. Nagy
Princeton University
School of Engineering and Applied Science
Department of Civil Engineering
Princeton, NJ 08540

Dr. J. Duffy
Brown University
Division of Engineering
Providence, RI 02912

Dr. J. L. Swedlow
Carnegie-Mellon University
Department of Mechanical Engineering
Pittsburgh, PA 15213

Dr. V. K. Varadan
Ohio State University Research Foundation
Department of Engineering Mechanics
Columbus, OH 43210

Universities (Con't.)

Dr. Z. Hashin
University of Pennsylvania
Department of Metallurgy and
Materials Science
College of Engineering and
Applied Science
Philadelphia, PA 19104

Dr. Jackson C. S. Yang
University of Maryland
Department of Mechanical Engineering
College Park, MD 20742

Professor T. Y. Chang
University of Akron
Department of Civil Engineering
Akron, OH 44325

Professor Charles W. Bert
University of Oklahoma
School of Aerospace, Mechanical,
and Nuclear Engineering
Norman, OK 73019

Professor Satya N. Atluri
Georgia Institute of Technology
School of Engineering Science and
Mechanics
Atlanta, GA 30332

Professor Graham F. Carey
University of Texas at Austin
Department of Aerospace Engineering
and Engineering Mechanics
Austin, TX 78712

Industry and Research Institutes

Dr. Jackson C. S. Yang
Advanced Technology and Research, Inc.
10006 Green Forest Drive
Adelphi, MD 20783

Dr. Norman Hobbs
Kaman AviDyne
Division of Kaman
Sciences Corp.
Burlington, MA 01803

Industry and Research Institutes (Con't.)

Argonne National Laboratory
Library Services Department
9700 South Cass Avenue
Argonne, IL 60440

Dr. M. C. Junger
Cambridge Acoustical Associates
1033 Massachusetts Avenue
Cambridge, MA 02138

Dr. V. Godino
General Dynamics Corporation
Electric Boat Division
Groton, CT 06340

Dr. J. E. Greenspon
J. G. Engineering Research Associates
3831 Menlo Drive
Baltimore, MD 21215

Dr. K. C. Park
Lockheed Missile and Space Company
3251 Hanover Street
Palo Alto, CA 94304

Newport News Shipbuilding and
Dry Dock Company
Library
Newport News, VA 23607

Dr. W. F. Bozich
McDonnell Douglas Corporation
5301 Bolsa Avenue
Huntington Beach, CA 92647

Dr. H. N. Abramson
Southwest Research Institute
8500 Culebra Road
San Antonio, TX 78284

Dr. R. C. DeHart
Southwest Research Institute
8500 Culebra Road
San Antonio, TX 78284

Dr. M. L. Baron
Weidlinger Associates
110 East 59th Street
New York, NY 10022

Industry and Research Institutes (Con't.)

Dr. T. L. Geers
Lockheed Missiles and Space Company
3251 Hanover Street
Palo Alto, CA 94304

Mr. William Caywood
Applied Physics Laboratory
Johns Hopkins Road
Laurel, MD 20810

Dr. Robert E. Nickell
Pacifica Technology
P.O. Box 148
Del Mar, CA 92014

Dr. M. F. Kanninen
Battelle Columbus Laboratories
505 King Avenue
Columbus, OH 43201

Dr. G. T. Hahn
Battelle Columbus Laboratories
505 King Avenue
Columbus, OH 43201

Dr. A. A. Hochrein
Daedalean Associates, Inc.
Springlake Research Center
15110 Frederick Road
Woodbine, MD 21797

Mr. Richard Y. Dow
National Academy of Sciences
2101 Constitution Avenue
Washington, DC 20418

Mr. H. L. Kington
Airesearch Manufacturing Company
of Arizona
P.O. Box 5217
111 South 34th Street
Phoenix, AZ 85010

Dr. M. H. Rice
Systems, Science, and Software
P.O. Box 1620
La Jolla, CA 92037

UNCLASSIFIED

SECURITY CLASSIFICATION OF THIS PAGE (When Data Entered)

REPORT DOCUMENTATION PAGE	READ INSTRUCTIONS BEFORE COMPLETING FORM
1. REPORT NUMBER (14) UILU-ENG-79-2005, SRS-461 2. GOVT ACCESSION NO.	3. RECIPIENT'S CATALOG NUMBER
4. TITLE (and Subtitle) (6) Boundary Integral Equation Solution of Plane Elasticity Problems with High Stress Concentrations.	5. TYPE OF REPORT & PERIOD COVERED (9) Technical Report.
	6. PERFORMING ORG. REPORT NUMBER SRS NO. 461
7. AUTHOR(s) (10) Hassan Nikooyeh, Arthur R. Robinson	8. CONTRACT OR GRANT NUMBER(s) (15) N00014-75-C-0164
9. PERFORMING ORGANIZATION NAME AND ADDRESS Department of Civil Engineering, University of Illinois at Urbana-Champaign, Urbana, Illinois 61801	10. PROGRAM ELEMENT, PROJECT, TASK AREA & WORK UNIT NUMBERS Project No. NR 064-183
11. CONTROLLING OFFICE NAME AND ADDRESS Office of Naval Research, CODE N00014, Department of the Navy, Arlington, Virginia 22217	(11) 12. REPORT DATE April, 1979; 13. NUMBER OF PAGES 122
14. MONITORING AGENCY NAME & ADDRESS (if different from Controlling Office) Material Science Division, Structural Mechanics Program (CODE 474), Office of Naval Research (800 Quincy Street), Arlington, Virginia 22217	15. SECURITY CLASS. (of this report) UNCLASSIFIED; 15a. DECLASSIFICATION/DOWNGRADING SCHEDULE

16. DISTRIBUTION STATEMENT (of this Report)

Approved for public release: Distribution Unlimited

17. DISTRIBUTION STATEMENT (of the abstract entered in Block 20, if different from Report)

(12) 143 p.

18. SUPPLEMENTARY NOTES

19. KEY WORDS (Continue on reverse side if necessary and identify by block number)

Plane Elasticity
Boundary Integral Equations
Stress Concentrations
Notches
Fillets

20. ABSTRACT (Continue on reverse side if necessary and identify by block number)

A numerical method for determination of stresses in two-dimensional elastic bodies with high stress concentrations is presented. Major emphasis is placed on bodies with a notch having a fillet of small radius and bodies with a crack of small width. These static boundary value problems are formulated in terms of boundary integral equations of a type used previously by Barone and Robinson for sharp notches and cracks.

276 020

DD FORM 1 JAN 73 1473 EDITION OF 1 NOV 65 IS OBSOLETE

SECURITY CLASSIFICATION OF THIS PAGE (When Data Entered)

20. (Continued)

For the fillet problem a small inner region containing the fillet and bounded by a circle is separated out and analyzed numerically under the loading system of each of the Williams' solution of the corresponding sharp notch. The results are then used to develop analytical solutions for the intermediate region adjacent to the fillet region. In this way the details of the boundary configuration of the fillet is reflected in a set of generalized displacements which characterize the intermediate field.

For the solution of the whole body including the loaded boundary, kernels developed by Barone and Robinson are used to pick out the generalized displacements of the intermediate region.

The solution of the wide crack problem is similar except that a perturbation scheme is required to ensure homogeneous boundary conditions at the actual edges of the crack.